UNIVERSITÀ DEGLI STUDI DI PADOVA

DIPARTIMENTO DI INGEGNERIA DELL'INFORMAZIONE

UNIVERSITY OF PADUA

DEPARTMENT OF INFORMATION ENGINEERING

MASTER'S DEGREE THESIS IN BIOENGINEERING

Analysis of legs stiffnesses in unilateral amputee elite athletes during treadmill running and track sprinting

Supervisor: Prof. Nicola Petrone

Candidate: Valerio Pelusi

Co-Supervisors: Eng. Andrea G. Cutti
Eng. Samira G. Breban

ACADEMIC YEAR 2022 – 2023

Date 17/04/2023

ABSTRACT

Leg Stiffness (K_{leg}) is a common parameter used to characterize leg function during bouncing gaits, like running and sprinting. In people with a lower limb amputation Running-Specific Prostheses (RSP) are designed to replicate the spring-like behaviour of the biological leg.

The aim of this study is to analyse the leg stiffness of the affected limb (AL) and the unaffected limb (UL) in unilateral amputee elite athletes, during treadmill running and track sprinting.

For this reason, a spring-mass model has been defined and implemented, using a custom MATLAB code, to describe and examine the running action during the stance phase. Moreover, not only the '*Leg Stiffness'* but also the '*Foot Stiffness'* of the prosthetic foot and the contribution of the residual limb have been investigated.

The data used for the analysis had been acquired from treadmill and track in-vivo experimental sessions, in which the participant, the 'Gold medallist' sprinter Ambra Sabatini, performed constant speed running. Each test session required specific protocols and specific instrumentations, including Motion Capture cameras, force platforms and wearable force sensors.

The results of the analysis were compared to highlight differences on the K_{leg} between the affected and unaffected limb, running on different types of surfaces (treadmill and track) and using different prothesis configuration. It has been confirmed that unilateral amputee wearing RSP present bilateral asymmetry in K_{leg} while running: in fact the K_{leg} was smaller in the affected limb than the unaffected limb. In addition, Leg Stiffness on track was greater than that on treadmill. Although several studies suggested that prosthetic alignment could influence running performance through the regulation of stiffness in lower-extremity amputees, from the data obtained in this work, not significantly changes has been observed considering the different socket alignments.

Since prosthetic leg stiffness is considerably lower than stiffness of the RSP, compliance of the residual leg should not be ignored; in fact, a substantial contribution of the residual leg to total leg stiffness was observed.

Due to the numerous assumptions and simplifications of the model, caution must be used in the interpretation of these results: further in-vivo experimental sessions will be taken place to overcome a good part of the limitations of this study and improve the quality of the analysis.

Contents

Introduction

OLIMPIA project

The research work described in this thesis has been carried out as part of the OLIMPIA project which aims to develop innovative technological solutions to improve performance and safety in Paralympic athletes during sport practice.

The project provides for the collaboration between the University of Padua and INAIL (National Institute for Insurance against Injuries at Work – Istituto Nazionale per l'Assicurazione contro gli Infortuni sul Lavoro).

The Prosthetic Centre INAIL of Vigorso di Budrio (BO – Italy) carries out significant scientific research, technological development, and clinical trials in fields of rehabilitation and prosthetics. It is specialized in design and manufacturing of custom-made prosthesis and orthosis for patients with lower and upper limb amputations [1].

In particular, the scientific research of OLIMPIA project, is focused on prosthesis and orthosis for running and jumping and on prosthesis and mono skis for alpine skiing. These devices are essential considering the different sport's application: in particular for amatorial and Paralympic running and sprint [2].

CHAPTER 1: Background

1. Human Running

Human running is a complex motion that engages the whole body, and it occurs in various forms in track and field competitions or team sports games. The running distance is covered through cyclic lower limb movements based on continuous acceleration and deceleration phases: therefore, it is comparable to a rapid sequence of jumps similar to the motion of a bouncing ball, in which each leg acts like a spring [3].

In the bouncing mechanism of running, potential energy and kinetic energy are in phase: this "in phase oscillation" of the centre of gravity is suggestive of an elastic rebound of the body, as the energy is alternately absorbed and restored by the muscle [4].

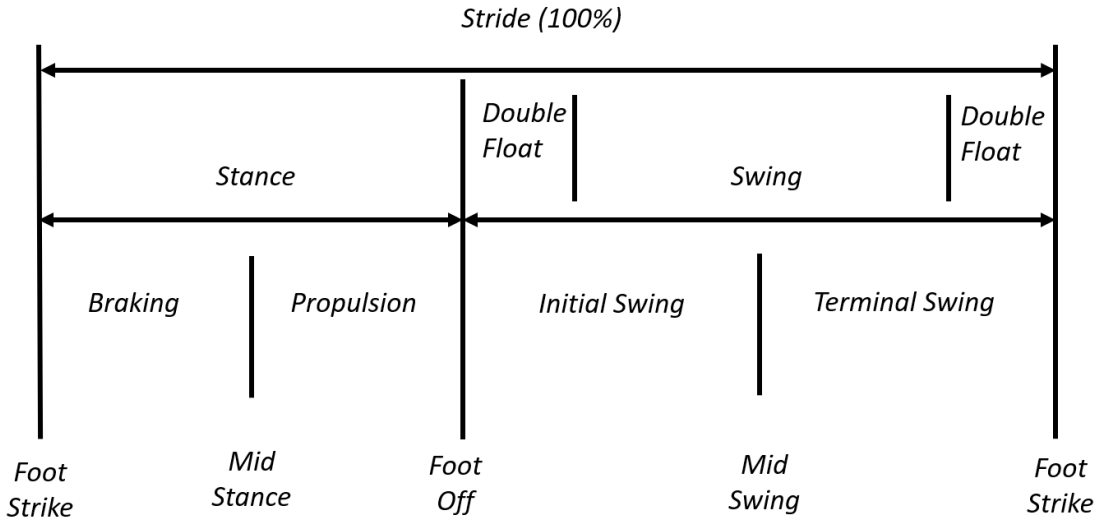

Figure 1.1: Running phases.

In the running cycle two principles phases can be distinguished: *Stance* and *Swing.*

The *Stance* phase starts with the *Foot Strike (FS)* and finishes in the *Foot Off (FO)*, with the extension of the lower limb. In *Swing*, the foot doesn't touch the ground. Furthermore, running has a *Double Float* instead of a *Double Stance* like in walking, when both feet are airborne twice during the running cycle, one at the beginning and one at the end of the *Swing*.

The *Stance* is around the 40% of the stride cycle, while the swing is the 60%: in elite sprinting this percentage could reach the 20% (stance) and 80% (swing) [5].

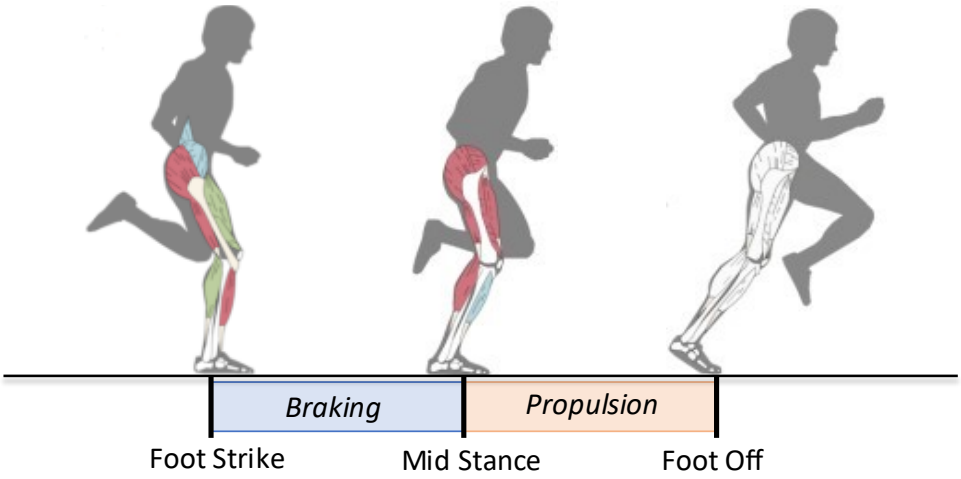

Figure 1.2: Stance events and phases in human running [Frank Angulo (Ossur) drawings adapted].

The stance phase can be divided in two phases identified by three events [6]:

During the braking phase (beetween the *Foot Strike (FS)* and *Mid Stance (MS)*) deceleration and energy absorption occur: in the first part the foot's support on the ground is cushioned by the eccentric action of the triceps suralis and the quadriceps femoris: hip, knee and ankle work together to absorb energy. Approaching the *Mid Stance* the muscles contract isomerically to keep the body stable.

The transition from absorption to propulsion happens during the *Mid Stance*: nearly all the leg muscles create a forward force and knee begins to extends while the ankle is pushing off.

The propulsion phase (beetween *Mid Stance (MS)* and *Foot Off (FO)*) is the acceleration or speed-generation phase: muscles use their elastic properties to project forward the body. As the foot pushes off, the lower leg generates more than twice the energy that was stored when the foot struck down [7].

The body during running is subjected to ripetitive impacts, that may cause injury or pain to the runner: therefore, there is some evidence that too little or too much lower extremity stiffness has implications for both performance and injury [8].

2. Amputee Running

Starting from the 1980s, when the advances in composites materials flooded the prosthetic industry, the usefulness of lower limb prosthesis improved tremendously. Carbon-fibers reinforced materials brought lightness, durability, strength, and biocompatibility to the design of the prosthetic feet [9].

2.1 Running Specific Prosthesis (RSP)

Passive-elastic carbon-fiber running-specific prostheses (RSPs) are designed to enable atheletes with lower limb amputation to run [10].

The main components to the design of the prosthesis are the socket, the prosthetic knee, the connecting organs (pylon, pyramidal attack) and the carbon blade foot.

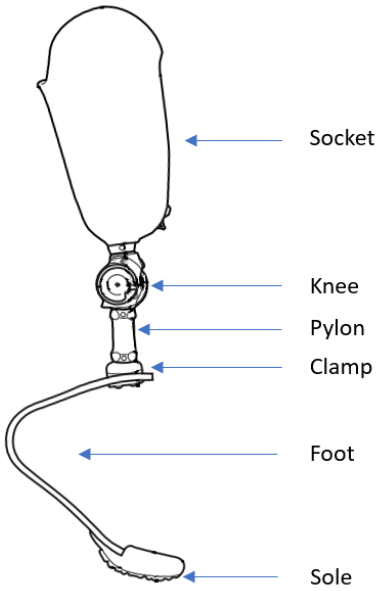

Figure 1.3: RSPs main components.

- *Socket*: carbon-fiber or fiber-glass negative composite of a residual limb; it represents the custom element of the prosthesis.
- *Knee:* the cylindrical, hydraulic joint that connectes the socket to the RSP in trasfermoral amputees. It has a single - axis mechanism that works like a hinge, allowing the athlete to make a more natural swing movement and it locks automatically the knee when it has to support loads.
- *Pylon*: is a rigid tubular member connecting the socket to the knee unit or directly to the foot, helping the prosthesis in shock-absorption and weight bearing.
- *Pyramidal attack:* allow to fix the foot to the pylon and adjust the angles of alignment of the foot, by acting on four fixing screws.

- *Sole:* it provides a specialized traction that has been optimized for the foot blade. A spiked sole ensures grip with the Tartan surface of the athletics tracks, while a rubber sole could be used in others ground surfaces, for example on a treadmill.

All the elements above, from the socket to the foot, the so-called 'RPF- *Running Prosthesis Foot*', are part of the 'RSP - *Running Specific Prosthesis*'. RSPs are essentially characterised by their shape, category and height.

Figure 1.4: Different models of Running Specific Prostheses

RPFs are shaped like the uppercase letters “C” or “J”, attach in - series to residual limbs. The shape, depends on the type of running performed and on whether the prosthesis is attached directly to the socket or below it.

RPF category is a number representing the relative stiffness of the blade: the stiffer the foot, the bigger the category. Each prosthetic manufacter recommends prostheses based on body mass and intended activity, such as slow or fast running [7].

RSP height is set at the discretion of the athlete and /or their prosthetist in accordance with the International Paralympic Committee (IPC) guidelines [11]. The height is based on the unaffected leg and residual limb length. The total height of the affected limb, when unloaded, is usually set about 5 cm longer than the intact limb to compensate body deflection during loading [12], [13].

Using carbon fibre material, the running prosthetic foot allows to store and then to return elastic energy during the contact to the ground.

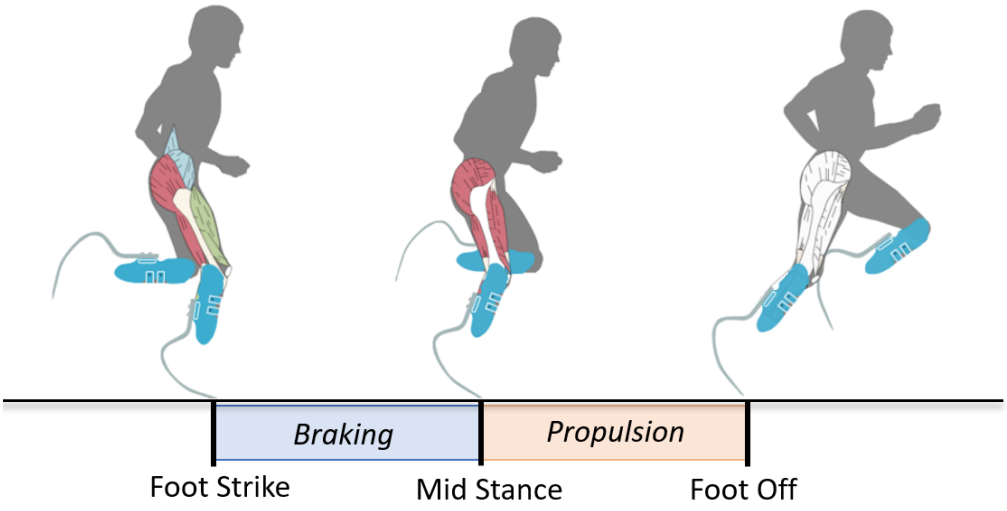

Figure 1.5: Stance events and phases in amputee running
[Frank Angulo (Ossur) drawings adapted].

The stance phase can be still divided in two phases (braking and propulsion) identified by three events (*FS, MS, FO*).

During the braking phase blade compresses, storing energy, while the hip muscles help stabilize the knee and generate speed.

At the *Mid Stance*, the energy stored in the blade reaches the front edge: in this moment, hips must generate almost twice the energy of an able-bodied sprinter.

In the propulsion phase, the energy in the blade is released propelling the runner forward. Unlike biological ankles, running prosthetic feet cannot generate mechanical power anew and return only from 63% to 95% of the stored elastic energy during running [7].

2.2 **Socket alignment**

The *'alignment'* is defined as the position of the sockect with respect to knee and foot. During the latest studies [14], [15] , including the experimental sessions that will be described later in this work, different socket alignments have been tested with Paralympic transfemoral sprinters.

The alignment procedure should be done in the condition of mid stance, which is reproduced on a bench during the design phase and in vivo during test sessions: the mid stance was defined as the instant of the stance phase in which the projection of the Greater Trochanter on the ground passes through the prosthetic knee centre for the prosthetic side. Prior to bench alignment, the subject's thigh orientation and hip mobility should be measured with the so-called *Thomas' Angle,* which is the degree of hip flexion contracture measured with the Thomas' Test [16].

The prosthetist does the procedure of alignment adjusting all the prosthetic components and defining the '*Alignment Axis*' and the '*Socket Axis*' for the identification of the *'Socket alignment angle'*.

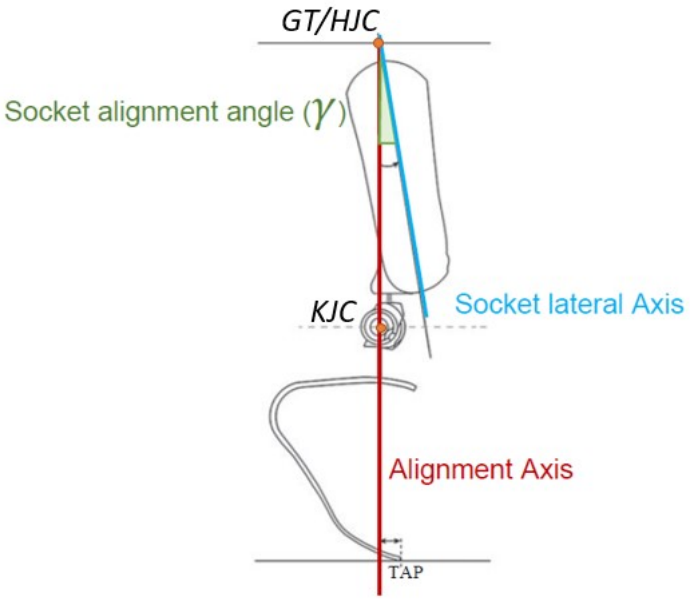

Figure 1.6: Alignment axis and socket lateral axis used to individuate the alignment angle (γ) [14], [16]

The '*socket axis'* is identified as the intersection between frontal and sagittal mid-planes of the socket. The lateral axis of the socket has also to be marked and it represents the incidence of frontal plane with the socket. Then, a plumb line is used to obtain the *'Alignment Axis'*, which is the vertical axis passing through the Greater Trochanter (GT), approximating the Hip Joint Centre and which, in condition of mid stance, should pass through the Knee Joint Centre (KJC).

Once identified these axes, is possible to define the *Socket tilt angle (γ)*, which is basically the angle in the sagittal plane between the *lateral axis of the socket* and the *Alignment Axis*.

For a running prosthesis, the socket tilt should range from 5° up to 15° plus the patient-specific *Thomas' Angle*.

Table 1: socket Alignments features (Socket tilt angle has to be added to the Thomas' Angle) [Migliore et al,.*[16]*]*

Alignment	Socket tilt*(γ) [°]
A0	5
A1	9
A2	12
A3	15

3. Definition of Stiffness

The concept of stiffness of a spring or elastic element has its origin in physics as part of the Hooke's Law:

$$F = K\,\Delta l$$

It was developed to describe the behaviour of elastic deformable bodies under application of external forces stating a proportional relationship between the force (F) and the displacement (Δl) [8].

Therefore, *stiffness* (K) was defined as the ratio of the amount of deforming force to the unit of displacement.

$$K = \frac{F}{\Delta l}$$

Stiffness has been used to model the way in which the lower body responds to landing during cyclic motions such as running and jumping [3].

3.1 Leg Stiffness

Human running is often modelled using a *'spring - mass'* model, in which the supporting leg behaves as a massless mechanical spring loaded by a body mass centred over the spring, which depicts the runner during stance phase [17]–[20].

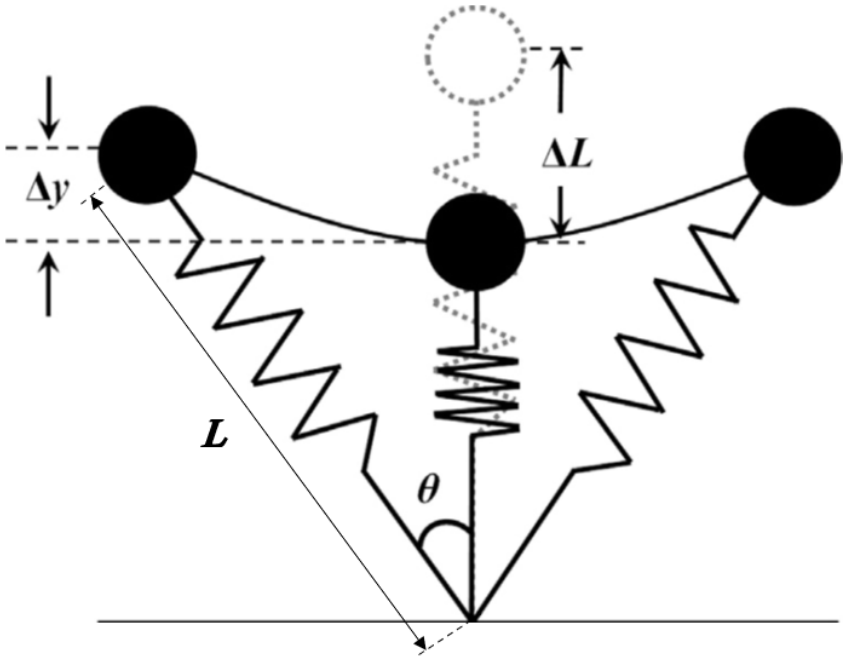

Figure 1.7: "Spring–mass model" for running: Δy is the maximal vertical displacement of the centre of mass; ΔL is the maximal leg compression; θ denotes half of the angle swept by the leg during the ground contact (Blickhan, 1989; McMahon and Cheng, 1990)

In mechanics and physics, a linear spring is characterized by its spring constant K, which is a measure of the spring's stiffness. In the context of gait analysis, the stiffness of the spring is called *Leg Stiffness (Kleg)* and it is an important parameter that influence the running performance.

Leg stiffness can be generally expressed by the following equation [3]:

$$K_{leg} = \frac{F}{\Delta l}$$

where F is the deforming force (the causes of the change in length), Δl denotes the change in "leg-spring" length (leg shortening). It is importatant to underline that this is a general definition: indeed there are lots of models in the literature which define the deforming force and the leg shortening in multiple ways.

It is thougth that the stiffness of the supporting leg greatly influences several running variables, such as speed, stride frequency and energetic cost [17].

Studies have examined the relationship beetween stiffness and running performance, support that as the physical demands of the activity increases, leg stiffness also increases. The biomechanical parameters that mostly influence K_{leg} are stride frequency and speed [3], [8], [21], [22].

On one hand with the increasing of running velocity, leg stiffness remains relatively constant or increases during running, on the other hand it is possible to change the leg stiffness value more than twice by increasing stride frequency at a given running: increasing the frequency of the stride results in a decrease in the lowering of the centre of mass and consequently an increase in K_{leg}. Moreover, leg stiffness is not strongly related to the aerobic demand of running and fatigue [3], [21].

Increasing leg stiffness brings to an increment of loading rates, which have been associated with increased shock to the lower extremity. In addiction, increased peak forces, loading rates and shock are all believed to place athletes at a greater risk for bony injuries. From another point of view, studies suggest that too little stiffness may be associated with soft tissue injury [8].

During running tasks, leg stiffness is expected to be greater in athletes than nonathletes: therefore, increases in leg stiffness make it theoretically possible for runners to absorb greater loads that may be important in training programs [3].

Able-bodies runners are capable of modulating and to adapting leg stiffness to change step frequency or to accommodate to different surface stiffness [23]. Different components have a contribution in leg stiffness variations: tendons, ligaments, muscles, cartilage, and bone. In addiction the overall stiffness of the leg is related to the mechanical behaviour of soft and hard tissues, contraction speed and viscoelastic properties of the muscle, delay in reflex and activation under Central Nervous System [8].

For these reasons, the estimation of the leg stiffness plays a key role in the assessment of the sport performance and in the subsequent improvement of training methods.

3.2 Leg Stiffness in amputees runners

In amputee runners the total leg stiffness is depending on the stiffness and configuration of the residual joints together with the stiffness of the prosthesis [24].

Carefull selection of the RPF stiffness is crucial to optimize performance in athletes with lower limb amputation: currently, athletes are assigned a stiffness category based on the body mass and intended activity level, rather than performance based metrics of the prosthesis [7].

It has been shown that the stiffness of the RPF is not a constant but depends on loading conditions and by changing the direction of loading of the blade the prosthetic stiffness could be changed. For example, by changing the angle of attack of the leg at initial contact or the angle of alignment of the RPF beneath the socket, the stiffness could change. Thus, not only the RPF category is essential, but also the alignment of the blade relative to the socket need to be taken into account [7], [23]. Therefore the calculation of the leg stiffness has a further function: thanks to it, it is possible to assess the best alignment of the prosthesis for each athlete.

Although stiffness of the RPF dominated total leg stiffness, the stiffness of the residual leg has been shown to contribute significantly to total leg stiffness. Nevertheless, athletes using a RSP seemed not capable of regulating the stiffness of the residual leg to adjust the total leg stiffness [25]. RPF category and RSP height could be expected to have an effect on the stiffness of the affected leg, but it came out that the main influence is on the K_{leg} of the sound leg [26].

Many studies reported differences in K_{leg} between the affected (AL) and unaffected limb (UL). The modulation of the stiffness of the intact and residual limb can vary according to running speed and step frequency.

McGowan et al. [27] showed that stiffness for legs without amputations was constant or increased with speed (when speeds exceeds 6 m/s), whereas stiffness for legs with RSPs decreased with speed.

In athlete with transtibial amputation, Hobara et al.[26] suggest that the prosthetic leg has lower stiffness than the sound leg. In both limbs K_{leg} remain constant during running at submaximal speeds, from 2.5 to 3.5 m/s [26], while McGowan et al.[27] found that intact side stiffness remained constant or increased with speed. These differences are likely due to different experimental setup.

Sano et al. [28] and Hobara et al.[29] demonstrated that leg stiffness in prosthetic limb was significantly smaller than unaffected limb in transfemoral amputees. Moreover, results show a decrease in K_{leg} with increasing speed across a range of running velocity for the affected limb, whereas no change was present in the unaffected limb.

These results are congruent with previous finding demonstrating that transtibial amputees wearing RSP have bilateral asymmetry in K_{leg} during running [26], [27]. Along with previous data, these studies suggest that bilateral asymmetry in spring-like leg behaviour may be a common biomechanical characteristic among lower extremity amputees wearing the RSPs while running.

In summary, the modulation of the stiffness of the intact and residual limb can vary according to running speed: K_{leg} in transtibial and transfemoral amputee sprinters remained constant or increased with speed in intact limbs, while it remained constant or decreased in limbs using RSPs. This also suggest that the spring-like behaviour and K_{leg} regulation during running using RSPs may not necessarily depend on amputation level.

Finally, considering the stiffness regulation at different step frequencies at a given running speed in unilateral transfemoral amputees, it was found that K_{leg} increases with increasing step frequency for the unaffected limb (according to Farley et al. [21]), but not for the affected limb [30]. This also suggest that the stiffness regulation strategy during running differs between the affected and unaffected limb.

3.3 Modeling of Leg Stiffness

Accurate calculation of leg stiffness in human running required the use of direct kinematic-kinetic measuraments [17].

According to a recent overview [3] and a previous Thesis work [31], in literature there are several mathematical models which allow the estimation of leg stiffness. In general, these models are of three different types: unidimensional, bidimensional and three-dimensional, depending on the number of components of force used in calculation. In the master's Thesis study, after a literature analysis to find all the mathematical models, applying some exclusion criteria, 7 papers were chosen, and 12 different models were selected [17], [21], [23], [32], [33]. With the aim of choosing a mathematical model for the estimation of leg stiffness to be applied to the track running data of a transfemoral amputee sprinter, all available models were tested with a public dataset: data from treadmill trials at different speeds (2.5 m/s and 4.5 m/s.) were analysed. In the chosen dataset the maximum speed reached by the subjects is comparable to that of non-elite transfemoral amputees sprinters.

Among the selected models, the 'gold standard' is considered the one described in the study of Liew et al, [33]. In this model, the leg is represented by a 3D vector from the Hip Joint Centre (HJC) to the centre of pressure (COP); the leg shortening (ΔL) is given by the difference between the leg length at initial contact and the leg length at peak resultant projected GRF. The leg stiffness is calculated by taking the ratio between the peak magnitude of the resultant projected GRF, and the resultant change in leg length [33].

This model appears to be the most consistent with reality, but also the most complex in its application: since all three force and markers trajectory components are required, indeed force platforms and optoelectronic system are necessary as instrumentation for experimental session.

Among the goals of the Olimpia project there is the implementation of new models in order to estimate the leg stiffness using the data acquired during in-vivo experimental sessions which better represent running in amputee athletes.

4. Aim of this work

The aim of this study is to analyse the *Leg Stiffness* of the affected limb (AL) and the unaffected limb (UL) of a unilateral elite amputee athlete, during treadmill running and track sprinting.

For this reason, a spring-mass model has been implemented to describe the running action during the stance phase.

Given the model, with its assumptions and simplifications, it is then possible to study and quantify additional considerations regarding the leg stiffness. Therefore, the research questions investigated through the present Thesis work are the following:

a) What is the difference on the K_{leg} between AL e UL?
b) What is the difference on the K_{leg} between Treadmill and Track?
c) Are there any changes on the K_{leg} considering different socket alignment? (A1, A2, A3)

Furthermore, it is possible to investigate the influence of the prosthetic foot, with its foot stiffness, and the residual limb on the overall leg stiffness.

It should be noted that different method for calculating the stiffness will likely produce different results. Therefore, these methods should be clearly defined, and caution should be exercised when making comparison beetween studies using different mehods.

CHAPTER 2: Simplified Model

In this chapter the spring-mass model implemented in this work is explained. The model has been named as '*Simplified Model*' because a model that accounts for all the components that influence motion would be very complicated and becomes impractical: so many assumptions and simplifications have been made.

The model used to calculate the Leg Stiffness is called *'Leg Stiffness Model'* to be distinguished from the model used to calculate the stiffness of the prosthetic foot. This second model is named *'Foot Stiffness Model'*.

1. Leg Stiffness Model

Preliminary assumptions

• The model is applied to the entire leg (it should be noted that the knee is always extended in stance in transfemoral amputees).

• It does NOT assume "sagittal symmetry": the symmetry of movement of the proximal point with respect to mid stance in the sagittal plane.

1.1 Leg Length

The *Leg Length* (***L***) is represented by the magnitude of the 3D vector from the proximal point (COM, HJC) to the centre of pressure (COP).

The vector is represented with the three components:

$$\vec{L} = \left[L_x\,, L_y\,,\, L_z\,\right]$$

where 'x' is the antero-posterior, 'y' the vertical and the 'z' is the medio-lateral component.

The magnitude is calculated as:

$$\left\|\vec{L}\right\| = \sqrt{L_x^2 + L_y^2 + L_z^2}$$

Besides, the versor (unit vector) identifies the 'leg direction':

$$\hat{L} = \frac{\vec{L}}{\left\|\vec{L}\right\|}$$

The following figure, gives a visual representation of the Leg Length considered in the model:

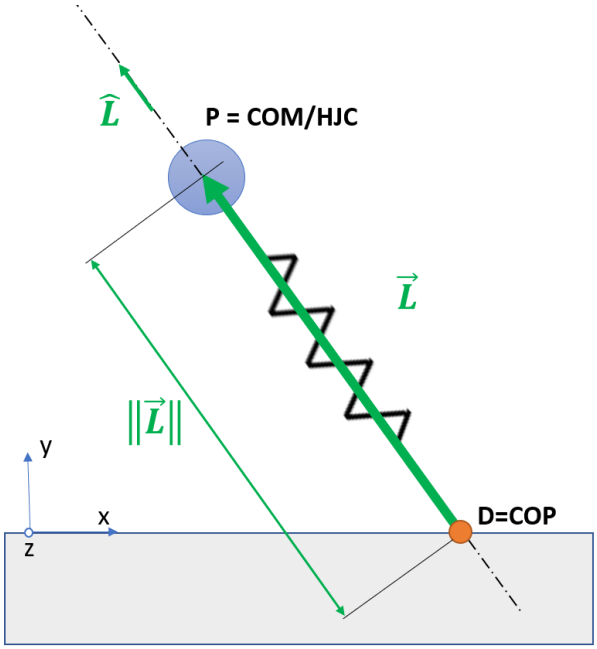

Figure 2.1: Leg Length between the proximal (P=COM/HJC) and distal point (D= COP).

- The *Reference Length* (**L0**) is defined as the Leg Length at the initial contact (Foot Strike), in each stance: this is consistent with Liew et al., 2017 [33].
- *Leg Shortening (*$\Delta \boldsymbol{L}$*)* is defined as the difference between the *Reference Length* (L0) and the *Leg Length* (L) in each frame during stance:

$$\Delta \boldsymbol{L} = \boldsymbol{L0} - \boldsymbol{L}(t)$$

The proximal point 'P' and the distal point 'D' must be defined: in particular, the choice of 'P' identifies the method of analysis of the leg stiffness:

- Method 1: P=COM
- Method 2: P=HJC

The proximal point P can be either 'COM' or 'HJC':

- *Centre Of Mass* (P=**COM**): looking at the full body.
  The COM is defined as the centroid of the markers placed on the anterior (RASIS, LASIS) and posterior (RPSIS, LPSIS) iliac spines. This is a conventional way to identify the COM, although this is not the real Centre Of Mass.

- Hip Joint Centre (P=**HJC**): looking at the lower limb.
  RHJC e LHJC, associated with pelvis, are calculated using Bell's method.

The distal point D is always the *Centre of Pressure* (D=**COP**).

The COP position with respect to the ground and to the foot's contact surface is a space-time variable quantity. For the type of running prosthetic feet on the market, the COP recedes after the first contact (anterior-posterior motion in the sagittal plane) due to the deformation of the foot and then it advances (posterior-anterior motion in the sagittal plane).

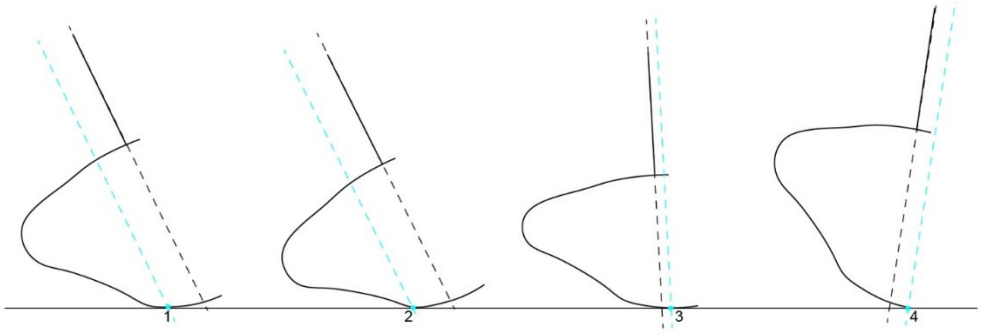

Figure 2.2: Qualitative position of COP in relation to the foot geometry:

1.Initial contact /2. Point of maximum retreat /3.Generic midpoint /4. Point of maximum advance.

Since it was not possible a direct measure of the Centre of Pressure, different approximations of the COP position are used for both the treadmill and track tests.

In treadmill trials the COP corresponds to the ground projection of the marker placed on the second metatarsal head for the healthy foot, while for the prosthetic foot it was assumed that the COP varies linearly from the midpoint of the FD2-FD3 markers and the tip of the foot FD1.

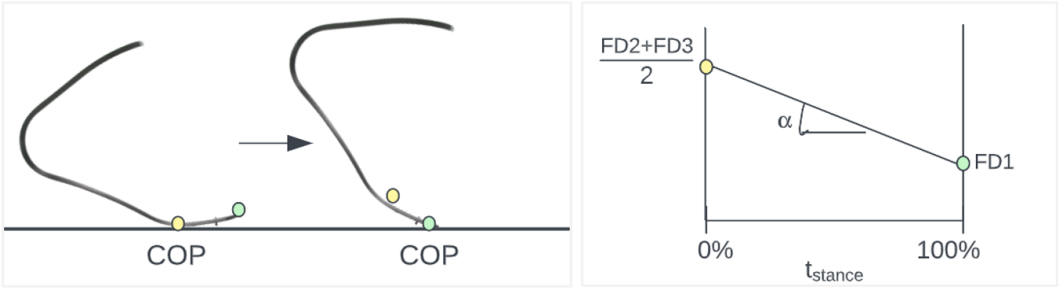

Figure 2.3: Schematic representation of COP displacement [14]

In track trials the identification of the coordinates of the COP come from the force and torque signals measured through the load cell.

Further details on how these input quantities have been implemented are explained in the 'Data Analysis' section of the Chapter 4.

1.2 Leg Orientation

The *Leg Orientation* (*Theta Leg-* Θ_L) is the angle between $\vec{L}$ and the vertical line, during stance.

Considering the vector:

$$\vec{L} = [L_x, L_y, L_z]$$

in the sagittal plane: $L_z = 0.$

The components are:

$$\begin{cases} L_x(t) = \|\vec{L}\| \sin(\Theta(t)) \\ L_y(t) = \|\vec{L}\| \cos(\Theta(t)) \end{cases}$$

The *Theta Leg* is calculated as:

$$\Theta_L(t) = \tan^{-1}\left(\frac{L_x(t)}{L_y(t)}\right)$$

In the figure below, the *Leg Orientation* is represented:

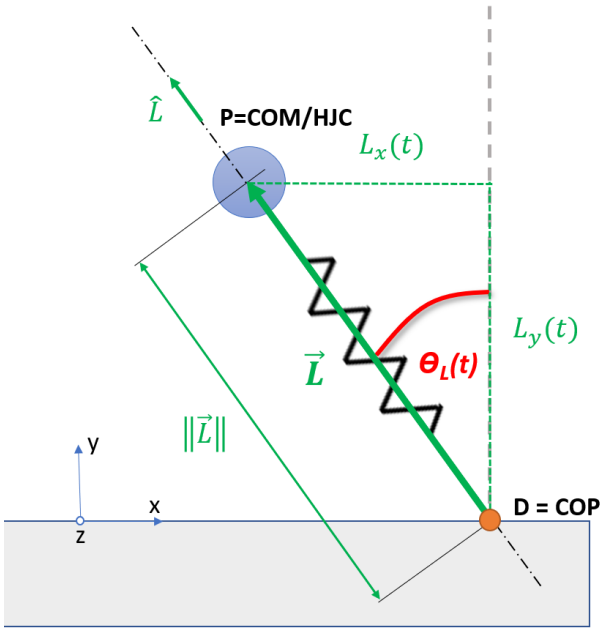

Figure 2.4: Leg Orientation (Theta Leg Θ_L*)*

1.3 Leg Stiffness

Before defining the Leg Stiffness, it is important to clarify what is the projected GRF on leg direction: $\overrightarrow{GRFp}$.

The versor (unit vector) identifies the 'leg direction':

$$\hat{\mathrm{L}} = \frac{\vec{\mathrm{L}}}{\|\vec{\mathrm{L}}\|}$$

The GRF vector is projected onto the respectively dimensioned leg vector by taking the dot product of the GRF vector by the unit vector of the leg.

Calculating the dot product between the Ground Reaction Force ($\overrightarrow{\mathrm{GRF}}$) and the versor, the magnitude of the projected GRF is obtained:

$$\left|\overrightarrow{\mathrm{GRFp}}\right| = \overrightarrow{\mathrm{GRF}} \bullet \hat{\mathrm{L}}$$

With a multiplication, the vector with all the 3D components is calculated:

$$\overrightarrow{\mathrm{GRFp}} = \left|\overrightarrow{\mathrm{GRFp}}\right| * \hat{\mathrm{L}}$$

The figure shows the projected GRF on the leg direction:

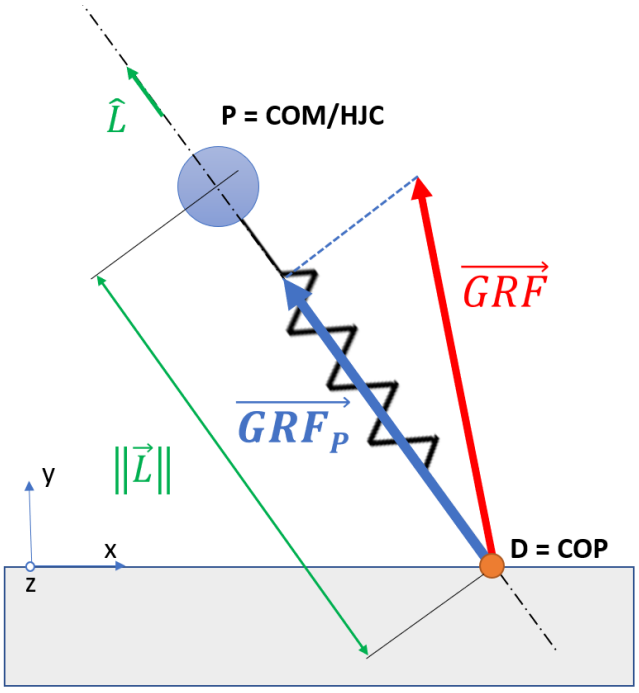

Figure 2.5: Projected GRF on the leg direction

In this model the *Leg Stiffness* is calculated by taking the ratio between the peak magnitude of the projected Ground Reaction Force ($|\overrightarrow{GRF_p}|_{max}$) and the resultant *Leg Shortening* $\Delta L(|\overrightarrow{GRF_p}|_{max})$.

The resultant *Leg Shortening* is calculated considering the *Reference Length* (L0) minus the Leg Length at the instant in which the $|\overrightarrow{GRF_p}|$ is maximum.

The following formula and graph illustrate the definition of the *Leg Stiffness*, that has been implemented with this model:

$$K_{leg} = \frac{|\overrightarrow{GRF_p}|_{max}}{\Delta L\left(|\overrightarrow{GRF_p}|_{max}\right)}$$

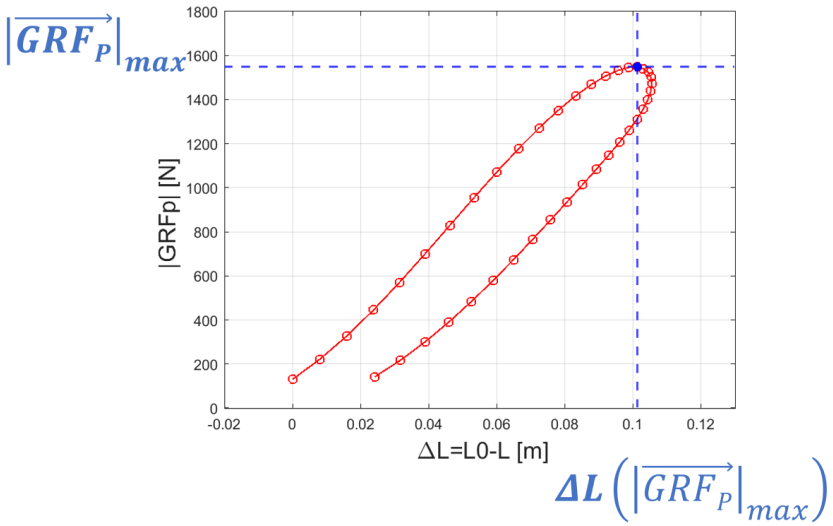

Figure 2.6: Leg Stiffness is calculated by taking the ratio between the peak magnitude of the projected Ground Reaction Force and the resultant Leg Shortening.

As it was written before, the choice of 'P' identifies the method of analysis of the leg stiffness:

- Method 1: P=COM
- Method 2: P=HJC

A summary of the two methods implemented with the terminology and quantities are shown in the next pages. The nomenclature for the events considered is the following:
FS=Foot Strike | MS=Mid Stance | FO=Foot Off

Definition of Mid Stance (MS): the MS is defined as the instant in which the vertical projection of the HJC (Hip Joint Centre) on the ground, overlaps the COP. In other words, it was found the instance in which HJC and COP have the same value on anterior-posterior axis.

Method 1: P=COM

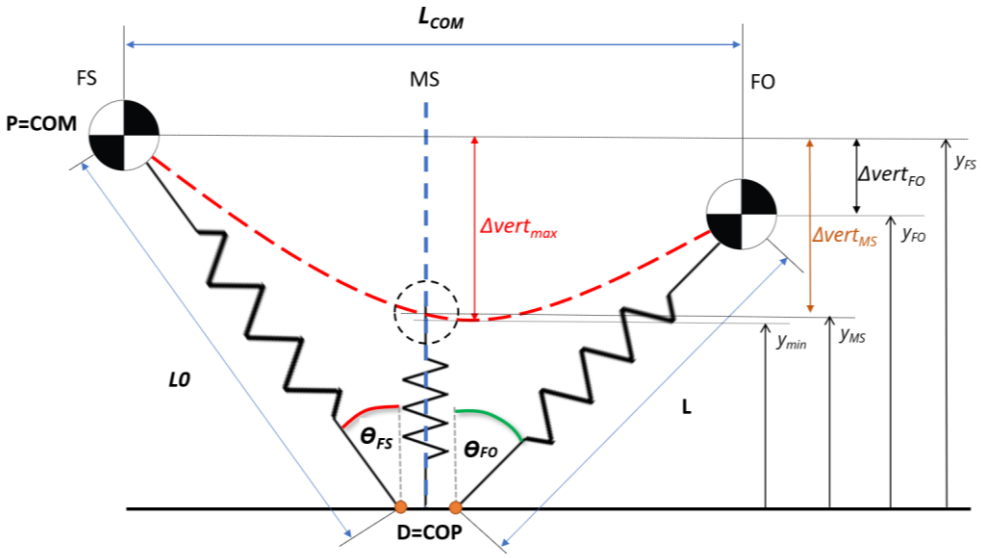

TERMINOLOGY: all the quantities presented in the model are listed below.

- Proximal point: **P=COM**

- Distal point: **D=COP**

- *Leg Length* (***L***) defined as the module of the vector: $\vec{L} = (\overrightarrow{COM - COP})$.

- *Reference Length* (***L0***): defined at Foot Strike (FS).

- *Leg Shortening*: $\Delta \boldsymbol{L} = L0 - L(t)$

- *Leg Orientation* (*Theta Leg*- $\boldsymbol{\theta_L}$): at Foot Strike (Θ_{FS}) and at Foot Off (Θ_{FO}).

- COM trajectory during stance.

- y_{FS} = absolute "initial" altitude of COM (at Foot Strike - FS).

- y_{FO} = absolute "final" altitude of COM (at Foot Off - FO).

- y_{MS} = altitude at Mid Stance (MS) of COM.

- y_{min} = minimum altitude of COM, during stance.

- $\Delta vert_{MS}$ = vertical lowering of COM between Foot Strike and Mid Stance.

- $\Delta vert_{max}$= maximum vertical lowering of COM during stance, compared to Foot Strike.

- $\Delta vert_{FO}$ = vertical lowering of COM between Foot Strike and Foot Off.

- L_{COM} = forward trajectory length of COM, during stance.

Method 2: P=HJC

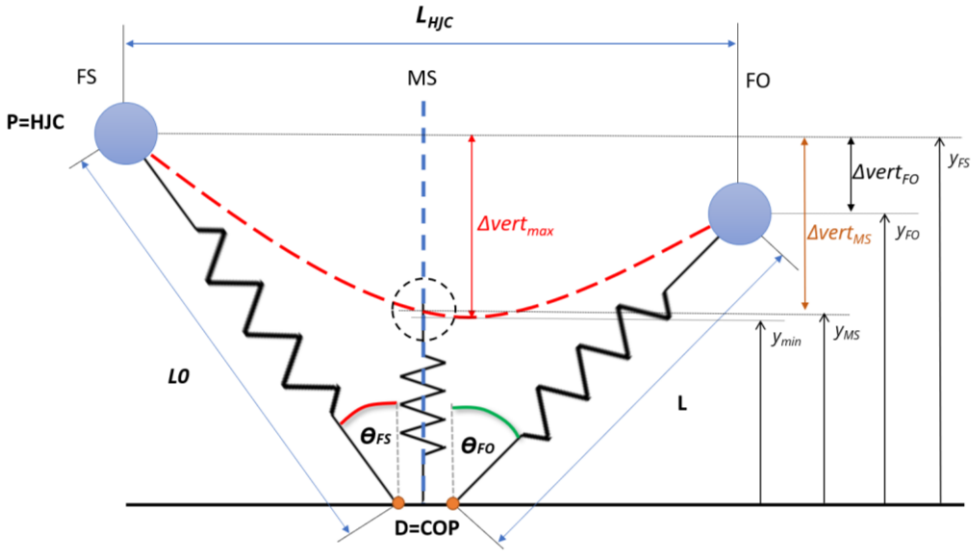

A similar terminology to the *'Method 1'* is used for this method. The quantities are:

- Proximal point: **P=HJC**

- Distal point: **D=COP**

- *Leg Length* (***L***) defined as the module of the vector: $\vec{L} = (\overrightarrow{HJC - COP})$.

- *Reference Length* (***L0***): defined at Foot Strike.

- *Leg Shortening*: $\Delta L = L0 - L(t)$

- *Leg Orientation* (*Theta Leg*- $\boldsymbol{\theta_L}$): at Foot Strike (Θ_{FS}) and at Foot Off (Θ_{FO}).

- HJC trajectory during stance.

- y_{FS} = absolute "initial" altitude of HJC (at Foot Strike - FS).

- y_{FO} = absolute "final" altitude of HJC (at Foot Off - FO).

- y_{MS} = altitude at Mid Stance (MS) of HJC.

- y_{min} = minimum altitude of HJC, during stance

- $\Delta vert_{MS}$ = vertical lowering of HJC between Foot Strike and Midstance

- $\Delta vert_{max}$= maximum vertical lowering of HJC during stance, compared to Foot Strike

- $\Delta vert_{FO}$ = vertical lowering of HJC between Foot Strike and Foot Off.

- L_{HJC} = forward trajectory length of HJC, during stance.

2. Foot Stiffness Model

This model focuses on the RPF with the aim to investigate the effect of the prosthesis on the total leg stiffness of the affected limb.

Preliminary assumptions

• The model is applied to the prosthetic foot.

• It does NOT assume "sagittal symmetry": the symmetry of movement with respect to mid stance in the sagittal plane.

2.1 Foot Length

The *Foot Length* (***d***) is represented by the magnitude of the 3D vector from the proximal point (CL=Clamp) to the centre of pressure (COP).

The vector is represented with the three components:

$$\vec{d} = [d_x\,, d_y\,,\, d_z\,]$$

where 'x' is the antero-posterior, 'y' the vertical and the 'z' is the medio-lateral component.

The magnitude is calculated as:

$$\boldsymbol{d} = \|\vec{d}\| = \sqrt{d_x^2 + d_y^2 + d_z^2}$$

Besides, the versor (unit vector) identifies the 'foot direction' (Clamp-COP):

$$\hat{d} = \frac{\vec{d}}{\|\vec{d}\|}$$

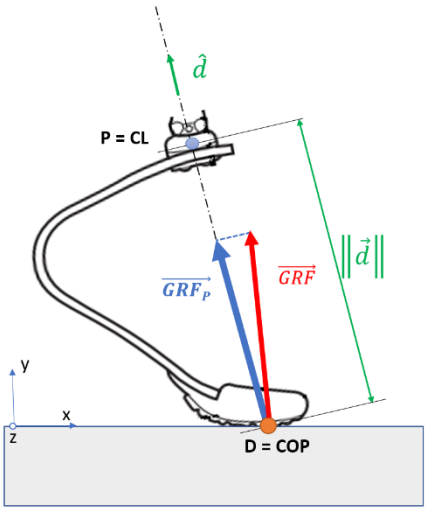

Figure 2.7: schematic representation of the RPF: the foot length ($\boldsymbol{d}=\|\vec{d}\|$) and the versor ($\hat{d}$) in green.

- The *Reference Foot Length* ($\boldsymbol{d_0}$) is defined as the Foot Length at the initial contact (Foot Strike), in each stance.
- *Foot Shortening* ($\Delta\boldsymbol{d}$) is defined as the difference between the *Reference Foot Length* ($\boldsymbol{d_0}$) and the *Foot Length* ($\mathbf{d}$) in each frame during stance:

$$\Delta \boldsymbol{d} = \boldsymbol{d}_0 - \boldsymbol{d}(t)$$

The distal point D is always the *Centre of Pressure* (D=**COP**) that is the same defined before in the 'Leg Stiffness model', either in treadmill or track tests.

The proximal point P is the centre of the clamp of the prosthetic foot (P=CL): this point is calculated considering the centroid of the four markers FP1, FP2, FP3 and FP4, as it is shown in the figure:

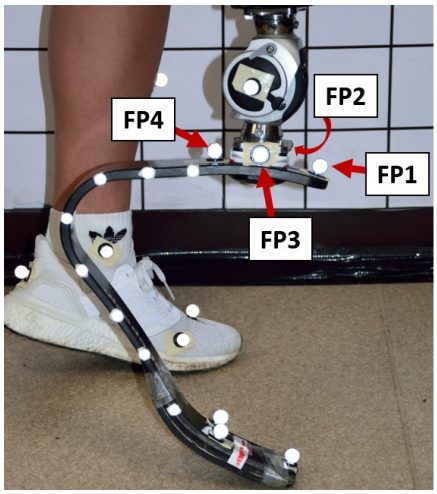

Figure 2.8: FP1, FP2, FP3 and FP4 identifies the proximal point considered (P=CL).

2.2 Foot Orientation

The *Foot Orientation* (*Theta* - Θ) is the angle between $\vec{d}$ and the vertical line, during stance.

The *Theta* angle is calculated as:

$$\Theta(t) = \tan^{-1}\left(\frac{d_x(t)}{d_y(t)}\right)$$

2.3 Foot Stiffness

The foot direction (Clamp-COP) is identified with the versor ($\hat{d}$):

$$\hat{d} = \frac{\vec{d}}{\|\vec{d}\|}$$

The magnitude of the projected GRF on this direction is calculated with the dot product between the Ground Reaction Force ($\overrightarrow{GRF}$) and the versor ($\hat{d}$):

$$\left|\overrightarrow{GRFp}\right| = \overrightarrow{GRF} \bullet \hat{d}$$

With a multiplication it is then possible to calculate the vector with all the 3D components:

$$\overrightarrow{GRFp} = \left|\overrightarrow{GRFp}\right| * \hat{d}$$

The figure below shows the projected GRF ($\overrightarrow{GRFp}$) on the direction CL - COP:

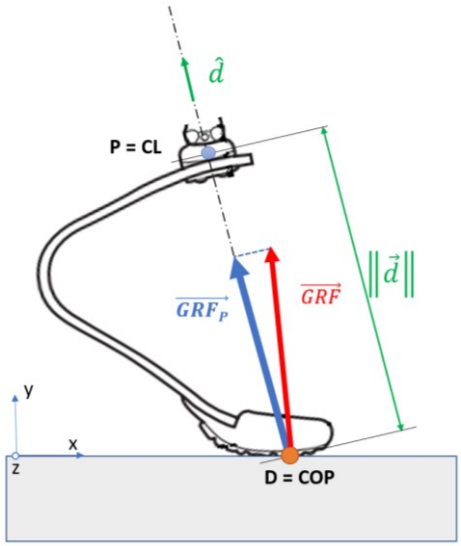

Figure 2.9: schematic representation of the RPF with GRF in red, projected GRF ($\overrightarrow{GRF_p}$) in blue and the foot length (***d***=$\|\vec{d}\|$) in green.

The *Foot Stiffness* is calculated by taking the ratio between the peak magnitude of the projected Ground Reaction Force ($\left|\overrightarrow{GRF_p}\right|_{max}$) and the *Foot Shortening* $\Delta d(\left|\overrightarrow{GRF_p}\right|_{max})$ at the instant in which the $|\overrightarrow{GRF_p}|$ is maximum.

The following formula illustrates the definition of the *Foot Stiffness*, that has been implemented with this model:

$$K_{foot} = \frac{\left|\overrightarrow{GRF_p}\right|_{max}}{\Delta d\left(\left|\overrightarrow{GRF_p}\right|_{max}\right)}$$

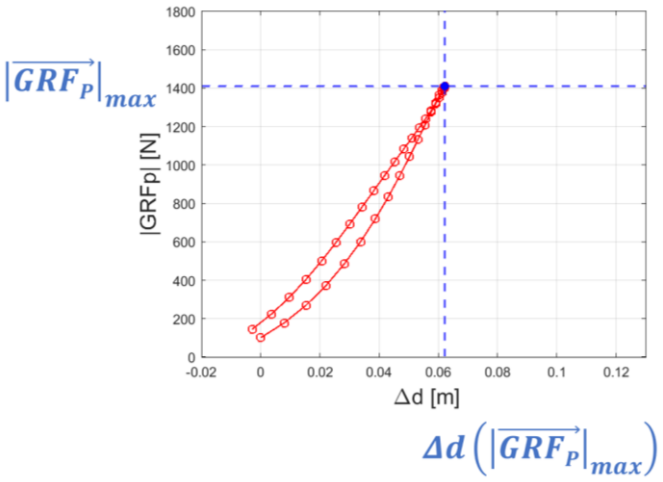

Figure 2.10: Foot Stiffness is calculated by taking the ratio between the peak magnitude of the projected Ground Reaction Force and the resultant Foot Shortening.

3. Residual leg stiffness

Finally, a further analysis can be made while looking at the effect of the RPF stiffness on the overall leg stiffness of the affected limb: the contribution of the residual leg.

The overall leg stiffness is modelled as two in-series massless linear springs: the RPF is attached in series to the residual limb.

$$\frac{1}{K_{leg}} = \frac{1}{K_{Foot}} + \frac{1}{K_{stump}}$$

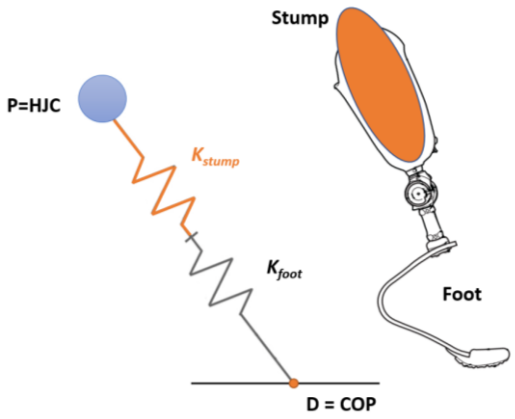

Figure 2.11: Spring-mass model of running with an in-series leg spring.

The contribution of the residual limb is defined as '*stump stiffness*' (K_{stump}) and it can be calculated with the following equation:

$$K_{stump} = \frac{K_{leg} * K_{foot}}{K_{Foot} - K_{leg}}$$

CHAPTER 3: Materials and Methods

The description of the in-vivo test performed in treadmill and track session are described in this chapter, considering the instrumentation and the methods adopted.

1. TREADMILL session

The treadmill session named as “Olimpia Session 2” took place at the Sports Engineering Laboratory in the Industrial Engineering Department of the University of Padua.

1.1. **Participant**

Ambra Sabatini (AS), 100 m gold medallist in Tokyo Paralympic Games 2020 for category T63 participated in the experiment. The athlete used the Running Prosthetic Foot (RPF) Ottobock 1E91 standard, category 3.5 and a monoaxial prosthetic knee Ottobock 3S80.

Figure 3.1:Prosthetic Knee Ottobock 3S80 and the Ottobock RPF1E91- cat 3.5

1.2. **Materials**

The instrumentation adopted during the tests consisted in:

a. Technogym Skillrun treadmill;
b. Eight BTS Smart Capture-DX 6000 cameras for motion capture;
c. Four BTS P 6000 force platforms;

In addition, high-speed cameras and smartphones were used to record videos while the athlete was running on the treadmill, from frontal and sagittal view, to also have a video support during the motion capture’s data analysis.

a. Treadmill

The treadmill used during the test is a commercial treadmill *Technogym Skillrun*: it can operate at a maximum speed of 30 km/h or at controlled resistance; it is also capable of vary its inclination: either positive and negative position.

Figure 3.2: Tecnogym Skillrun Treadmill [Technogym.com]

To adapt the treadmill to the tests, the screen, its supports frame, and the handrail were removed. This was done to reduce noise deriving from the vibration of the devices and to avoid obstructing the view on the athlete's leg. Indeed, the treadmill speed was regulated by another person, not the runner. Therefore, a custom-made frame was placed around the treadmill to support the athlete and ensure her safety.

BTS acquisition system

The BTS acquisition system of the Sport Engineering laboratory consists of a workstation that controls the BTS motion capture cameras and the BTS force platforms.

b. BTS Motion Capture Cameras

The *BTS Smart Capture – DX 6000* is a system of digital cameras used for motion analysis, typically for medical purpose: the system has a maximum acquisition frequency of 340 Hz.

For these tests, 8 cameras with a frequency of 250 Hz had been chosen and were positioned around the laboratory where the treadmill and the target volume were identified. Each camera emits infrared light, which is reflected off the markers applied on the athlete's body. Thanks to an internal algorithm, with a specific process called '*triangulation*', the cameras allow the determination of the three-dimensional location of the marker in the space. The markers were placed in specific positions on the body and on the prosthesis, according to a previously established protocol.

Figure 3.3: BTS Smart DX Camera

Defining a reference system is a crucial aspect before starting the data acquisition with a motion capture system. During the procedure called '*static calibration'*, the reference system can be defined using a special triad made of three orthogonal wands representing the three axes of the absolute reference system.

Moreover, a second smaller L-frame is placed on one force platform at a time to locate the force platforms in the capture space.

Figure 3.4: Triads on the treadmill representing the absolute reference frame and the smaller L-frame to locate the force platform.

c. BTS Force platforms

Force platforms are typically used in gait analysis to measure the Ground Reaction Forces, moments and the centre of pressure. With a motion capture system, the combination of kinematic and kinetic data is possible thanks to the interaction of the force platforms with the motion capture system.

The force platform *BTS P-6000* is a multicomponent force plate that works as a six-axis load cell: it has eight output signals that can be converted into six load components, such as forces Fx, Fy, Fz and moments Mx, My, Mz. Its maximum acquisition frequency is 1000 Hz, and the vertical load capacity is 3500 N.

The treadmill was placed over the four force platforms, that were positioned to have their centre aligned with one foot of the treadmill, which were used simultaneously: the load components were summed to obtain the resultant ground reaction force.

Figure 3.5: Force platform BTS P-6000

The final experimental set up, is shown in the figure below:

Figure 3.6: Set up for the treadmill session.

Agreement between the results of Breban et al., [34] and literature confirms that the proposed setup gives sufficient confidence in the evaluation of the sprint technique. In fact, the work showed that GRFs measured using a treadmill placed on four external force platforms can provide horizontal and vertical kinetic quantities useful to evaluate athlete's performance.

1.3. **Methods**

The athlete had to test four different socket alignments: A0, A1, A2, A3. The different socket tilts used in the test are shown in the following table:

Alignment	Socket tilt [°]
A0	5°
A1	9°
A2	12°
A3	15°

The test condition performed during this session and studied in the present work, in which the treadmill operates in controlled speed mode, is named **"*Steady State Running (SSR)*"**.

Figure 3.7: Steady State Running on treadmill.

In an *SSR*, first, the athlete hangs on the handrails of the external frame while the treadmill reaches a speed of 10 km/h. The athlete jumps on the belt and starts running. Then, the speed of the treadmill is led to a maximum value of 18 km/h and the athlete has to continue running at this constant speed for at least 7 seconds.

Test preparation

Once all the hardware is ready to be used with BTS cameras and force platforms connected to the workstation, these are the following steps:

- The treadmill is placed over the four force platforms with each of its supports in the centre of one force platform.
- The BTS cameras are distributed all around the treadmill: they must be in a fixed position. The capture volume should be clear from people, markers or reflective objects or surfaces creating phantom markers. Then the calibration of the system can be performed: it is required to establish a 3D reference system for the cameras, that is to determine the X, Y and Z axes along which the three dimensions of the markers position is measured.
- Opening the SMART Analyzer software on the BTS workstation is possible to check what the cameras are looking at: the focus and lens' aperture have to be adjusted in order to clearly see each marker inside the acquisition volume. At this point, the windows of the laboratory are covered with black panels, to minimize possible reflection.
- The *calibration* procedure is characterized by three steps. As first step, the wand has to be moved all around the calibration volume, in particular in the treadmill area. The second step consists in the placement on the treadmill of the reference triad with reflecting markers: this points it's the origin of the three-dimensional volume. The third step is represented by positioning on the corners of each platforms the small L-frame with reflecting markers, once at a time.
- The calibration file of the instrumentation (cameras and platforms) is loaded using the *BTS SMART Clinic* software: further, this software is used to monitor and check what the cameras are looking at and what load is measured by the platforms. It is needed also for the creation of a new session of data collection considering the different trials, that must have different names.
- If everything is working, the systems are ready for the data acquisition.

Subject preparation

Before the athlete gets on the treadmill to run, she has to wear the socket, that was previously prepared by an orthopaedic technician in terms of alignment angle. Then, a climbing harness has to be worn for safety reason, securing the athlete to the ceiling in case of fall. In the end, in accordance with the previous established protocol, the markers are attached to the body: the full

marker set is composed of 56 markers, placed on specific anatomical landmarks and on the prosthesis.

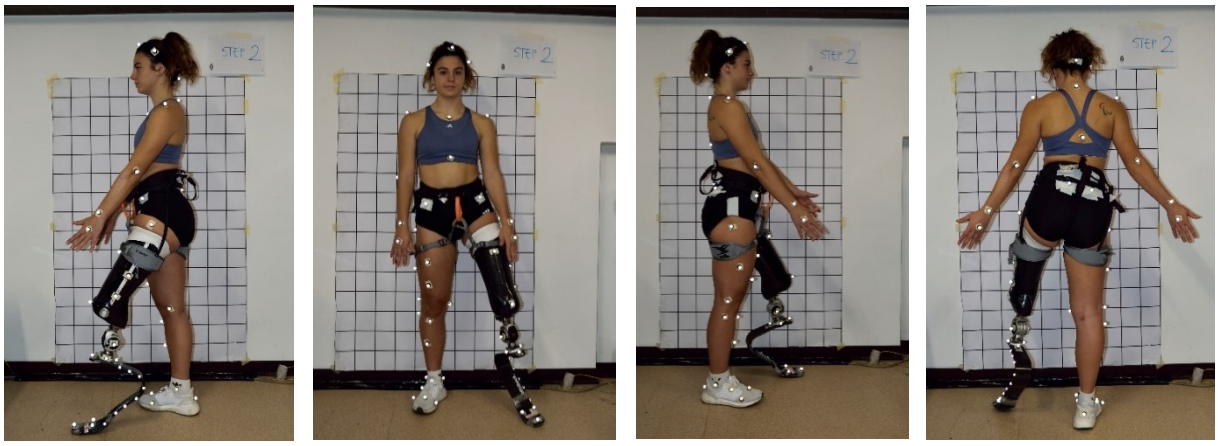

Figure 3.8: Full marker set of treadmill session.

Test procedure and data collection

Before starting the test, all devices have to be switched on and ready to acquire: on the BTS workstation new Patient and test are inserted and a new folder is created where all the data during the test would be saved.

For each different socket, the procedure followed is:

- **Static trial**

During the static trial, the athlete has to remain on the treadmill in a standing still position for few seconds, within the volume previously calibrated. The data acquisition is started, stopped, and saved using the *BTS Smart Capture* software.

Afterwards, the procedure called "*Static Calibration*" is performed. It consists in other acquisitions with the athlete in the same standing position, while another person points at some anatomical landmarks or at specific points on the prosthesis with a specific wand, that has two markers in known position with respect to its tip. With a geometrical reconstruction, this procedure allows to locate the position of some points, would not be clearly visible otherwise or which are too small to be correctly located with a marker. Each of these points requires a separate acquisition.

At the end, markers not needed for the dynamic acquisitions are removed.

- **Dynamic trial:**

Before the acquisition, the athlete has to suspend on the handrails for few seconds in order to start the acquisition with a zero loading condition of the recorded signal.

During the Steady State Running, the treadmill is switched on and accelerated while the athlete is standing on the external borders or hanging on the handrails. After that, she jumps on the belt and starts running with treadmill increasing the speed until reaching 18 km/h, maintaining this speed for 7 seconds. Then she suspends again on the handrails and the data acquisition is stopped from the BTS workstation.

The athlete performed a total of 35 tests, including both static and dynamic: in the following table, a synthesis of the trials performed is shown. The trials relative to the static calibration with the wand, repeated trials or not valid trials are omitted. 'Test number' refers to the progressive number given by the BTS acquisition software.

Subject	Test number	Test Type	Socket Alignment
AS	02	STATIC	A2
AS	13	SSR	A2
AS	19	STATIC	A1
AS	22	SSR	A1
AS	27	STATIC	A3
AS	28	SSR	A3
AS	33	STATIC	A0
AS	35	SSR	A0

2. TRACK session

The track session named as “Olimpia Session 3” took place at the Palaindoor of Padua, that is an indoor arena with a 200m track with six lanes and 60m straight runway with eight lanes and others multiple platforms for many athletics disciplines.

Figure 3.9: Palaindoor setup.

2.1. Participant

As for the previous session at the Sports Laboratory, Ambra Sabatini (AS) participated in the experiment. She used the same Running Prosthetic Foot (RPF) Ottobock 1E91 standard, category 3.5 and a monoaxial prosthetic knee Ottobock 3S80: to ensure a better grip with the Tartan surface of the track, the RPF had a spiked sole.

2.2. Materials

The instrumentation adopted during the tests consisted in:

a. 28 *Vicon* cameras for marker-based motion capture
   (25 *Vicon Vero* v2,2, 2 *Vicon Vantage* v16, 1 *Vicon Vantage* v5);
b. *DTS Slice Nano* acquisition system;
c. 6-axis load cell *SRI M3564F1*;
d. Triaxial accelerometer + triaxial gyrometer *DTS 6DX PRO-A;*

In addiction 2 high-speed cameras for sagittal and frontal recording and smartphone for slow-motion videos and for recording complete trials were used.

a. Vicon Motion Capture cameras

Vicon cameras were used for marker-based motion capture: 6 out of 28 Vicon cameras were placed on a framework in the middle of the track, while the remaining cameras were placed on tripods, placed along the 8th lane of the 60m straight runway.

Figure 3.10: Motion Capture Cameras. Vicon Vantage (left) and Vicon Vero (right).

b. DTS Acquisition systema

SLICE NANO is an ultra-small acquisition system provided by the company *'Diversified Technical Systems, Inc'*. It has a modular design, called SLICE 'Stack', with consist of one BASE+ SLICE, one BATTERY SLICE and up to eight additional sensor input modules (BRIDGE SLICE) having three input channels each. During the tests, four Bridge modules were employed: two were connected to the six-axis load cell and the remaining two were connected to the 6DX PRO-A, which is a triaxial accelerometer + triaxial angular rate sensor. The BASE+ SLICE contains a microprocessor, 16 GB flash data memory, USB cable to connect it to PC, power conditioning and control signals. BATTERY SCLICE is only a backup battery in case main power is lost.

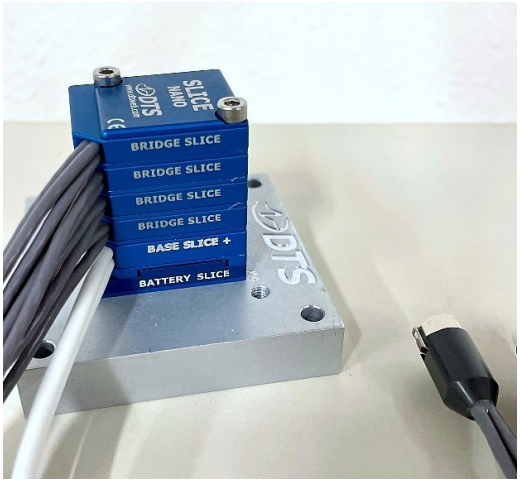

Figure 3.11: Acquisition System DTS

The system is provided with an End Of Chain (EOC) terminal, which enables attaching the battery, sending a trigger signal or monitoring the status of the SLICE system. A push button panel was designed and produced, in order to make the system easier to use. It has three buttons: one is to switch on and switch off the system, another is for the start and stop the record input and the last one for the events input signal. A led shows the status of the system.

Figure 3.12: SLICE NANO Base Cable Kit on the left: it includes the End-of-Chain (OEC) terminal, start-event switch, USB communication cable and power supply. The custom case on the right.

To manage and monitor the process of data collection using the DTS acquisition system, it is necessary to use the *DTS SLICEWare software*. With this software it is possible the definition of the test set up and the management of the sensor database, allowing real time sensor check-out, the execution of the tests and the export of the data acquired.

During this session, the data acquisition system DTS Slice NANO, the battery, the button panel and the power-bank were placed inside a trail-running backpack that the athlete was wearing during the test.

c. Load cell

The load cell (model M3564F1, produced by the SRI sensors company) is a circular (d=65 mm), light (190 g), extra-thin (10 mm), six-axis load cell: it has six coupled output channels, which can be decoupled thanks to calibration matrices to obtain three components of force, Fx, Fy and Fz and three components of moment, Mx, My and Mz.

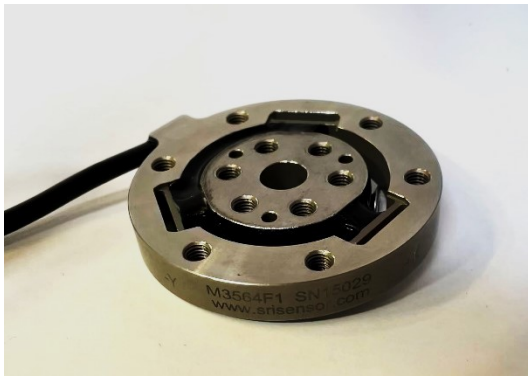

Figure 3.13: 6 -Axis Load Cell

The maximum measurable value along X and Y directions is 2500 N, while along Z direction the maximum is doubled. Regarding Mx and My, the maximum value is 2500 Nm, while for Mz it is 100 Nm.

d. Inertial sensor

6DX PRO-A is small, high-shock tolerant six degrees of freedom sensor package, which includes three angular rate sensors plus three accelerometers. It is a very versatile sensor, since it has large bandwidth options available and multiple sensor ranges. The triaxial accelerometer can measure linear accelerations in the range ± 500g along the three axes, while the triaxial angular rate sensor works in the range ±8000 deg/s.

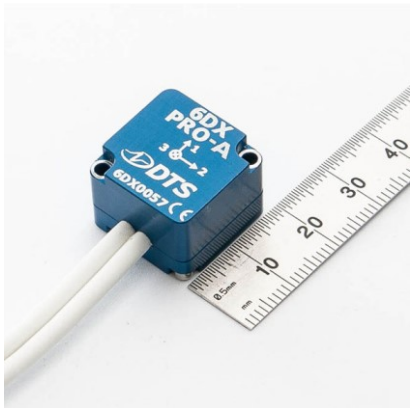

Figure 3.14: 6DX PRO-A inertial sensor.

The load cell was fixed between the prosthetic knee and the clamp, while the inertial sensor was placed on the inner surface of the proximal portion of the prosthetic foot.

Figure 3.15: Load cell and sensor set up.

These wearable sensors allow continuous measurement of the running gesture and can be used in whatever environment, including the outdoor athletics track: the 6 – axis load cell permits to measure the forces applied to the clamp, which represents in turn the effect of the Ground Reaction Forces transferred to the RPF, while the inertial sensor gives information about the linear acceleration and angular velocity of the foot.

This innovative solution is a consequence of a previous work (Petrone et al., [35]), where an instrumented Running Prosthetic Foot (iRPF) was developed at the University of Padua. This is a system of strain gauge bridges attached to the prosthetic foot which measuring forces acting on the foot clamp on multiple steps without modifying the RSP behaviour.

2.3. Methods

The test was performed by the athlete AS, wearing the same socket alignment A3.

Alignment	Socket tilt
A3	15°

The test condition performed during this session which was considered in the present work, is named **"*Steady State Running on Track (TSSR)*"**.

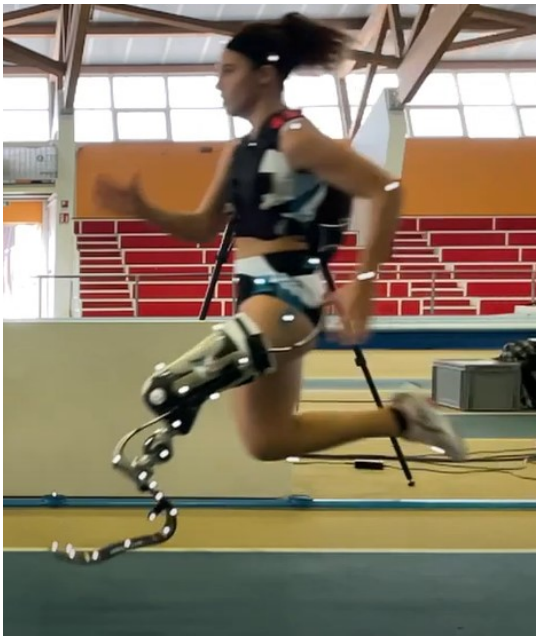

Figure 3.16:Steady State Running on Track.

In a TSSR, the athlete starts from standstill and has to reach a constant speed, equivalent to the 60% of the personal maximum speed (AS reached nearly 15 km/h), in about 15 meters and maintain that speed for about 20 meters, that was the part of the straight runway included in the acquisition volume.

Test preparation

Vicon Motion Capture cameras are mounted on temporary tripods which needed to be placed alongside the 8th lane of the straight runway and each camera is connected to the Vicon workstation through Ethernet cables.

Once all the cameras are mounted, before starting the acquisition, other steps follow. These steps can be monitored with the Vicon Nexus software 2.13:

- Adjust the position and tilt of each camera to have the intended framing: the regulation is made camera by camera, using the corresponding screw and moving it to one side or the opposite. During this operation, some markers were placed in the acquisition volume, and it was checked the quality of the operation watching at the Vicon Nexus software, in the central View pane. The camera is optimized when, while zooming on a marker, a thigh circular image is shown, with a cross exactly in the centroid of the marker blob, the centre of the blob is bright white and towards the edges there is a gradient of grayscale.
- The acquisition frequency of 300 Hz is set from the Nexus 2.13 software, in the Resource pane.

The calibration is performed, after removing all markers and any source of unwanted reflection from the acquisition volume: the procedure is managed from the Nexus software and needs the use of an 'Active Wand' as the instrument to perform the 'Full Calibration' type. The acquisition ends when every camera has collected enough data to be calibrated successfully.

Then also the origin of the acquisition volume must be set, either with three markers placed on the ground or with a calibration device, in this case an Active Wand. The position of the floor plane must be adjusted using some markers placed along the volume, to correctly align the coordinate system with the floor.

Subject preparation

The athlete AS, after a standard warm up, has to wear the instrumented prosthesis that was made specifically for this test. The 6-axis load cell is placed between the pyramidal attack below the knee and the clamp of the foot: the cables are strapped laterally to the socket to not be dangerous for the athlete's movements.

Sensors are connected to the DTS, that is placed inside a running backpack that is worn by the athlete. Inside the backpack there are also the battery, the button panel and the power bank needed to power the load cell.

The last preparation step consists in attaching the markers on the athlete's body and prosthesis according to the previously chosen protocol for the current session.

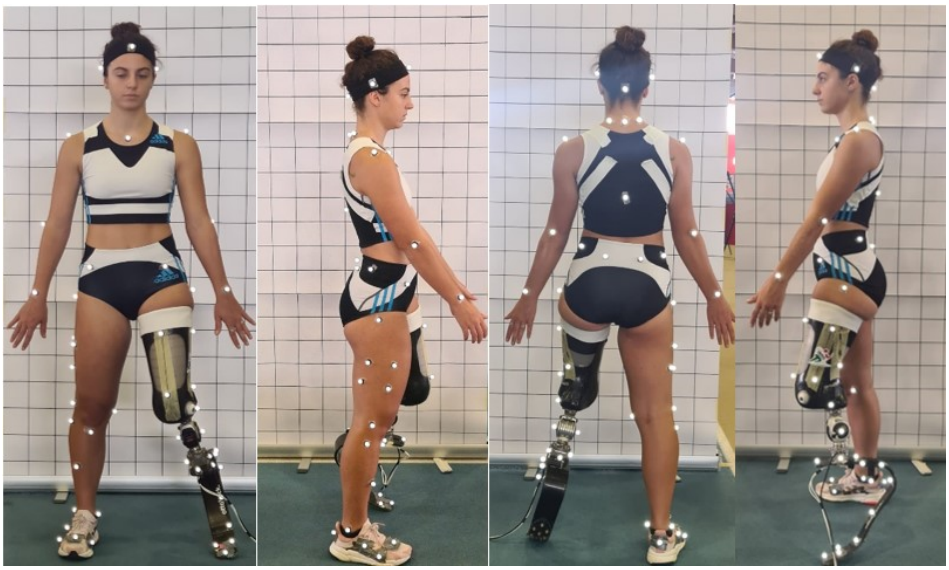

Figure 3.17: Full marker set of tracks session.

Test procedure and data collection

- **Static trial**

The athlete has to stay standstill in the middle point of the acquisition volume while an operator makes the acquisition using the *Nexus* software in 'Live' mode. Markers that were not placed directly on the body have been calibrated with a wand.

Once all the markers required for the static model have been captured, the markers not required for the dynamic trials are removed.

- **Dynamic trial**

Once the athlete is at the start of the lane, ready for the run, the following sequence of steps must be iterated:

- Start the acquisition from the software Nexus.
- Turn on the acquisition system (DTS), located in the backpack, and put it into acquisition mode with the START button.
- To have distinctive peaks in the sensors signal, the athlete lifts the prosthetic leg for three seconds and then performs three kicks on the ground and starts running.

During TSSR tests, the subject accelerates for about 15 meters and then maintains a constant speed while running across the acquisition volume. After the run, when the athlete is out of the volume, she can decelerate and the acquisition on Nexus is stopped. The athlete then executes

the same operation performed before starting, that is three seconds with the prosthetic leg lifted and three kicks on the ground. After that, the acquisition of the DTS system can be stopped.

During this track session, the athlete AS performed 18 tests, that are listed in the table below, with the test number representing the progressive number given by the Vicon system:

Subject	Test Number	Test Type
AS	2	STATIC
AS	8	TSSR 01
AS	11	TSSR 03
AS	13	TSSR 04

In the next Chapter the analysis of the data collected in these experimental sessions, will be illustrated.

CHAPTER 4: Data Analysis

The data collected during the in-vivo tests were processed to obtain meaningful quantities describing the running gesture. In her master's Thesis Barbacane [14] has contributed to the development of a software for the biomechanical analysis, which calculates the kinematic and kinetic parameters starting from raw data.

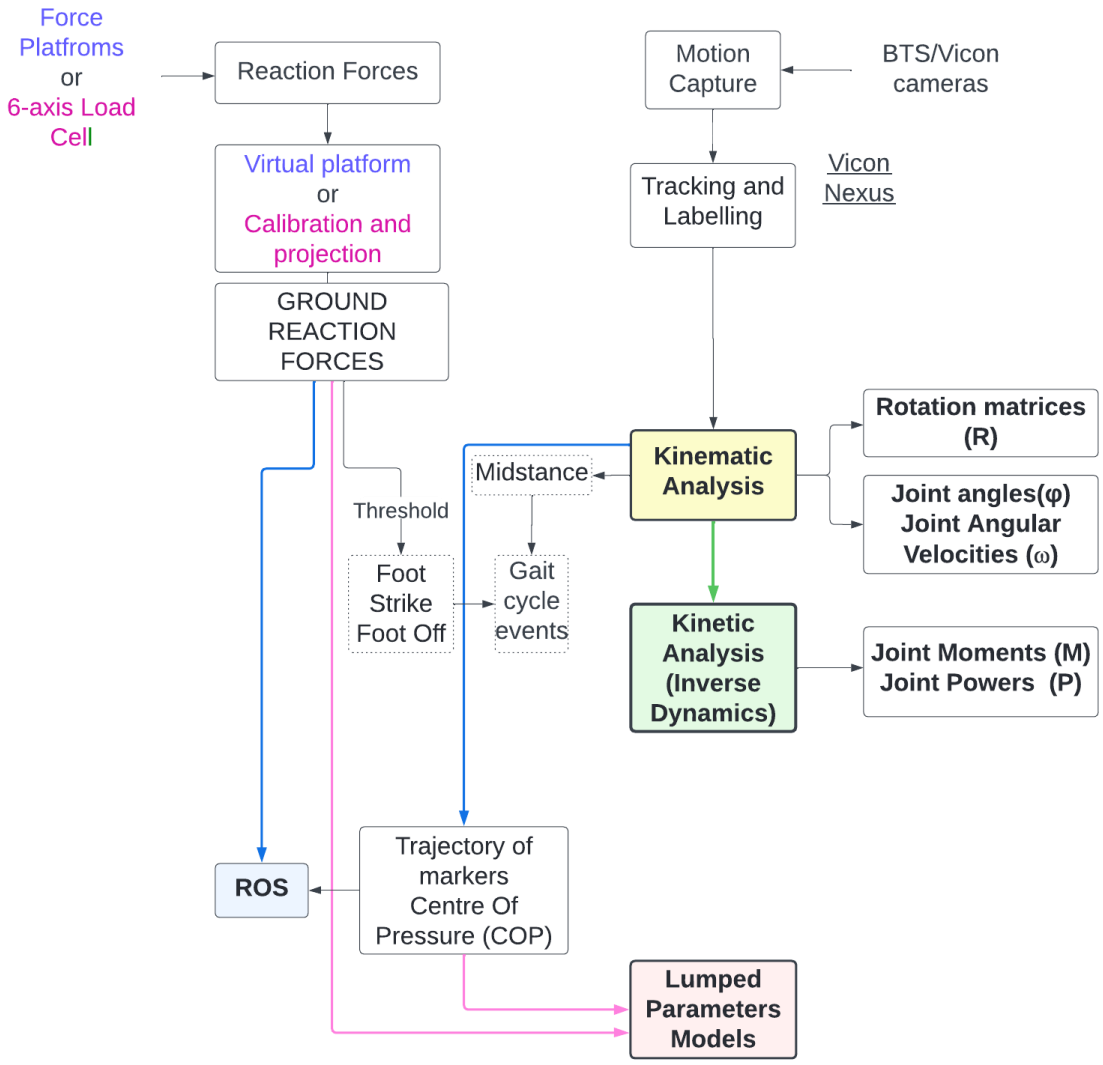

Figure 4.1: Flowchart of the Biomechanical Analysis Software Olimpia 1.0 [14]

In summary, the main two input sources are data from Motion Capture cameras and the data from the force platforms or from the wearable load cell.

Data acquired with Motion Capture needed some pre-processing prior to be used for the kinematic and kinetic analysis: the 'Labelling and Tracking' operations were done using the *Vicon Nexus Software* to reconstruct all the markers trajectories.

Data from the force platforms were processed to obtain a single resultant Ground Reaction Force vector and data from the load cell must be converted into the desired force components through a calibration matrix.

The kinematic analysis gives in output the matrices describing the orientation of each body segment in the three-dimensional space, the joint angles and the joint angular velocities. All these data, together with the filtered and segmented GRF and the running cycle events are the inputs for the kinetic analysis, which calculates joint moments and powers [14].

A MATLAB structure was created to save all the variables obtained from the biomechanical analysis. In particular the running cycle events and the resultant GRF vector were used to the analysis of the leg stiffness, which is the foremost aim of this thesis.

Lumped Parameters Models

This section addresses the implementation of the first model of the "Lumped Parameters Software": the general aim is to represents the running movement through simple elements like springs, masses and cams, considering the differences between the prosthetic and the sound limb, the influence of the socket alignments and the multidimensionality of the prosthetic foot stiffness.

The implementation of the '*Simplified Model*', described previously in Chapter 2, is now presented: the model, considering all the assumptions and simplifications explained, allows the calculation of the leg stiffness of the athlete.

Therefore, a custom code has been implemented using MATLAB: it is characterized by different modules in order to analyse different parameters.

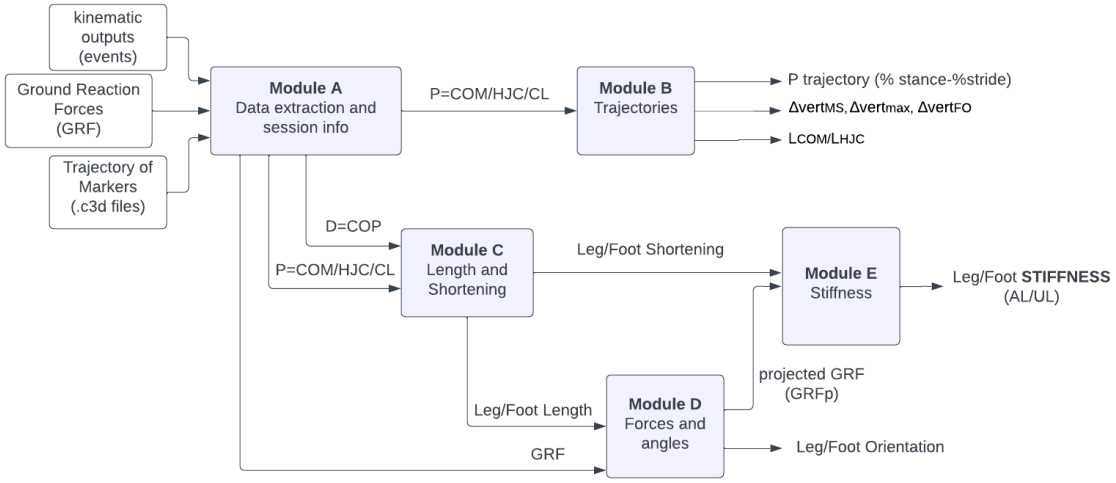

Figure 4.2: Flowchart of the Leg Stiffness Analysis

Module A: Data extraction and session info.

In this script the data of the subject (body mass and height) and the data structure '*outkine*' created in the kinematic analysis are loaded: in particular, the running cycle events and the ground reaction forces (GRFs) are considered in this analysis.

The optimized .c3d files were also loaded: in order to extract the data from these types of files the open-source MATLAB library *Biomechanical ToolKit - BTK* is used. The c3d files are used to store biomechanical information; the *BTK* library contains many functions useful to read and write c3d files, to get specific information like the number of markers, the acquisition frequency either for the stereo-photogrammetry or the kinematic data, and many others.

Once the c3d file is loaded with all the markers trajectories extracted, the markers coordinates are converted from millimetres to meters. Then to convert treadmill running to floor running the markers trajectories are multiplied to the treadmill speed, that was imposed during the in-vivo test.

The custom MATLAB function called '*coordswap'* [14] is used to make the Nexus coordinate system consistent with the one proposed by ISB (International Society of Biomechanics). In fact, the global reference frame used in *Nexus Vicon* is a right – handed triad having the x-axis pointing rightward, the y-axis pointing forward and the z-axis vertical, while the ISB reference is '*a right-handed orthogonal triad fixed in the ground with the + Y axis upward and parallel with the field of gravity. X and Z axes in a plane that is perpendicular to the Y axis*' [36].

The '*getEvents*' function (Olympia software 1.0) [14] gives as output the foot strike (FS) and foot off (FO) of both limbs. The pipeline consists of 3 steps:

- Force signal filtering using a second order band-pass filter with cut off frequencies of 15 and 35 Hz and a fourth-order low-pass frequency of 43 Hz.
- Down-sampling to obtain the stance events in the frame rate of the kinematic analysis (250 Hz).
- Threshold of 100 N to determine the stance events.

The MATLAB function '*getMidstance2*' gives as output the Mid Stance (MS) events: the MS is defined as the instant in which the vertical projection of the HJC (Hip Joint Centre) on the ground, overlaps the COP (2nd metatarsal head for the healthy limb or COP calculated with '*synthCOP*' [14] for the prosthetic limb). In other words, it was found the instance in which HJC and COP have the same value on anterior-posterior axis.

In this part of the code is possible to choose the proximal point P to consider for the model, defining the method of the analysis of the leg stiffness:

- Method 1: P=COM
- Method 2: PR=RHJC and PL=LHJC (where the prefix 'R'/'L' is for 'Right'/'Left').

For this reason, it is crucial to define and explain how these proximal points have been calculated.

- The '*COM_calculation*' function calculates the **Centre of Mass *(COM)*** of the athlete: the COM is approximated, and it is calculated as the centroid of the markers placed on the anterior (RASIS, LASIS) and posterior (RPSIS, LPSIS) iliac spines.

- The ***Hip Joint Centres (HJC)***, either for the right (RHJC) and the left limb (LHJC) are associated with the pelvis and they are calculated using Bell's method.

This is a predictive method that uses regression equations to estimate the hip joint centre position from measurable anthropometric quantities. Bell's method has been implemented in the custom function '*bellHJC*', which first calculates pelvis width as Euclidean distance between the markers placed on the superior anterior iliac spines, then multiplies it for three regression coefficients to obtain the three-dimensional coordinates of HJC expressed in the pelvis local reference frame [14], [37].

$$PW_{(pelvis\ width)} = |\ RASIS - LASIS|$$

$$RHJC^{LOC} = [-0.10 * PW;\ -0.30 * PW; +0.36 * PW]$$

$$LHJC^{LOC} = [-0.10 * PW; -0.30 * PW; -0.36 * PW]$$

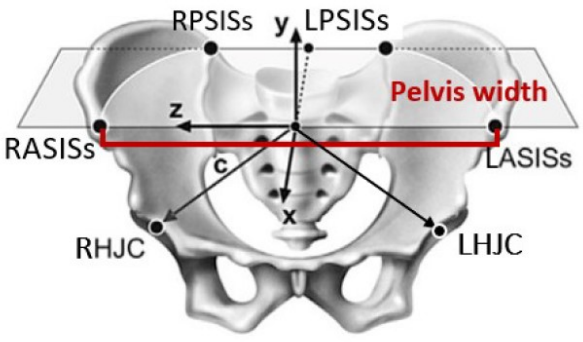

Figure 4.3: Hip Joint Centre with respect to Pelvis Coordinate System.

It is possible to focus the analysis on the prosthetic foot: thus, the proximal point P is the centre of the Clamp, calculated as the centroid of the markers FP1, FP2, FP3 and FP4.

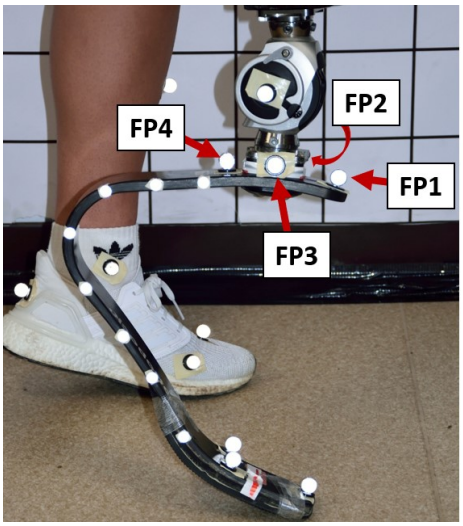

Figure 4.4: FP1, FP2, FP3 and FP4 markers on RPF.

The distal point D is always the Centre of Pressure (COP): since it was not possible a direct measure of the Centre of Pressure, different approximations of the COP position are used for both the treadmill and track tests.

The COP used for the treadmill trial is named: *'**vCOP – Virtual COP**'*. The Centre of Pressure corresponds to the ground projection of the marker placed on the second metatarsal head for the healthy foot, while for the prosthetic foot it was assumed that the COP varies linearly form the midpoint of the FD2-FD3 markers and the tip of the foot FD1. This is calculated in the function '*synthCOP*'[14].

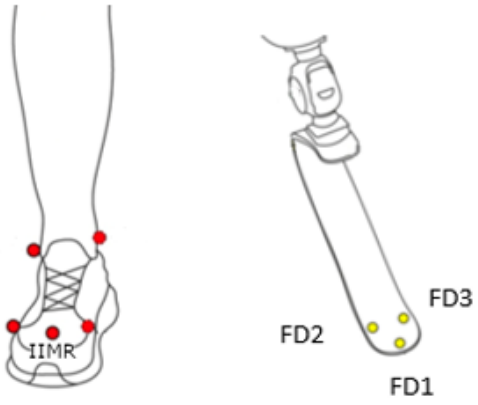

Figure 4.5: 2nd metatarsal head marker (IIMR) and markers used in 'synthCOP' function (FD1, FD2, FD3).

The COP used for the Track trial is the **'eCOP'- estimated COP**'. the identification of the coordinates of the COP are from the force and torque signals measured through the load cell.

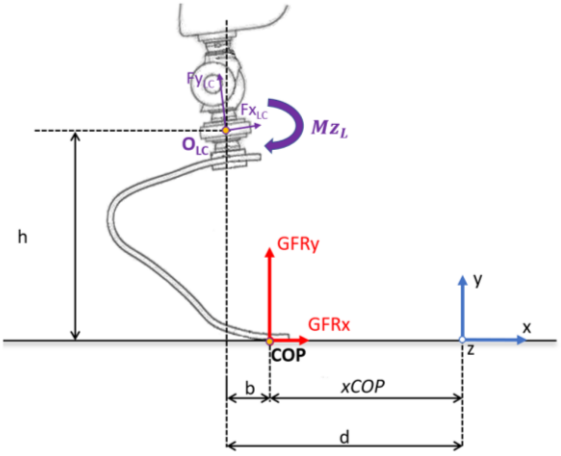

Figure 4.6: estimation of COP position trough load cell.

The COP position is estimated given:

- the matrix describing the orientation of the load cell with respect to the ground, forces can be projected from the local reference system (load cell) onto the global reference system: **GRFx** and **GRFy**
- the coordinates of the origin of the local Coordinate Systems of the load cell: $\boldsymbol{O_{LC}}$
- the vertical distance of the load cell from the ground: **h**
- the horizontal distance of the load cell respect to origin of the global reference system: **d**
- the torque about the z-axis, measured by the load cell: $\boldsymbol{Mz_L}$

$$Mz_L = GRF_y * b + GRFx * h$$

The relative horizontal distance between the origin of the load cell (O_{LC}) and the point of application of the force (COP) can be calculated as:

$$b = \frac{Mz_L - GRFx * h}{GRFy}$$

The absolute x-coordinate of the COP can be then obtained as:

$$xCOP = d - b$$

The y-coordinate of the COP is zero and the z-coordinate is assumed as the medio-lateral component of the marker 'LFD1' located on the tip of the foot.

These methods would be validated in future tests when athletes will be running on force platforms.

Module B: Trajectories

In this part the trajectory of the proximal point is analysed. The input are the markers of the proximal point P (COM or HJC) and the events. The output is the P trajectory during stance and stride and the following parameters:

- $\Delta vert_{MS}$ = vertical lowering of P between Foot Strike and Mid Stance

- $\Delta vert_{max}$= maximum vertical lowering of P during stance, compared to Foot Strike

- $\Delta vert_{FO}$ = vertical lowering of P between Foot Strike and Foot Off.

- L_P = forward trajectory length of P, during stance.

- y_F = maximum altitude of P during flight.

- $\Delta vert_F$ = maximum vertical elevation of P during flight.

In addiction the *tangential angle* (α) of P trajectory (at Foot Strike and Foot Off) is calculated: first the tangency line to the trajectory of P is calculated and then, the angle (α) between the tangency line and the horizontal which is the tangential angle of P.

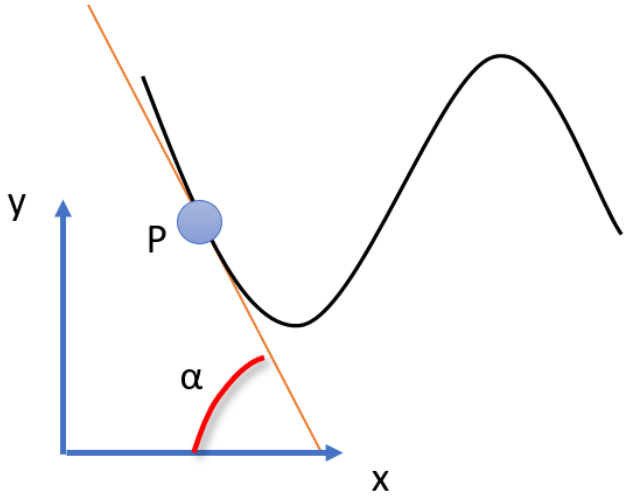

Figure 4.7: tangential angle (α)

Module C: Length and Shortening

The inputs at this part are the chosen proximal point P, the COP, and the events.

If P=COM or P=HJC is calculated the Leg Length and the Leg Shortening, otherwise if the focus is on the foot (which means that P=CLAMP), it is calculated the Foot Length (distance between the Clamp and the COP) and the Foot Shortening.

Once the COP is defined, and the proximal point P is chosen, the length is calculated through the custom function '*getLength*': it returns in output the components, the magnitude and the versor of the vector representing the length.

The *Reference Length* is calculated at the Foot Strike, for each stance, while the *Shortening* is calculated as the difference between the *Reference Length* and the length in every frame of the stance.

Module D: Forces and angles

The input required are the events, the GRFs and the versor that represents the direction on which the GRF is projected.

GRFs are projected with the MATLAB 'dot product' function between the GRF and the versor considered: in the treadmill session is possible to do this calculation for both the limbs, whereas in the track test it is possible only for the affected limb, thanks to the load cell, because no GRF data were collected for the unaffected limb.

In addition, the Theta angle is calculated, during the stance phase for both limbs.

Module E: Stiffness

In this module the *Leg or Foot Stiffness* are calculated, depending on the chosen proximal point: it needs in input the events, the magnitude of the projected GRF ($|\overrightarrow{GRFp}|$) and the shortening.

It computes the maximum $|\overrightarrow{GRFp}|$ and it finds the respective shortening.

The *Leg Stiffness* (when P=COM or P=HJC) is calculated, in each step, for both the limbs on treadmill and only the affected limb on track:

$$K_{leg} = \frac{\left|\overrightarrow{GRF_p}\right|_{max}}{\Delta L\left(\left|\overrightarrow{GRF_p}\right|_{max}\right)}$$

The *Foot Stiffness* (when P=CL) is computed implementing the follow equation:

$$K_{foot} = \frac{\left|\overrightarrow{GRF_p}\right|_{max}}{\Delta d\left(\left|\overrightarrow{GRF_p}\right|_{max}\right)}$$

The data acquired during the treadmill and track session were analysed and the most meaningful quantities are presented in the next chapter.

Chapter 5: Results

The results of the analysis are described in this chapter.

First, the *Leg Stiffness Model* results with the two methods implemented (Method 1: P=COM and Method 2: P=HJC), for both in-vivo experimental sessions are presented.

The athlete during the treadmill session used four different sockets alignment: the test performed with 'A0' has not been analysed because the results from the kinematics were not good enough; this was probably due to fatigue reasons. For this motivation, only the results from the alignments A1, A2, A3 are shown from the treadmill session.

In the track session only one alignment was tested: A3. In particular the results of the test 'TSSR 04' are presented.

The table describes the test type and alignment analysed with the different models.

	Test Type	**Socket Alignment**	**Analysed Limb**
Treadmill	SSR	A1	AL/UL
	SSR	A2	AL/UL
	SSR	A3	AL/UL
Track	TSSR 04	A3 Track	AL

Later, the results from the *Foot Stiffness Model* are also shown, for the different alignments.

For the affected limb (AL) and the unaffected limb (UL) the meaningful quantities pictured in the analysis are:

- Vertical component of the proximal point P (COM/HJC) in % stance.
- Leg Length (**L**) in % stance.
- Leg Orientation (Theta Leg) in % stance.
- Leg Shortening ($\Delta \boldsymbol{L}$) in % stance.
- Module of the projected GRF ($\left|\overrightarrow{GRF_p}\right|$) in % stance.
- The projected GRF ($\left|\overrightarrow{GRF_p}\right|$) vs Leg Shortening ($\Delta \boldsymbol{L}$)
- The Leg Stiffness (K_{leg}) for each step of the acquisition.

1. Leg Stiffness Model

P=COM	Test Type	Socket Alignment	Limb
Treadmill	SSR	A1	AL/UL

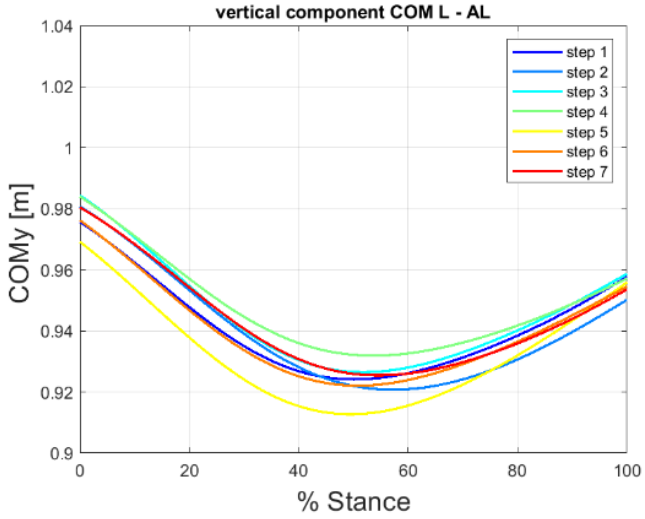

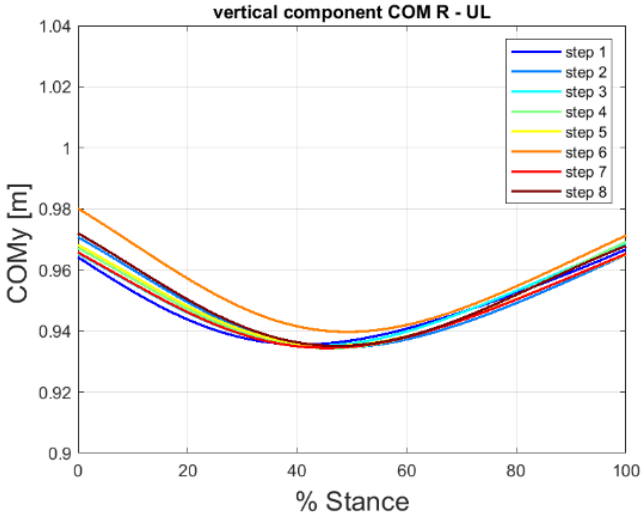

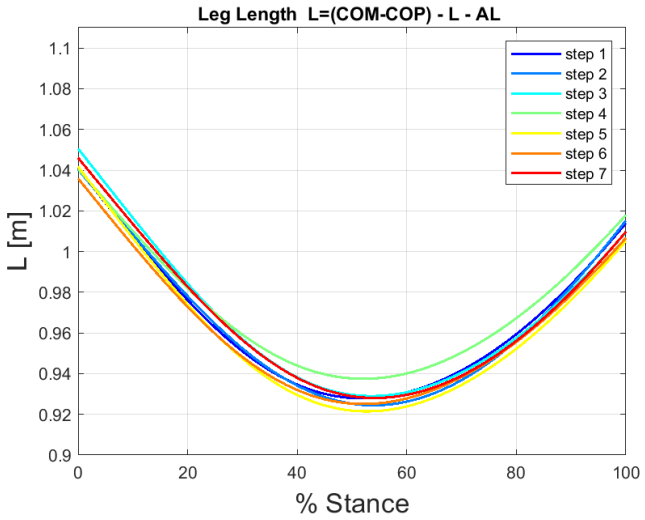

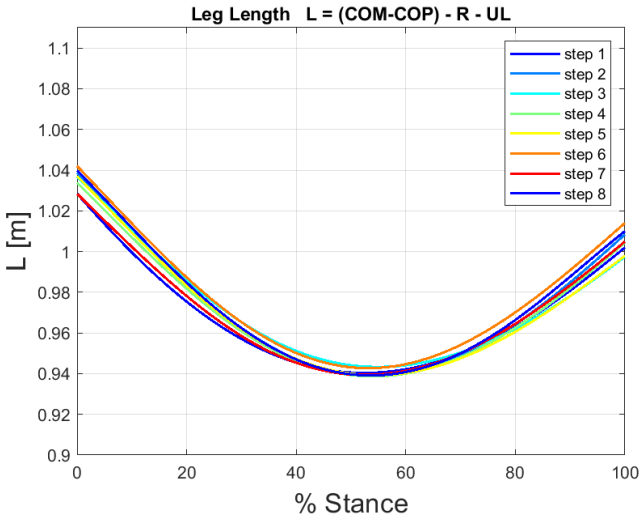

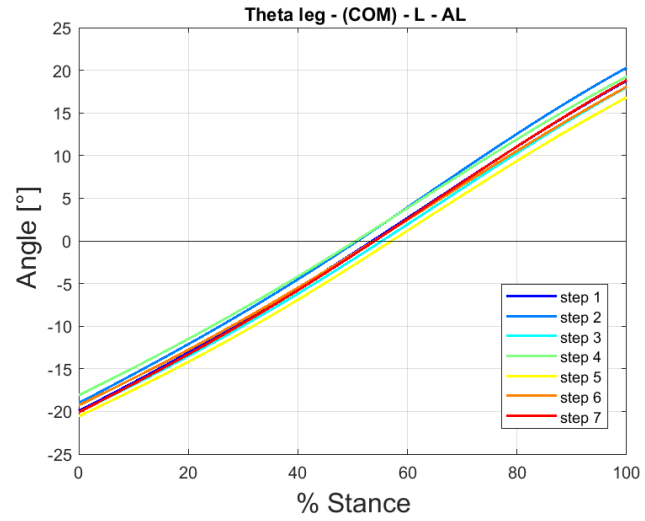

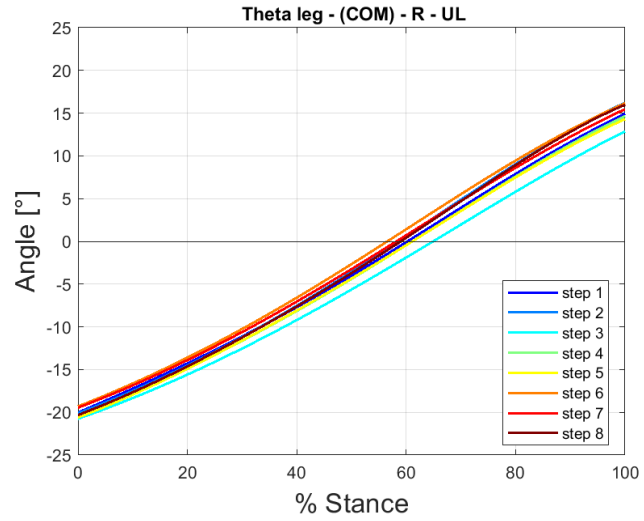

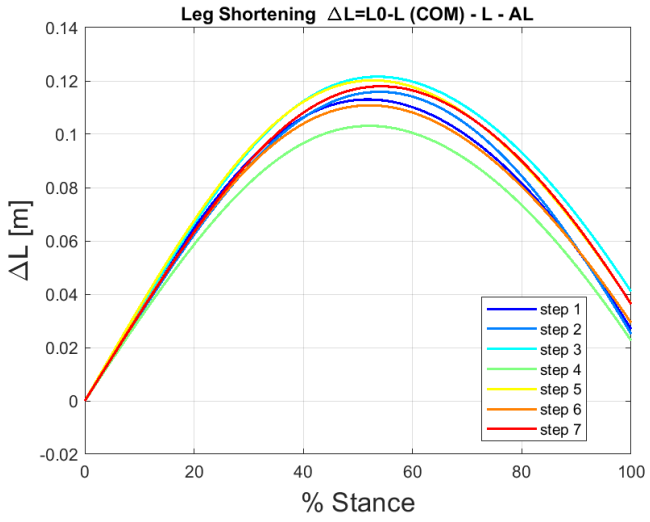
Leg Shortening ΔL=L0-L (COM) - L - AL
ΔL [m]
% Stance
step 1
step 2
step 3
step 4
step 5
step 6
step 7

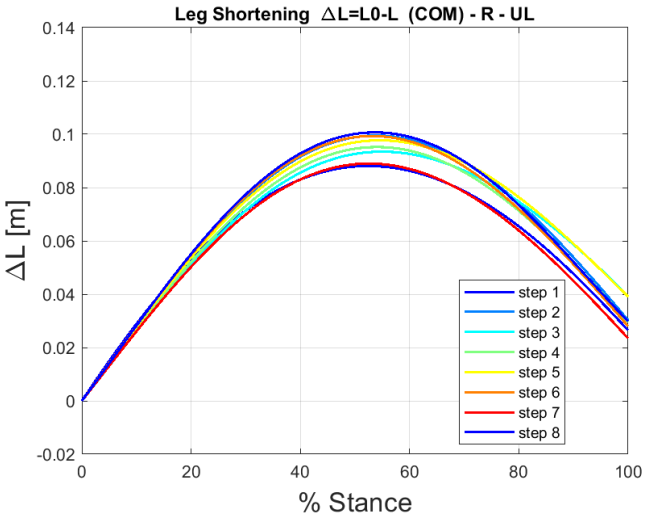
Leg Shortening ΔL=L0-L (COM) - R - UL
ΔL [m]
% Stance
step 1
step 2
step 3
step 4
step 5
step 6
step 7
step 8

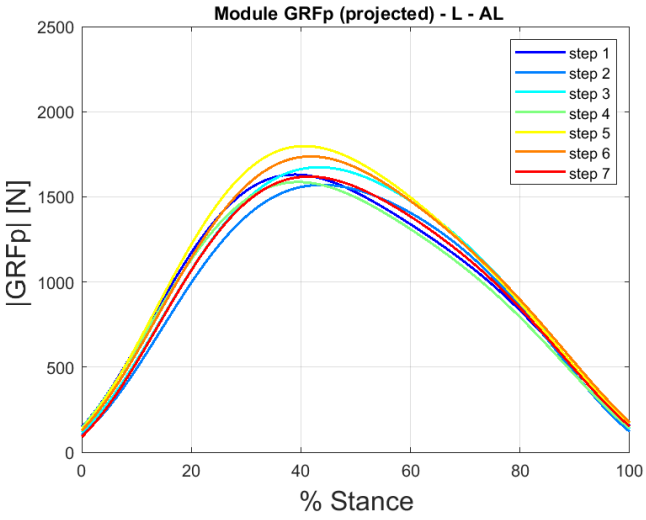
Module GRFp (projected) - L - AL
|GRFp| [N]
% Stance
step 1
step 2
step 3
step 4
step 5
step 6
step 7

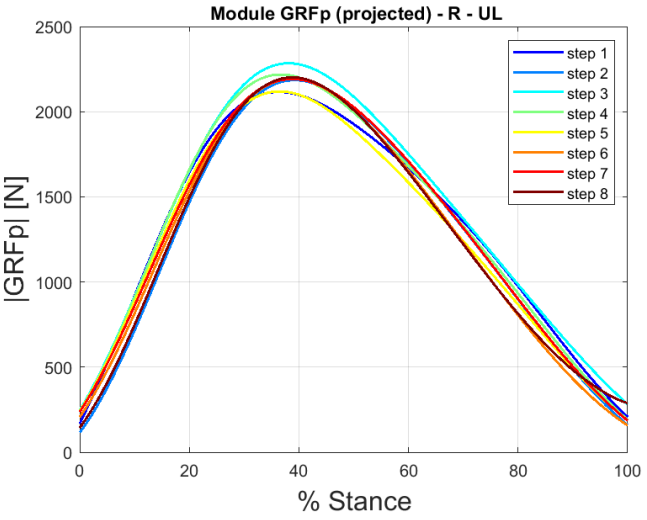
Module GRFp (projected) - R - UL
|GRFp| [N]
% Stance
step 1
step 2
step 3
step 4
step 5
step 6
step 7
step 8

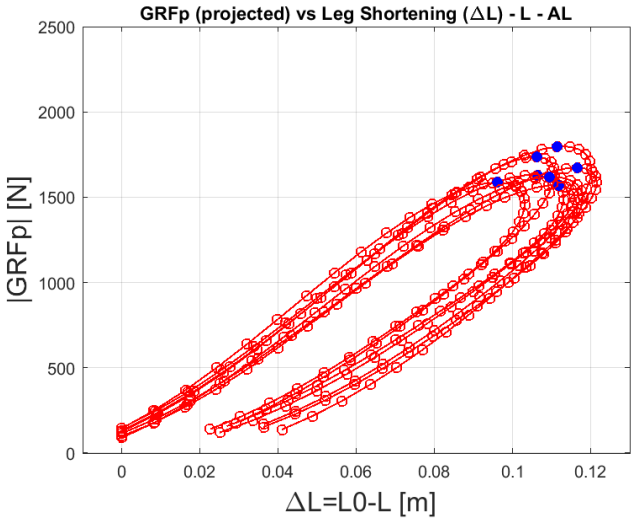
GRFp (projected) vs Leg Shortening (ΔL) - L - AL
|GRFp| [N]
ΔL=L0-L [m]

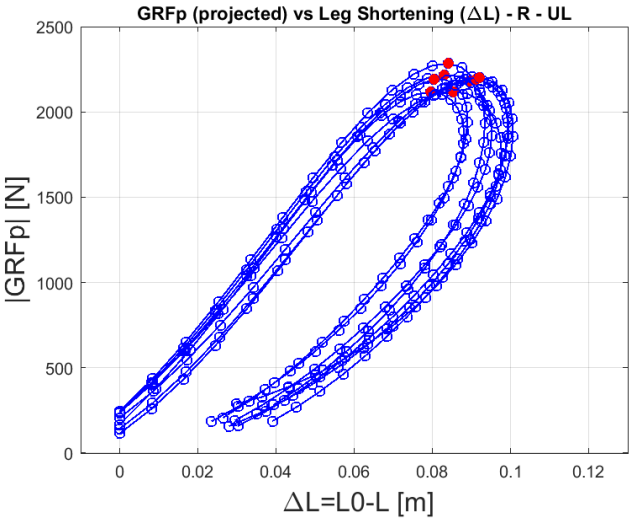
GRFp (projected) vs Leg Shortening (ΔL) - R - UL
|GRFp| [N]
ΔL=L0-L [m]

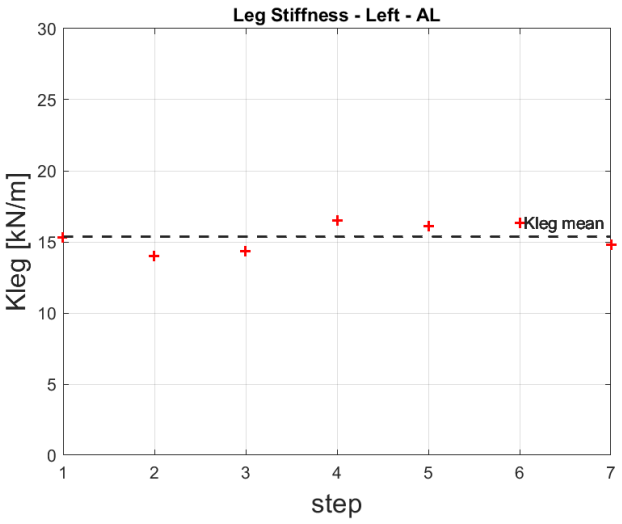

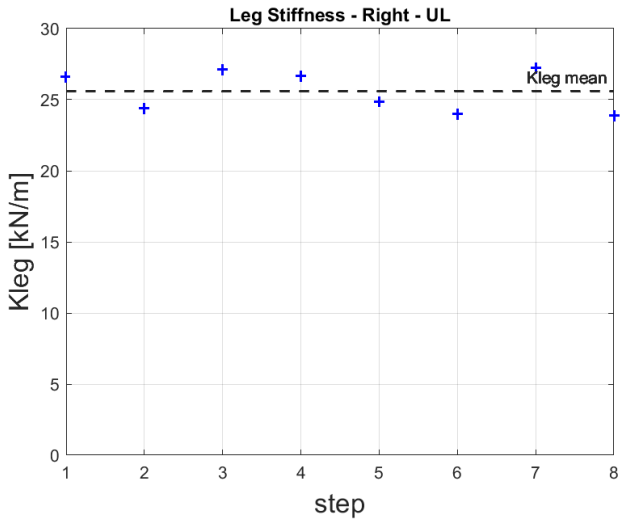

Leg Stiffness Model

Method 1: P=COM

Alignment: A1

The K_{leg} values for each step, with the mean and standard deviation:

AL – Affected Limb

	Step 1	Step 2	Step 3	Step 4	Step 5	Step 6	Step 7	**Mean**	**Std**
K_{leg_AL} [kN/m]	15.3	14.0	14.3	16.5	16.1	16.4	14.8	**15.4**	**1.0**

UL – Unaffected Limb

	Step 1	Step 2	Step 3	Step 4	Step 5	Step 6	Step 7	Step 8	**Mean**	**std**
K_{leg_UL} [kN/m]	26.6	24.4	27.1	26.7	24.9	24.0	27.2	23.9	**25.6**	**1.4**

P=COM	Test Type	Socket Alignment	Limb
Treadmill	SSR	A2	AL/UL

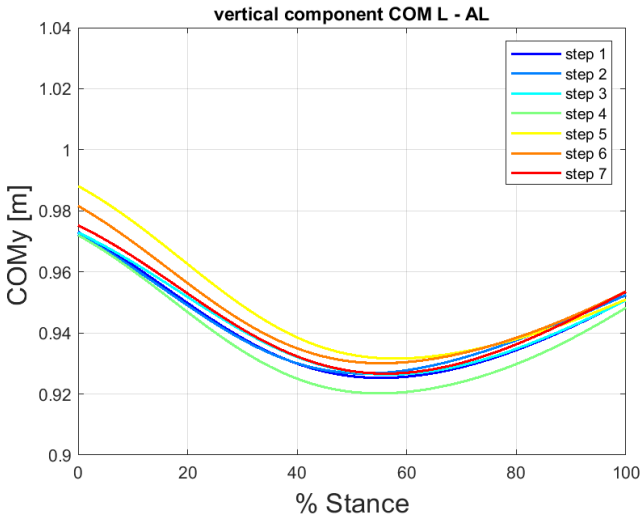

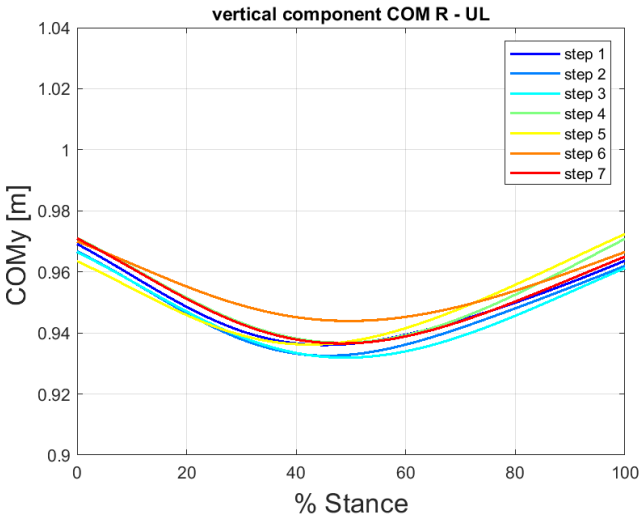

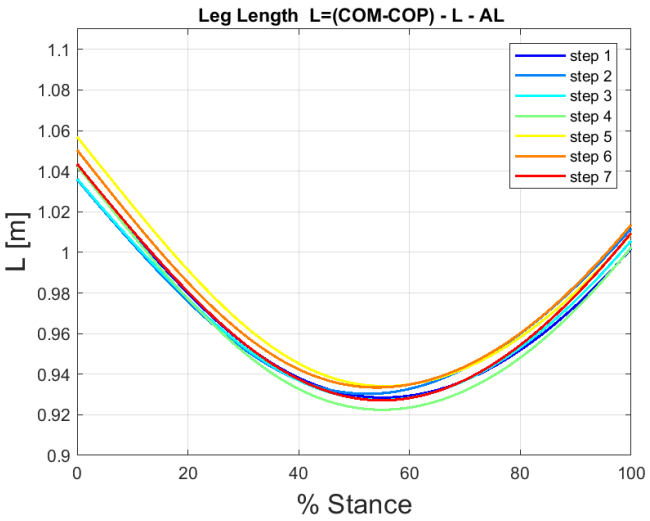

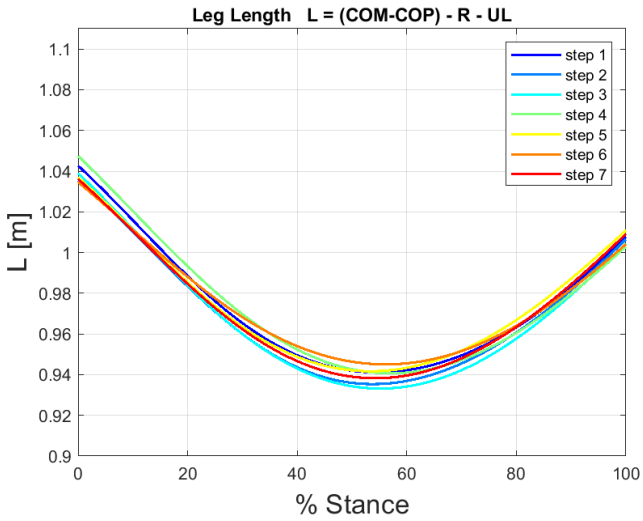

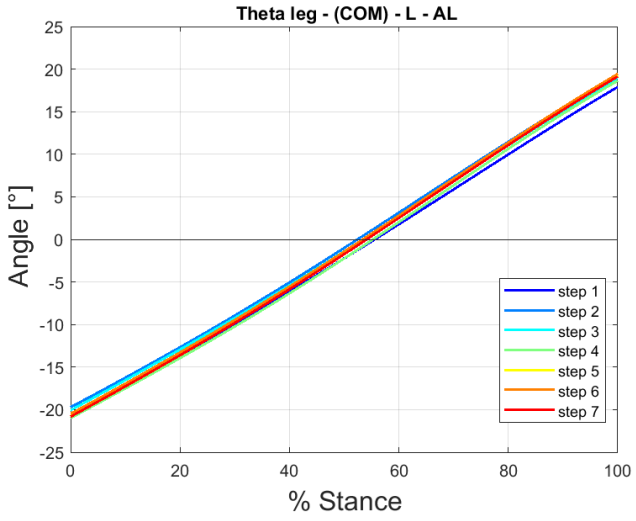

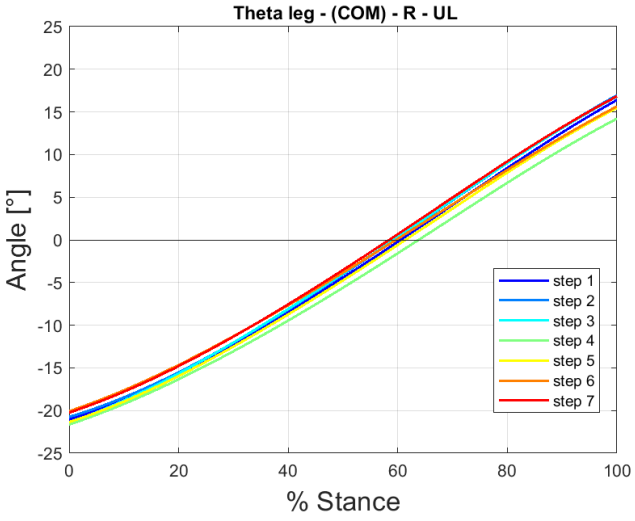

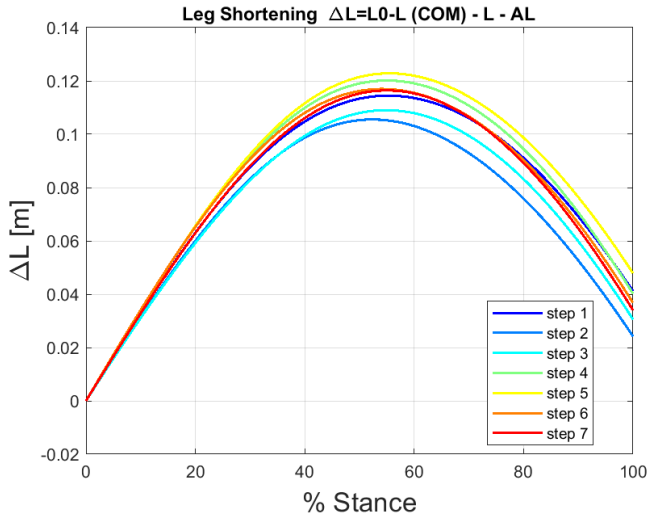
Leg Shortening ΔL=L0-L (COM) - L - AL
ΔL [m]
% Stance
step 1
step 2
step 3
step 4
step 5
step 6
step 7

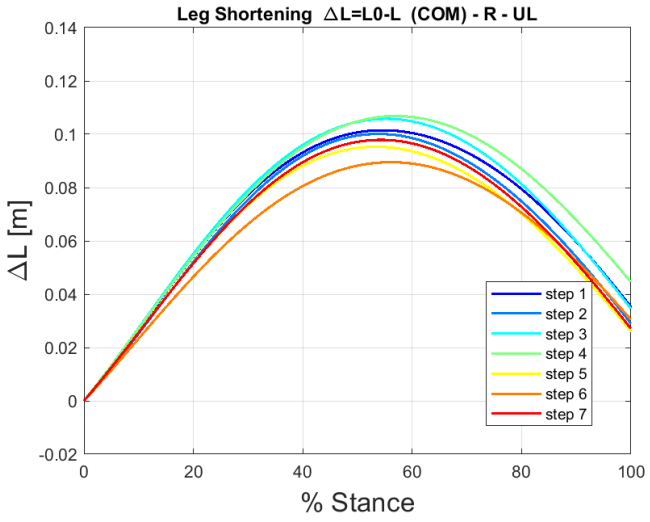
Leg Shortening ΔL=L0-L (COM) - R - UL
ΔL [m]
% Stance
step 1
step 2
step 3
step 4
step 5
step 6
step 7

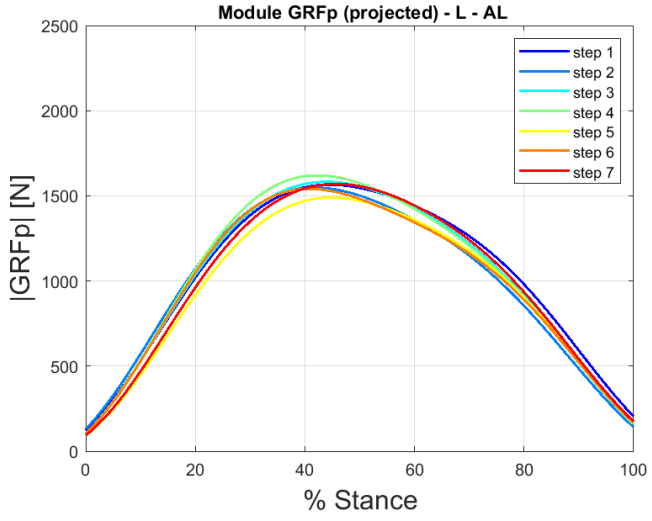
Module GRFp (projected) - L - AL
|GRFp| [N]
% Stance
step 1
step 2
step 3
step 4
step 5
step 6
step 7

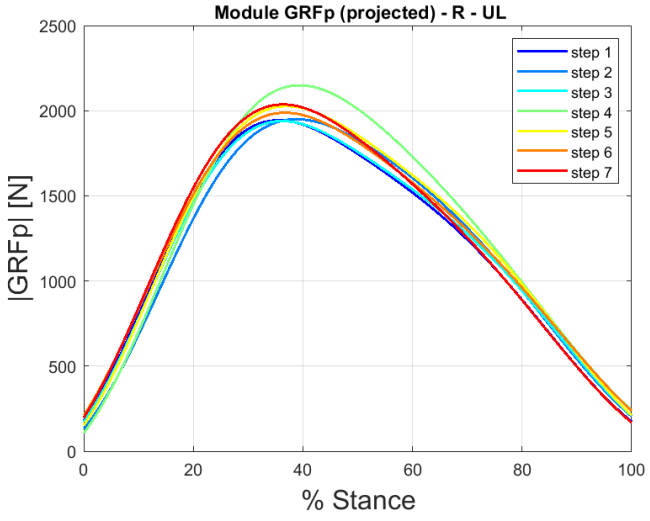
Module GRFp (projected) - R - UL
|GRFp| [N]
% Stance
step 1
step 2
step 3
step 4
step 5
step 6
step 7

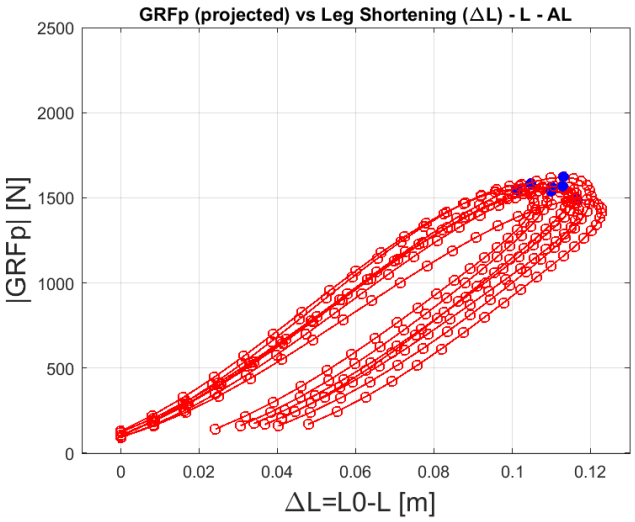
GRFp (projected) vs Leg Shortening (ΔL) - L - AL
|GRFp| [N]
ΔL=L0-L [m]

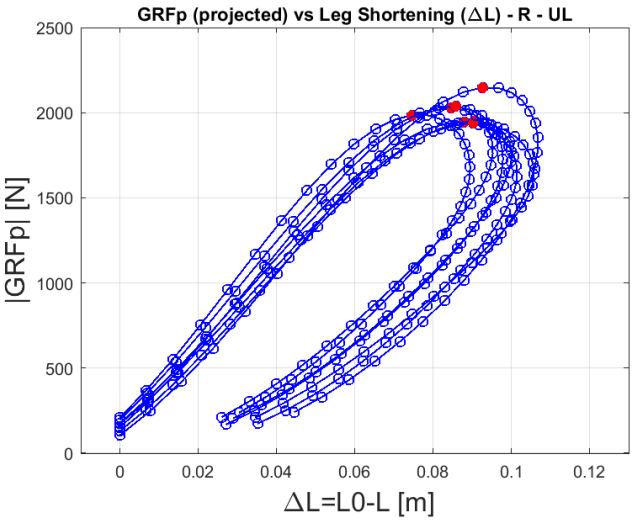
GRFp (projected) vs Leg Shortening (ΔL) - R - UL
|GRFp| [N]
ΔL=L0-L [m]

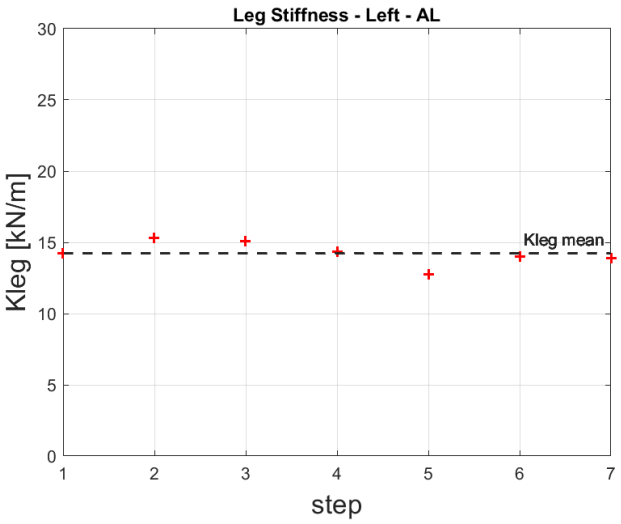

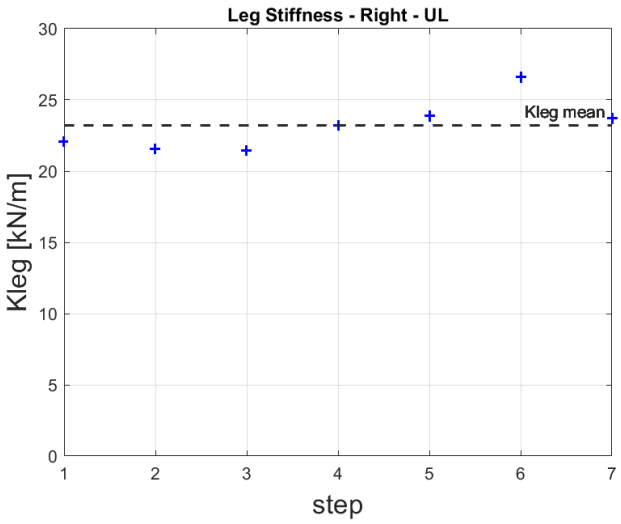

Leg Stiffness Model

Method 1: P=COM

Alignment: A2

The K_{leg} values for each step, with the mean and standard deviation:

AL – Affected Limb

	Step 1	Step 2	Step 3	Step 4	Step 5	Step 6	Step 7	**Mean**	**Std**
K_{leg_AL} [kN/m]	14.2	15.3	15.1	14.3	12.8	14.0	13.9	**14.2**	**0.8**

UL – Unaffected Limb

	Step 1	Step 2	Step 3	Step 4	Step 5	Step 6	Step 7	**Mean**	**std**
K_{leg_UL} [kN/m]	22.1	21.6	21.5	23.2	23.9	26.6	23.7	**23.2**	**1.8**

P=COM	Test Type	Socket Alignment	Limb
Treadmill	SSR	A3	AL/UL

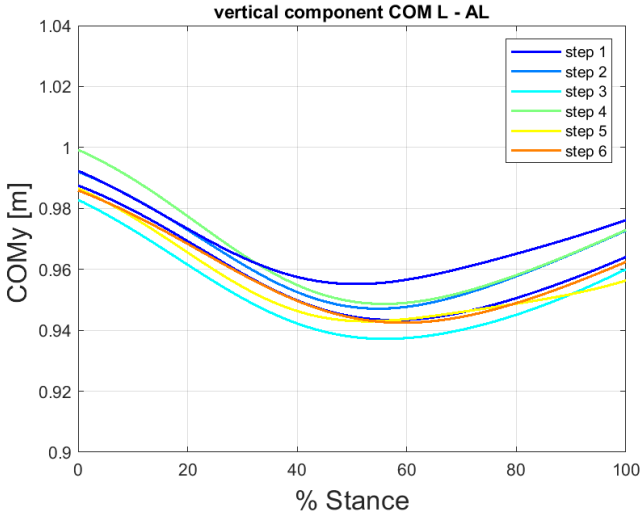

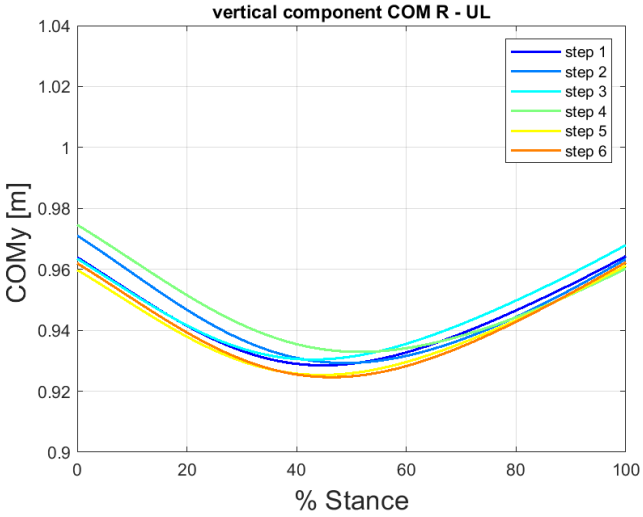

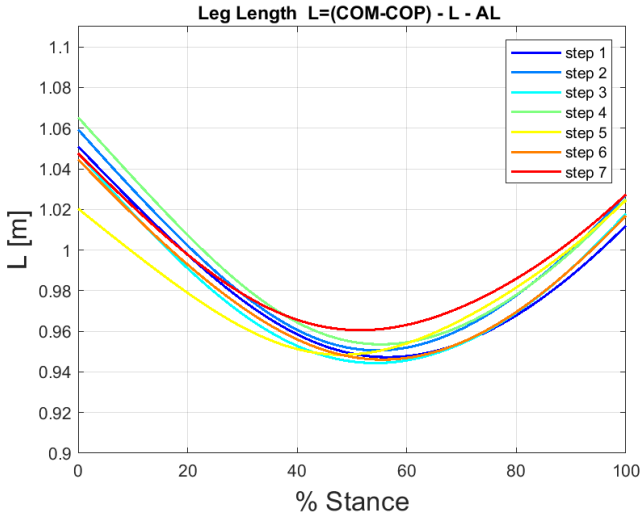

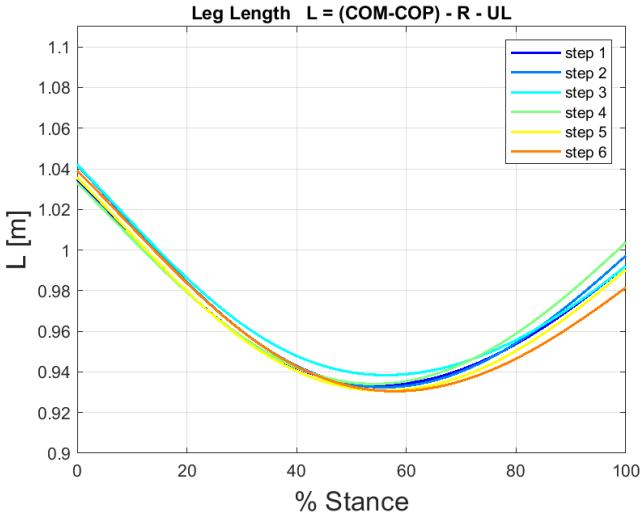

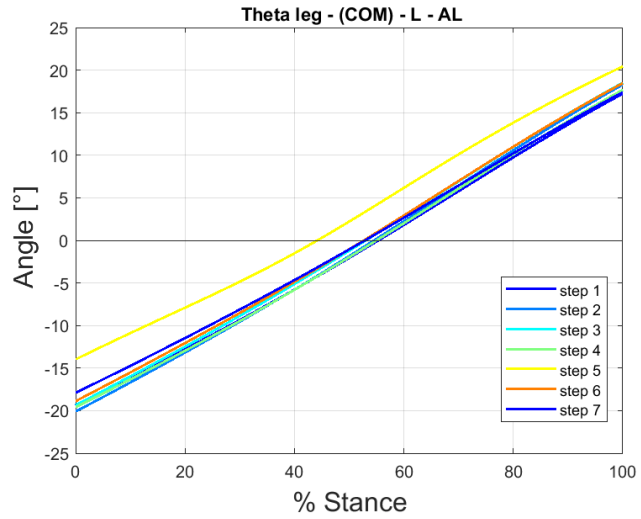

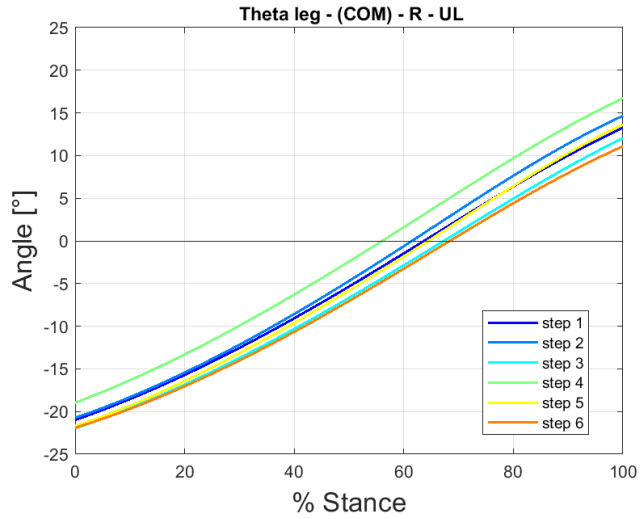

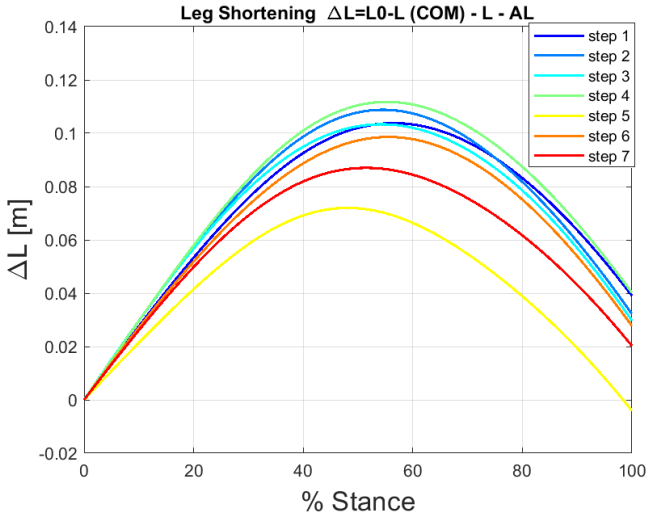
Leg Shortening ΔL=L0-L (COM) - L - AL
step 1
step 2
step 3
step 4
step 5
step 6
step 7
ΔL [m]
% Stance

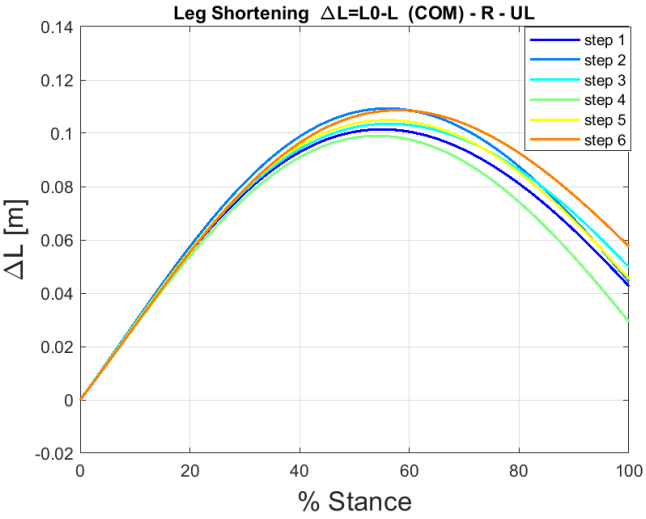
Leg Shortening ΔL=L0-L (COM) - R - UL
step 1
step 2
step 3
step 4
step 5
step 6
ΔL [m]
% Stance

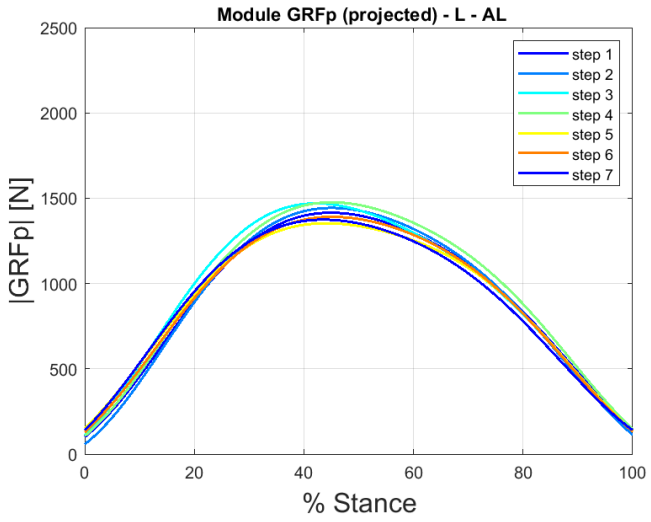
Module GRFp (projected) - L - AL
step 1
step 2
step 3
step 4
step 5
step 6
step 7
|GRFp| [N]
% Stance

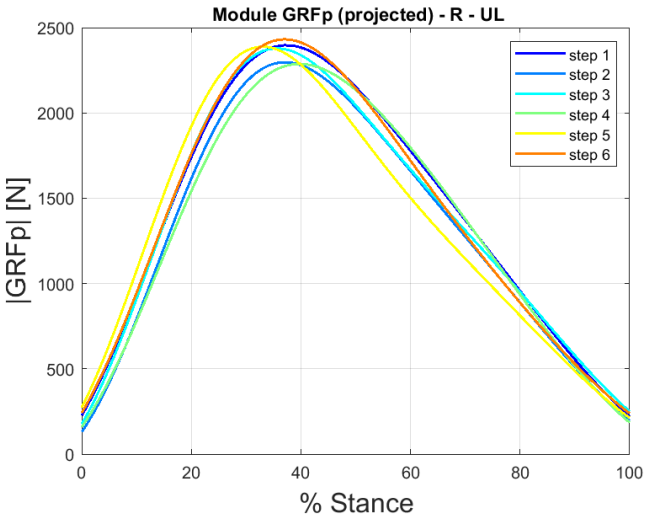
Module GRFp (projected) - R - UL
step 1
step 2
step 3
step 4
step 5
step 6
|GRFp| [N]
% Stance

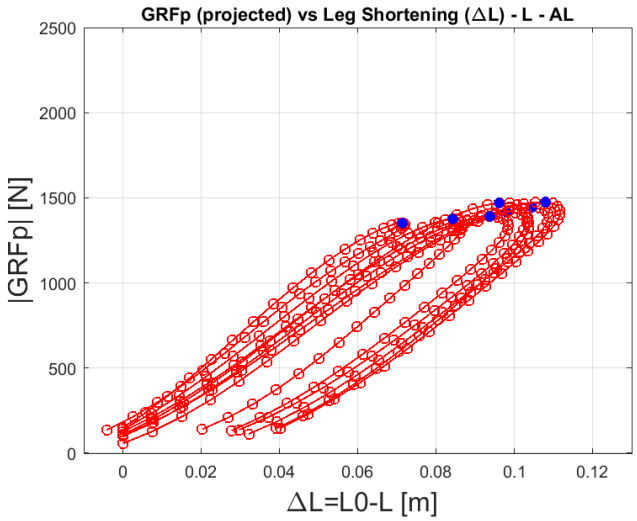
GRFp (projected) vs Leg Shortening (ΔL) - L - AL
|GRFp| [N]
ΔL=L0-L [m]

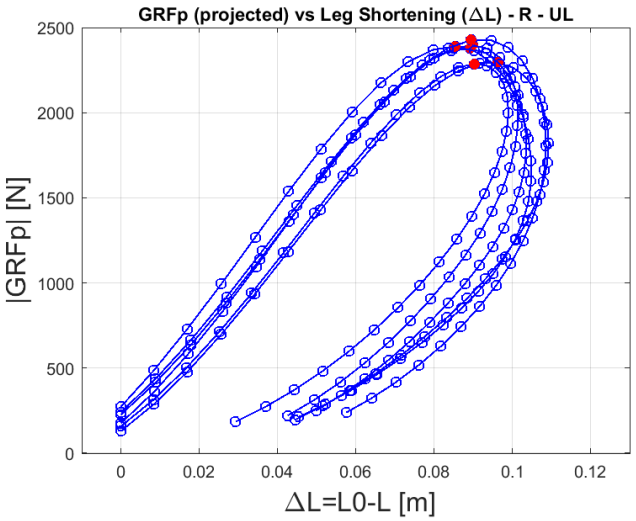
GRFp (projected) vs Leg Shortening (ΔL) - R - UL
|GRFp| [N]
ΔL=L0-L [m]

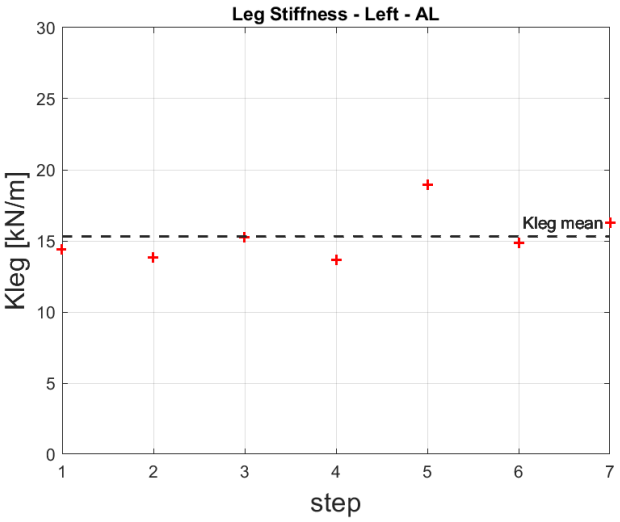

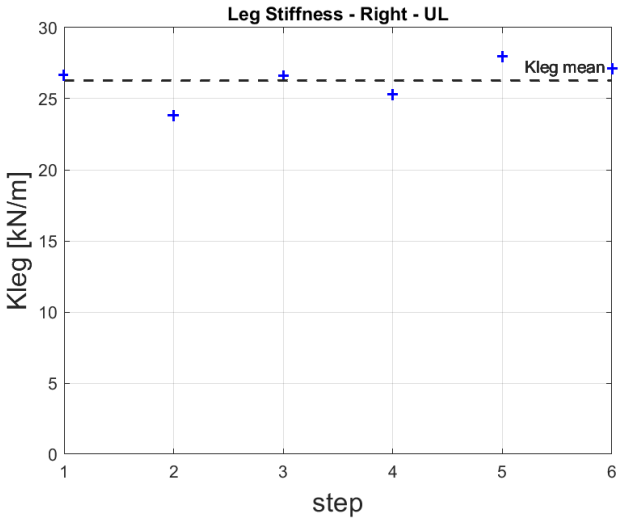

Leg Stiffness Model

Method 1: P=COM

Alignment: A3

The K_{leg} values for each step, with the mean and standard deviation:

AL – Affected Limb

	Step 1	Step 2	Step 3	Step 4	Step 5	Step 6	Step 7	**Mean**	**Std**
K_{leg_AL} [kN/m]	14.4	13.8	15.3	13.7	18.9	14.8	16.3	**15.3**	**1.8**

UL – Unaffected Limb

	Step 1	Step 2	Step 3	Step 4	Step 5	Step 6	**Mean**	**Std**
K_{leg_UL} [kN/m]	26.7	23.8	26.6	25.3	28.0	27.1	**26.3**	**1.5**

P=COM	Test Type	Socket Alignment	Limb
Track	TSSR 04	A3 Track	AL

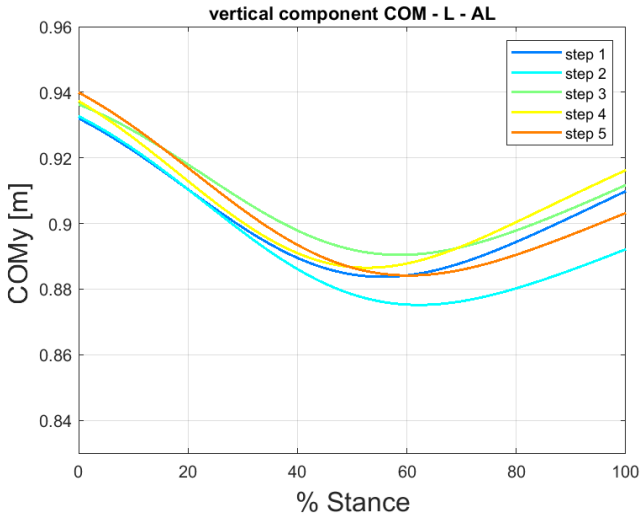

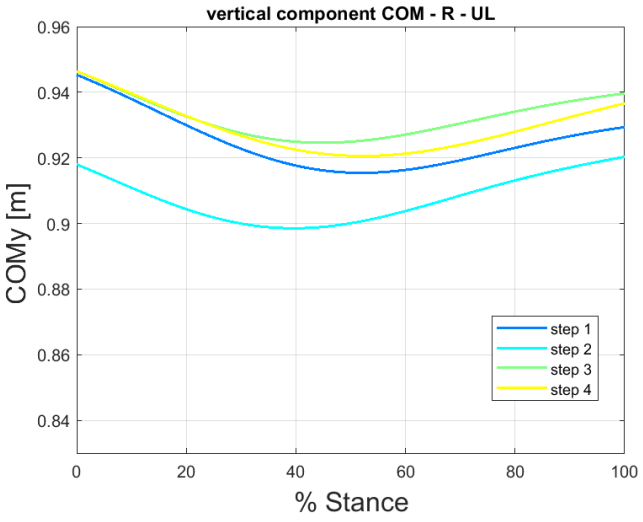

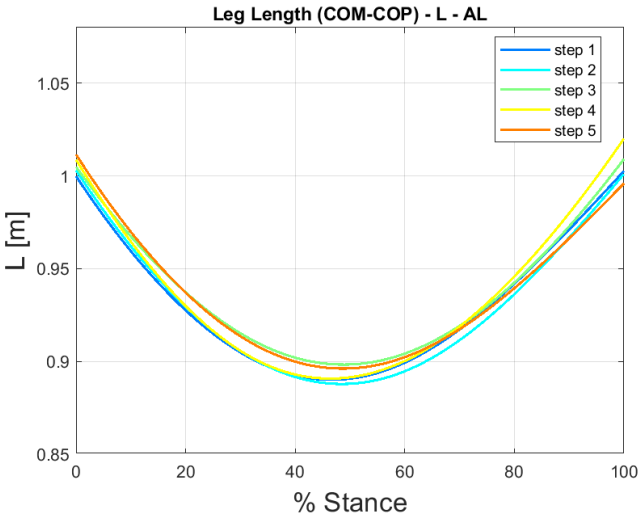

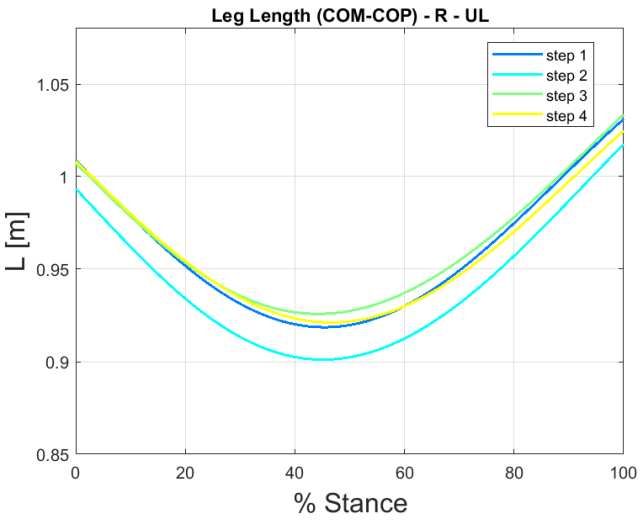

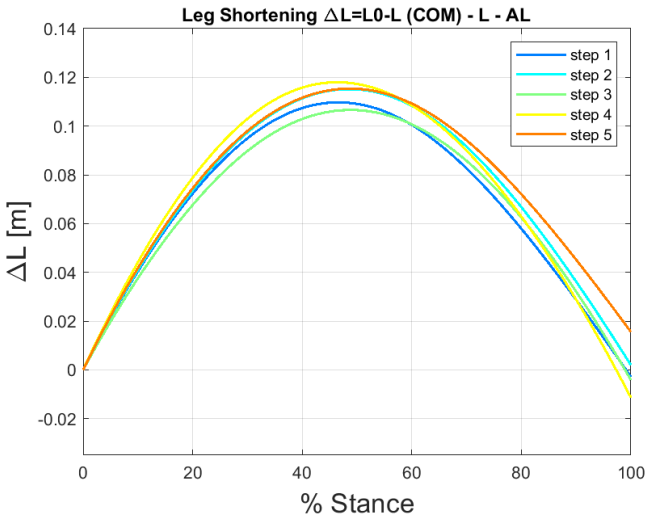

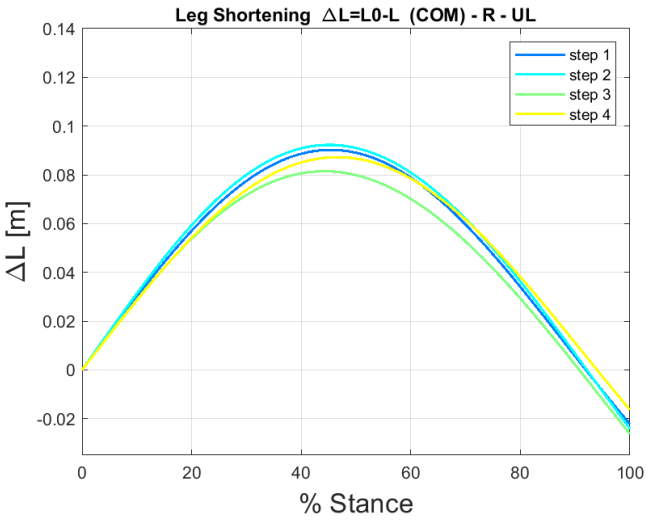

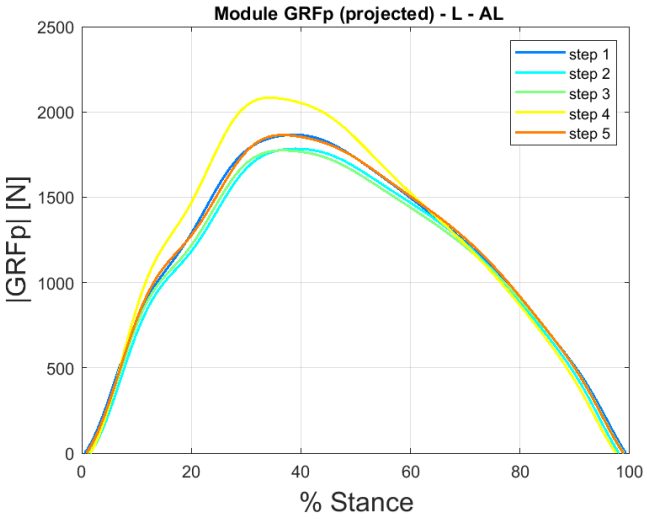

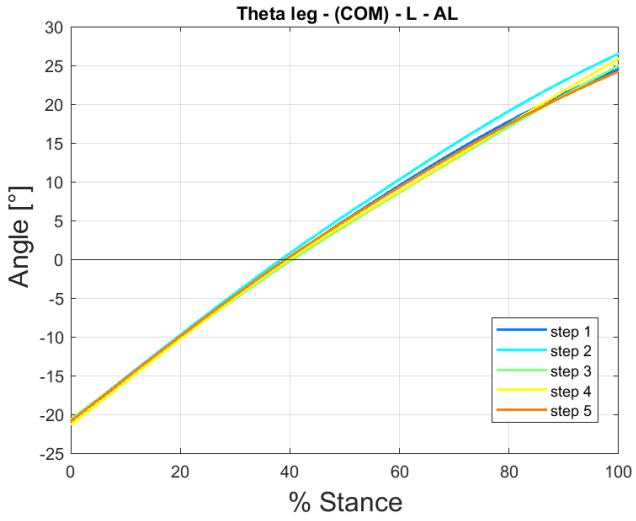

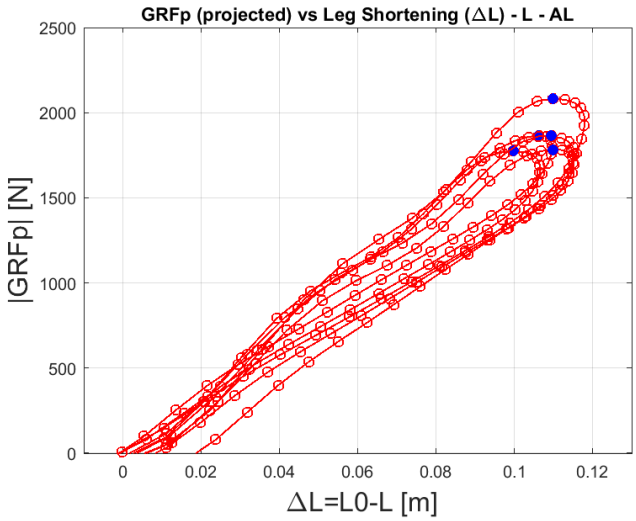

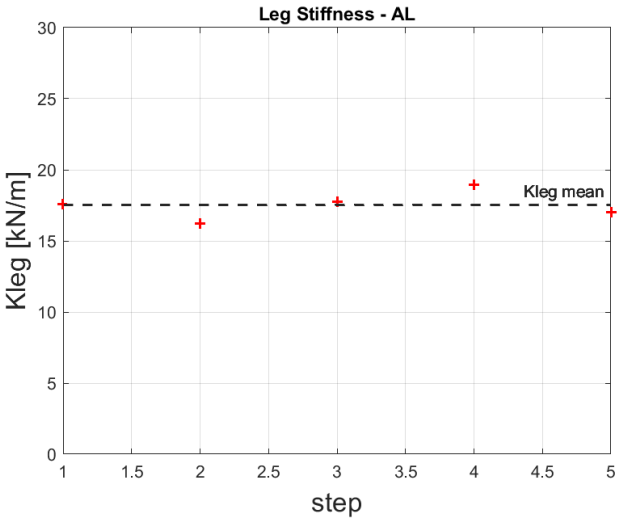

Leg Stiffness Model

Method 1: P=COM

Alignment: A3 Track (TSSR 04)

The K_{leg} values for each step, with the mean and standard deviation:

AL-Affected Limb

	Step 1	Step 2	Step 3	Step 4	Step 5	Mean	Std
K_{leg_AL} [kN/m]	17.6	16.2	17.8	19.0	17.0	17.5	1.0

The following bar plots synthesize the mean values of the Leg Stiffness (K_{leg}) calculated with the Method 1 (P=COM), for each alignment of treadmill and track test (A3 Track):

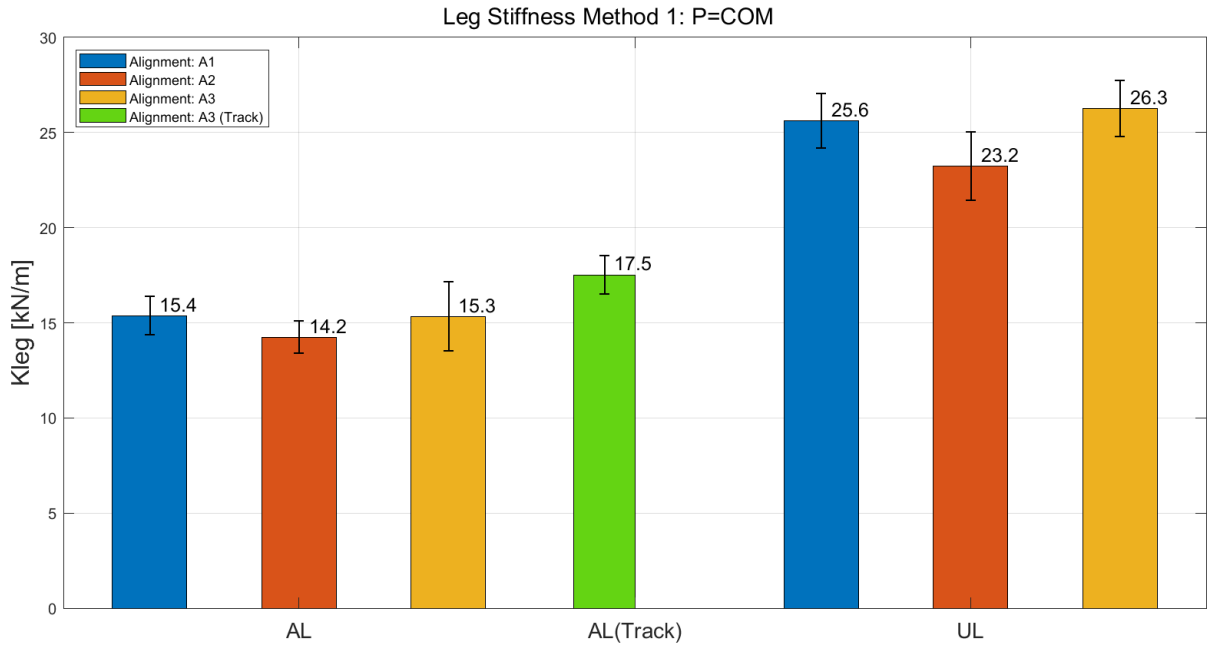

Figure 5.1: Leg Stiffness for the Affected Limb (AL) and Unaffected Limb (UL) for the alignments: A1 in blue, A2 in red and A3 in yellow; A3 (track) in green.

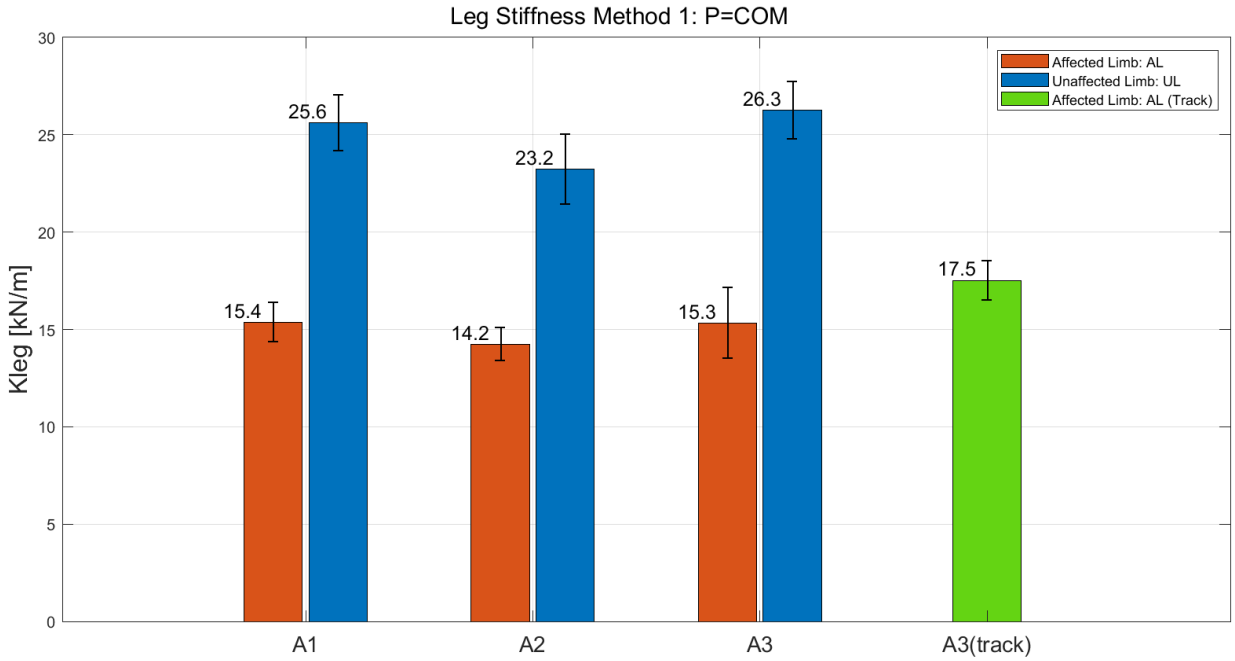

Figure 5.2: Leg Stiffness for all alignments (A1, A2, A3, A3 Track): in red the Affected Limb (AL), in blue the Unaffected Limb (UL) on treadmill. In green the Affected Limb on Track (A3 Track).

$\mathbf{L_{COM}}$ = forward trajectory length of COM, during stance – 'Contact Length'

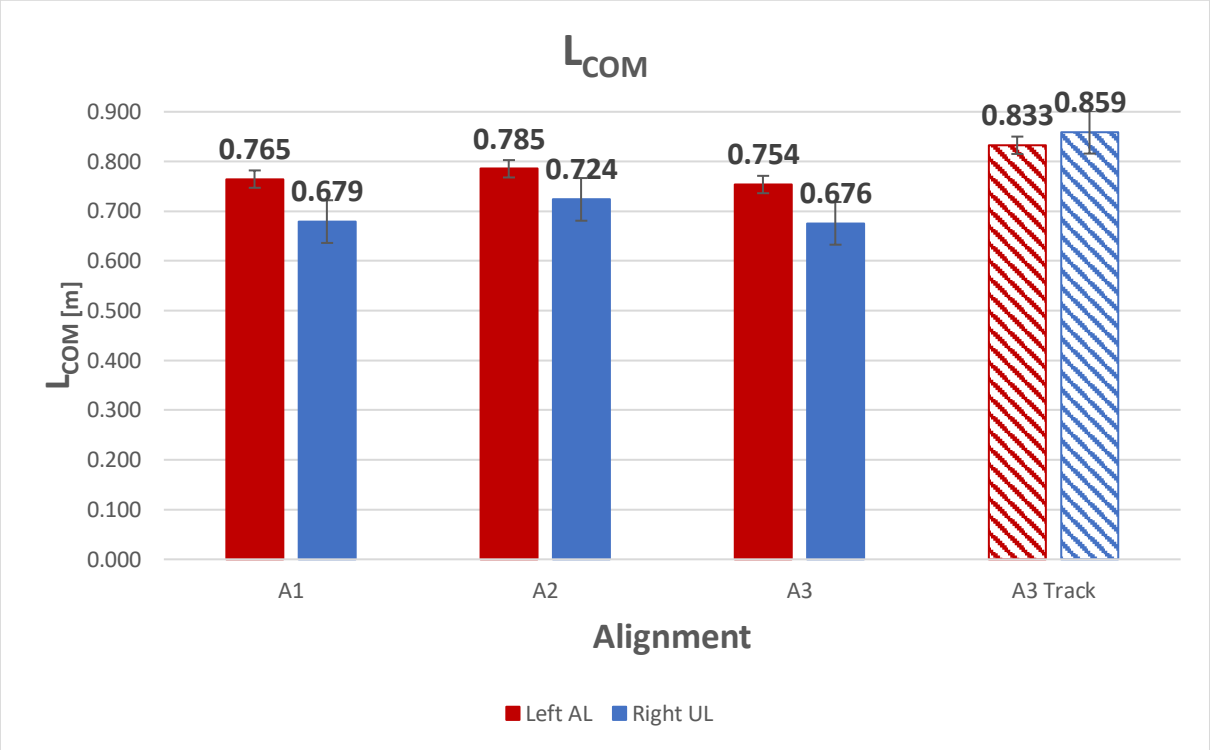

Figure 5.3: $\boldsymbol{L_{COM}}$ -Contact Length with Method 1(P=COM).

Method 2: P=HJC

P=HJC	Test Type	Socket Alignment	Limb
Treadmill	SSR	A1	AL/UL

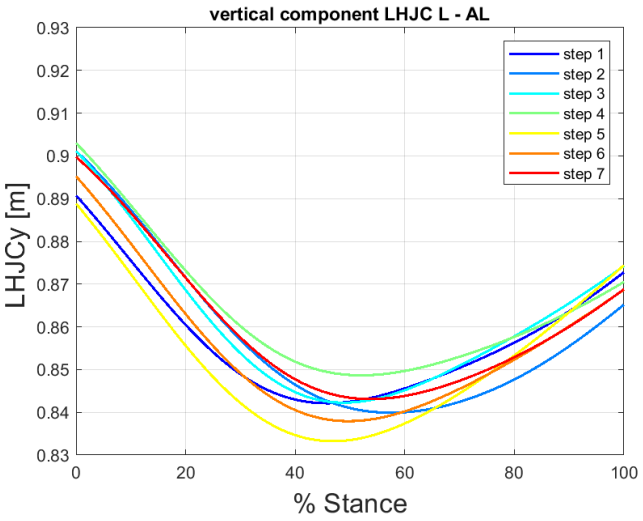

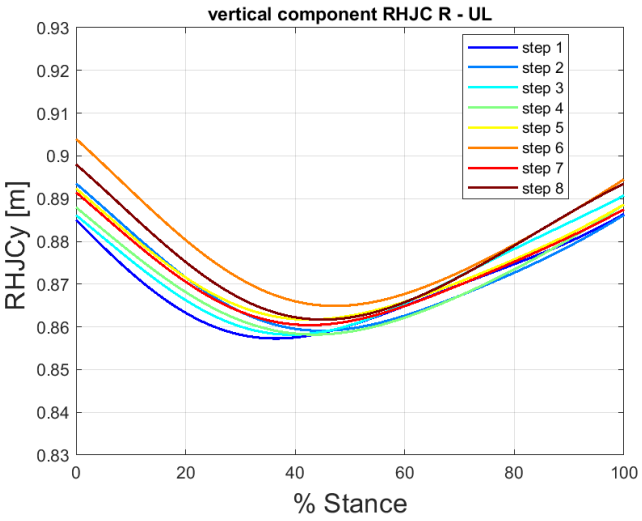

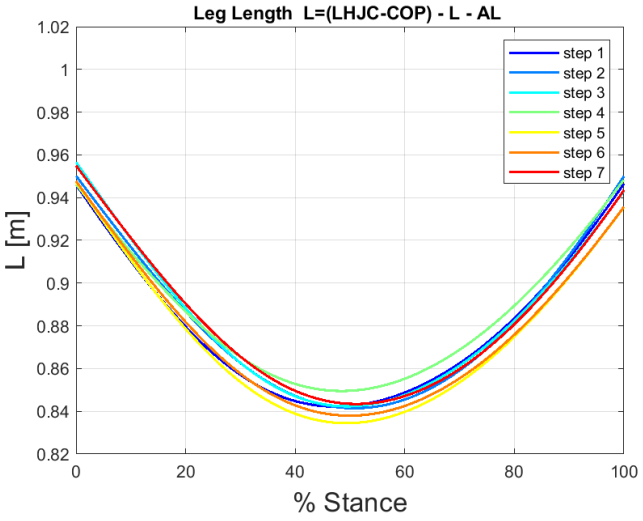

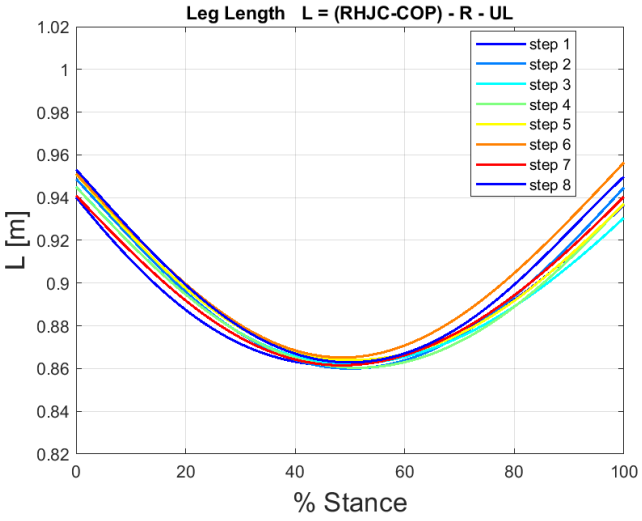

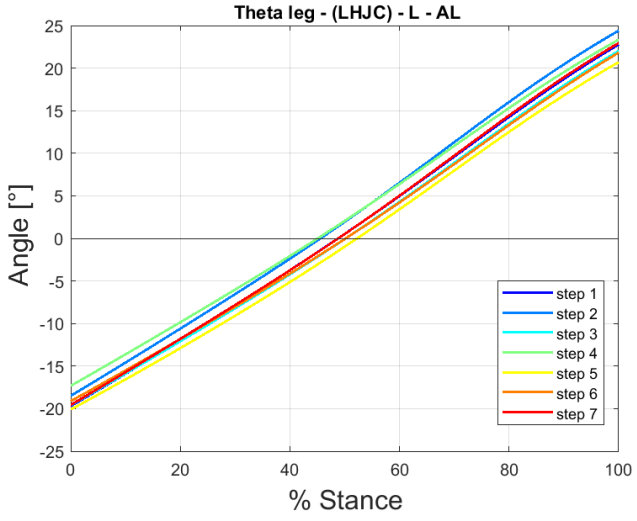

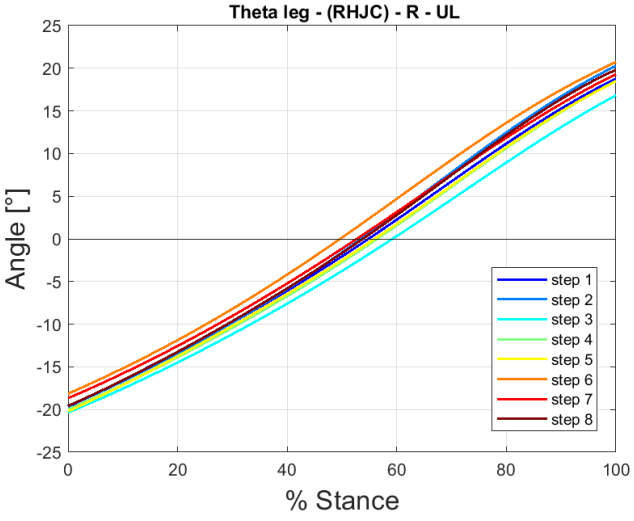

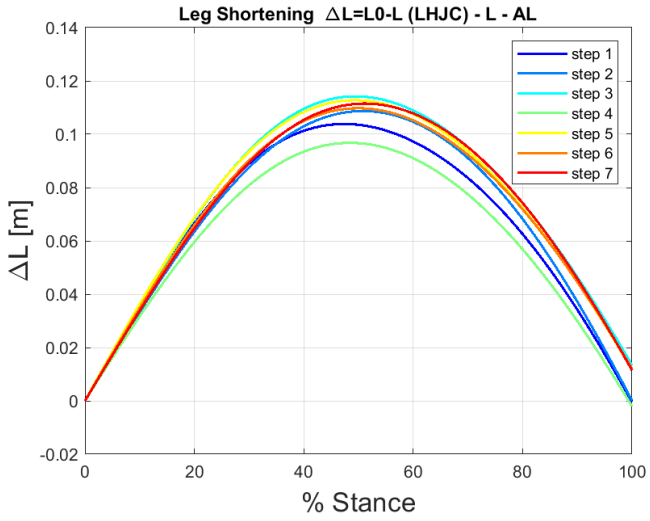
Leg Shortening ΔL=L0-L (LHJC) - L - AL
ΔL [m]
% Stance
step 1
step 2
step 3
step 4
step 5
step 6
step 7

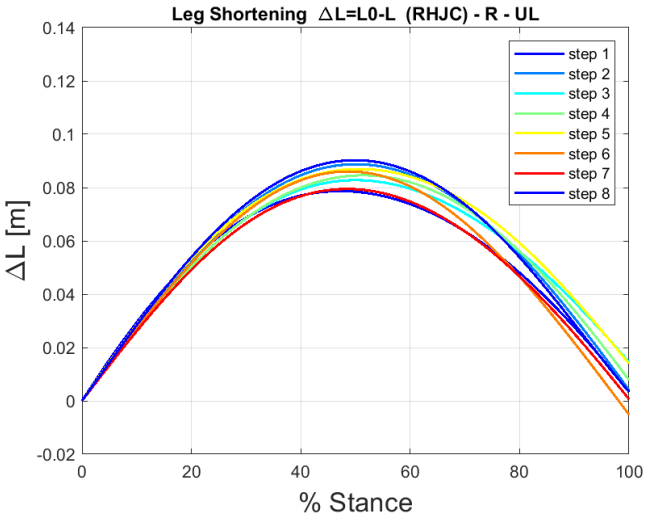
Leg Shortening ΔL=L0-L (RHJC) - R - UL
ΔL [m]
% Stance
step 1
step 2
step 3
step 4
step 5
step 6
step 7
step 8

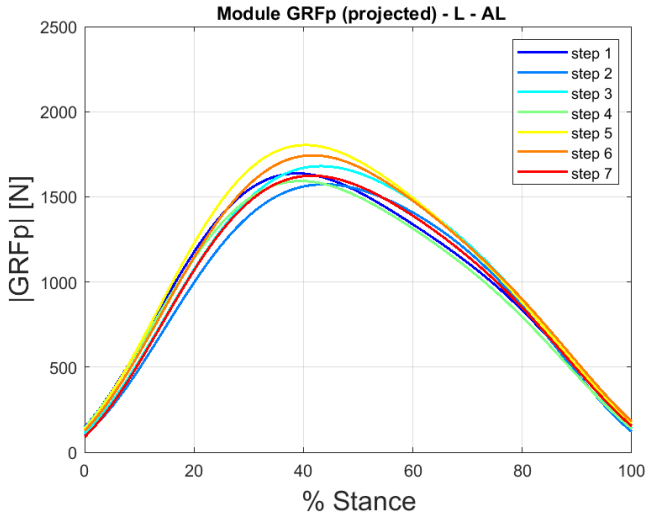
Module GRFp (projected) - L - AL
|GRFp| [N]
% Stance
step 1
step 2
step 3
step 4
step 5
step 6
step 7

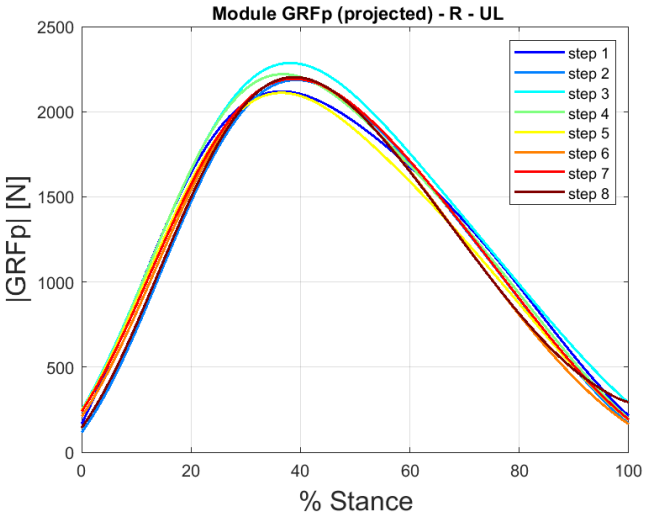
Module GRFp (projected) - R - UL
|GRFp| [N]
% Stance
step 1
step 2
step 3
step 4
step 5
step 6
step 7
step 8

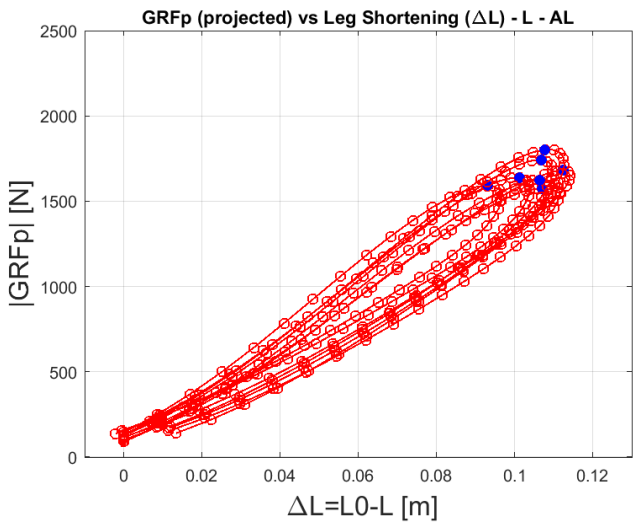
GRFp (projected) vs Leg Shortening (ΔL) - L - AL
|GRFp| [N]
ΔL=L0-L [m]

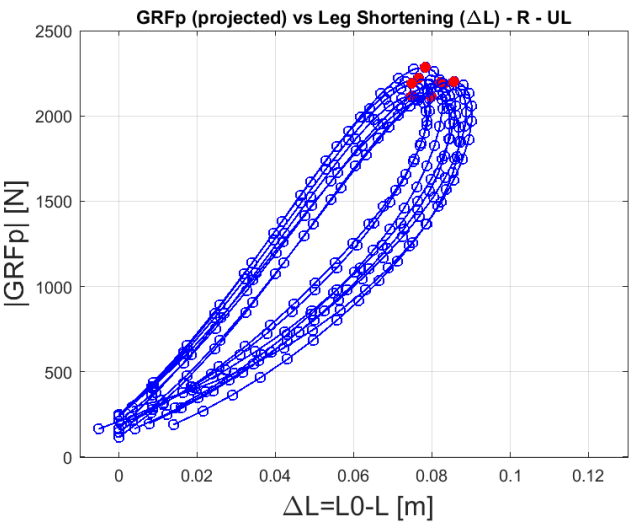
GRFp (projected) vs Leg Shortening (ΔL) - R - UL
|GRFp| [N]
ΔL=L0-L [m]

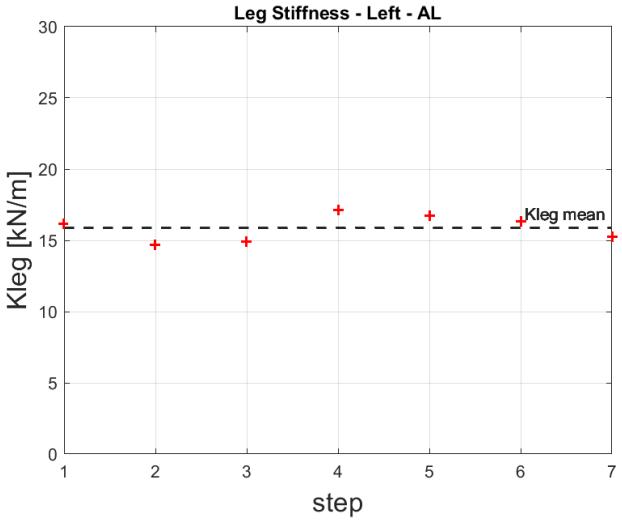

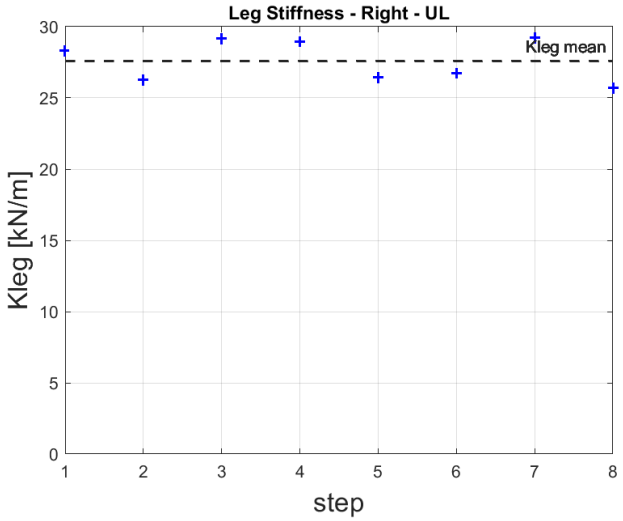

Leg Stiffness Model

Method 2: P=HJC

Alignment: A1

The K_{leg} values for each step, with the mean and standard deviation:

AL- Affected Limb

	Step 1	Step 2	Step 3	Step 4	step 5	Step 6	Step 7	**Mean**	**std**
K_{leg_AL} [kN/m]	16.2	14.7	14.9	17.1	16.7	16.3	15.3	**15.9**	**0.9**

UL – Unaffected Limb

	Step 1	Step 2	Step 3	Step 4	step 5	Step 6	Step 7	Step 8	**Mean**	**std**
K_{leg_UL} [kN/m]	28.3	26.3	29.2	29.0	26.4	26.7	29.2	25.7	**27.6**	**1.5**

P=HJC	Test Type	Socket Alignment	Limb
Treadmill	SSR	A2	AL/UL

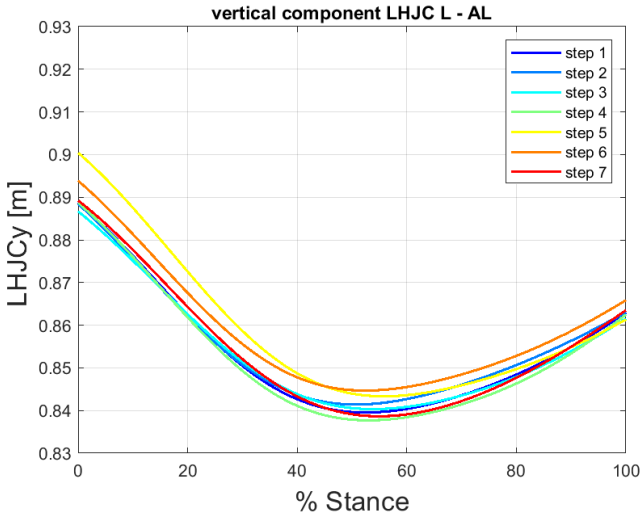

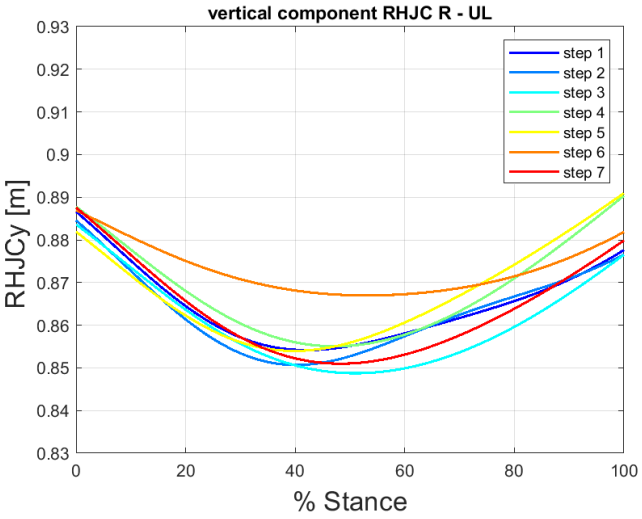

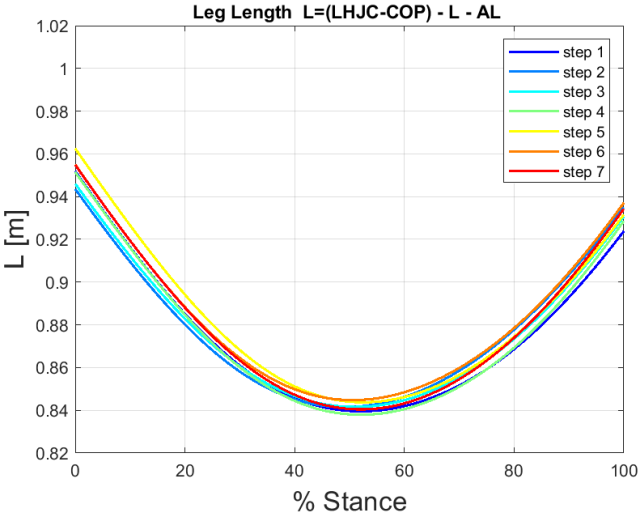

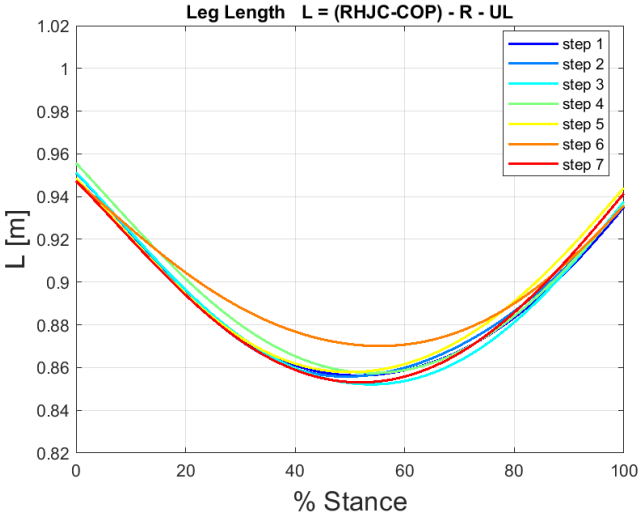

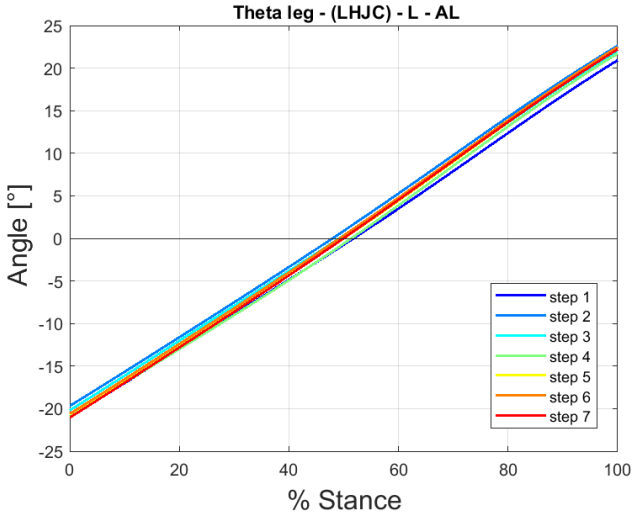

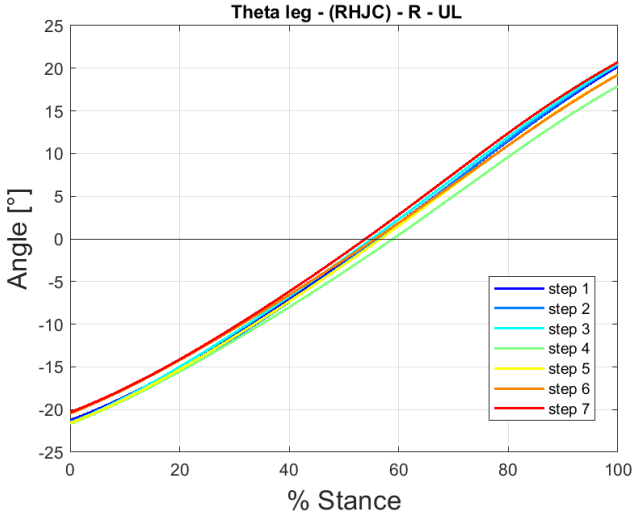

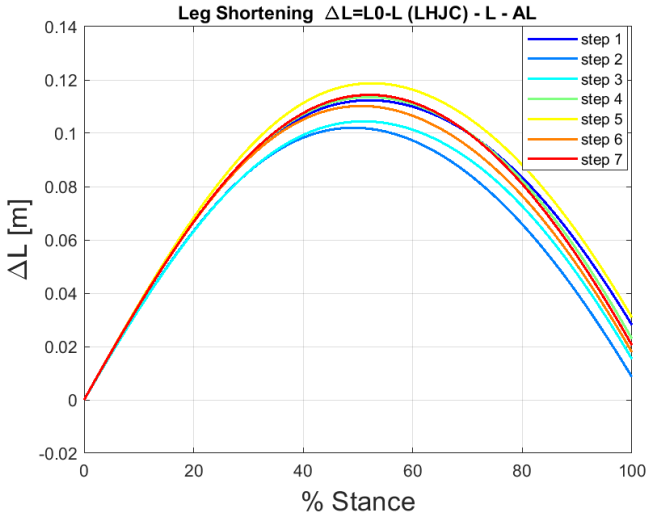
Leg Shortening ΔL=L0-L (LHJC) - L - AL
step 1
step 2
step 3
step 4
step 5
step 6
step 7
ΔL [m]
% Stance

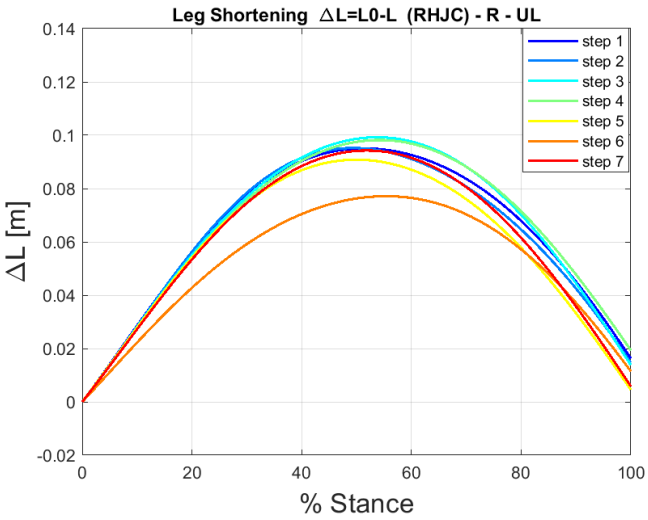
Leg Shortening ΔL=L0-L (RHJC) - R - UL
step 1
step 2
step 3
step 4
step 5
step 6
step 7
ΔL [m]
% Stance

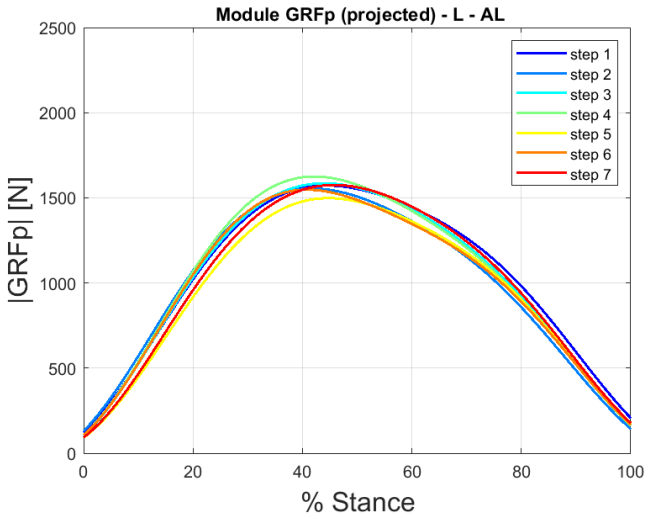
Module GRFp (projected) - L - AL
step 1
step 2
step 3
step 4
step 5
step 6
step 7
|GRFp| [N]
% Stance

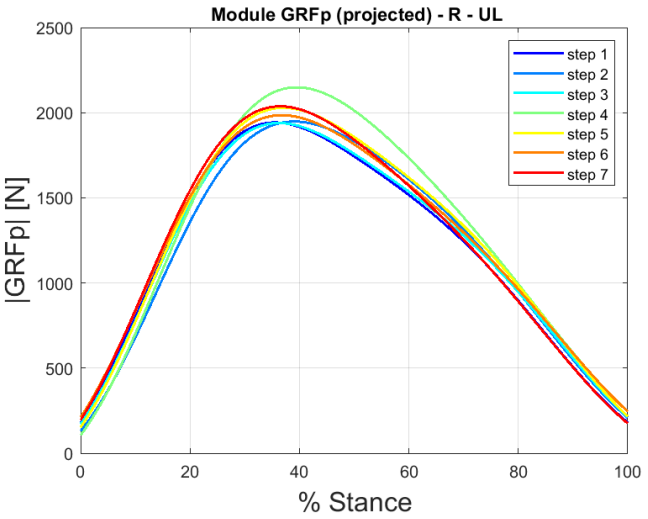
Module GRFp (projected) - R - UL
step 1
step 2
step 3
step 4
step 5
step 6
step 7
|GRFp| [N]
% Stance

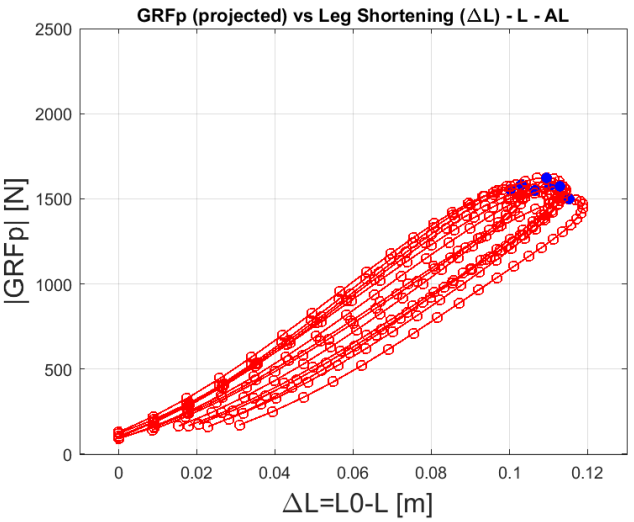
GRFp (projected) vs Leg Shortening (ΔL) - L - AL
|GRFp| [N]
ΔL=L0-L [m]

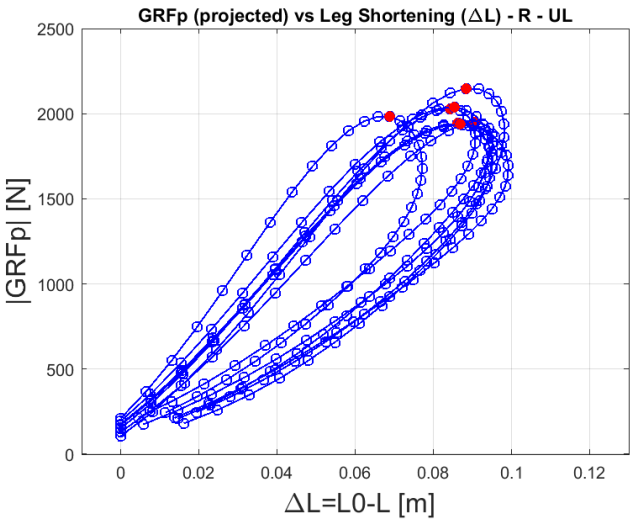
GRFp (projected) vs Leg Shortening (ΔL) - R - UL
|GRFp| [N]
ΔL=L0-L [m]

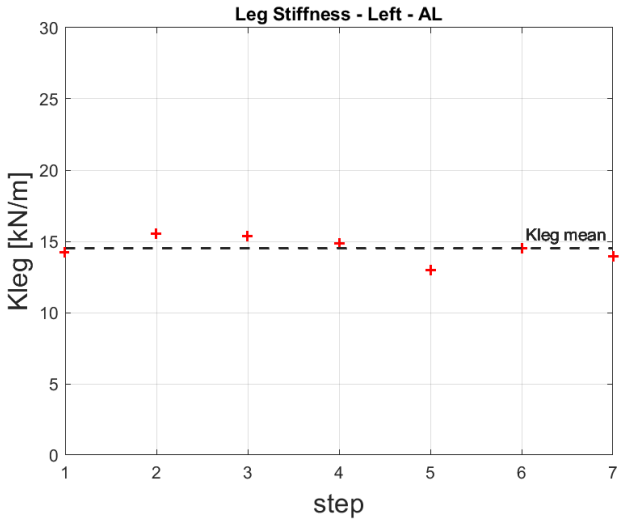

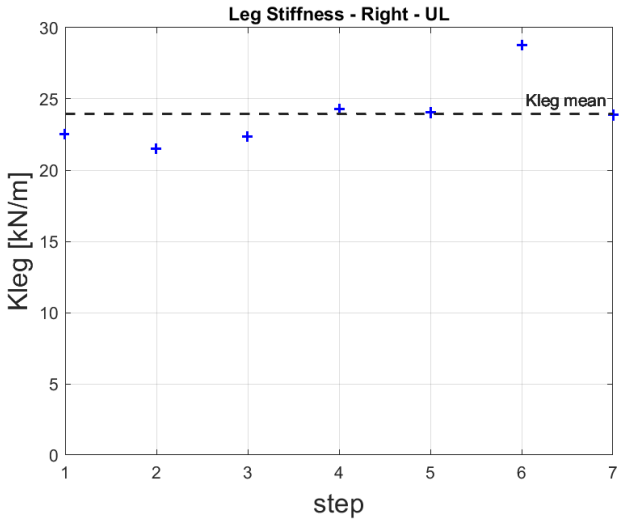

Leg Stiffness Model

Method 2: P=HJC

Alignment: A2

The K_{leg} values for each step, with the mean and standard deviation:

AL- Affected Limb

	Step 1	Step 2	Step 3	Step 4	step 5	Step 6	Step 7	**Mean**	**std**
K_{leg_AL} [kN/m]	14.3	15.5	15.4	14.8	13.0	14.5	14.0	**14.5**	**0.9**

UL- Unaffected Limb

	Step 1	Step 2	Step 3	Step 4	step 5	Step 6	Step 7	**Mean**	**std**
K_{leg_UL} [kN/m]	22.5	21.5	22.3	24.3	24.1	28.8	23.9	**23.9**	**2.4**

P=HJC	Test Type	Socket Alignment	Limb
Treadmill	SSR	A3	AL/UL

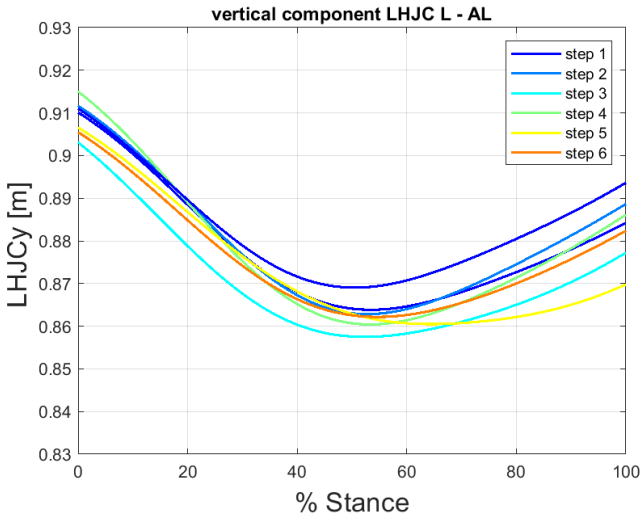

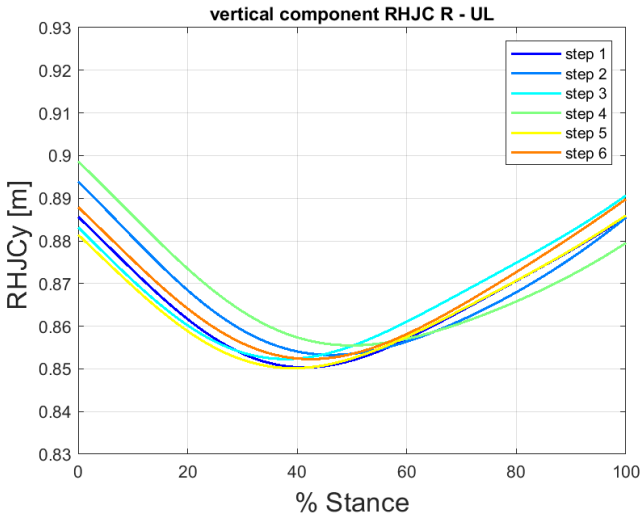

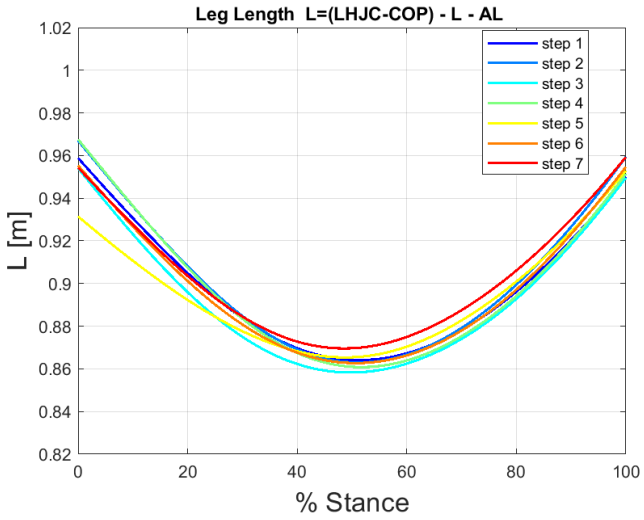

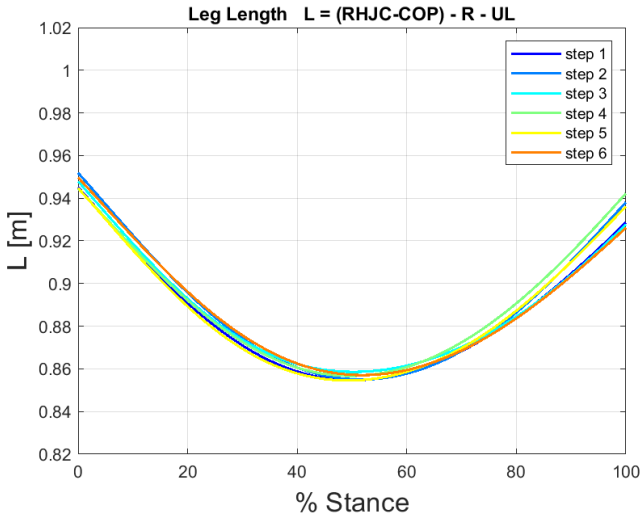

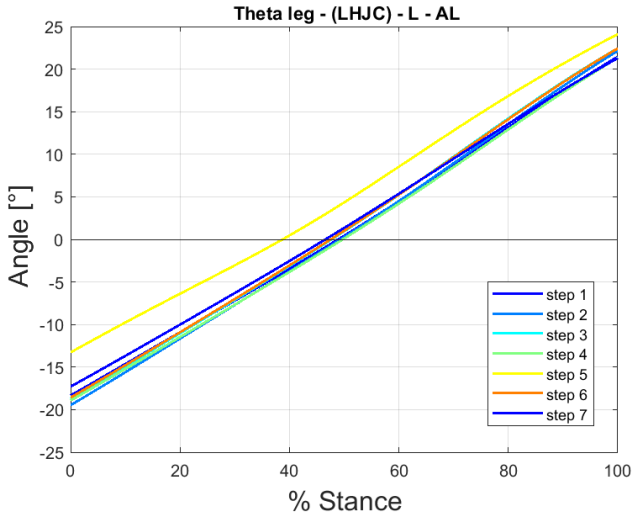

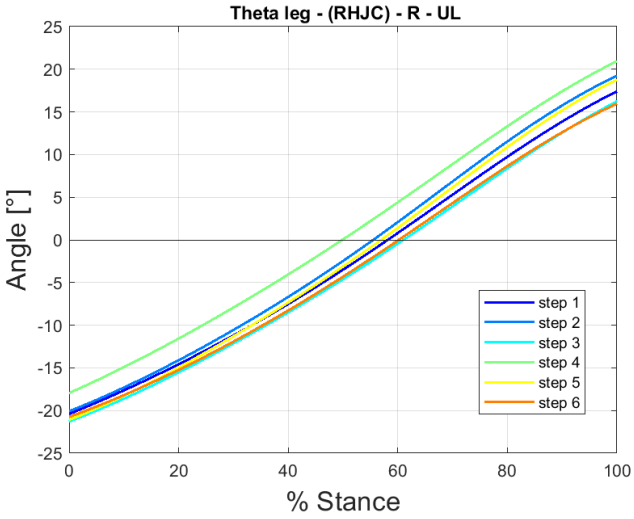

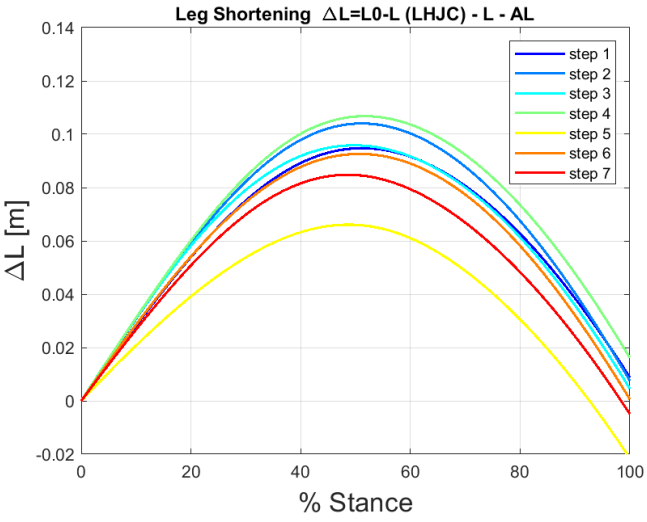
Leg Shortening ΔL=L0-L (LHJC) - L - AL
ΔL [m]
% Stance
step 1
step 2
step 3
step 4
step 5
step 6
step 7

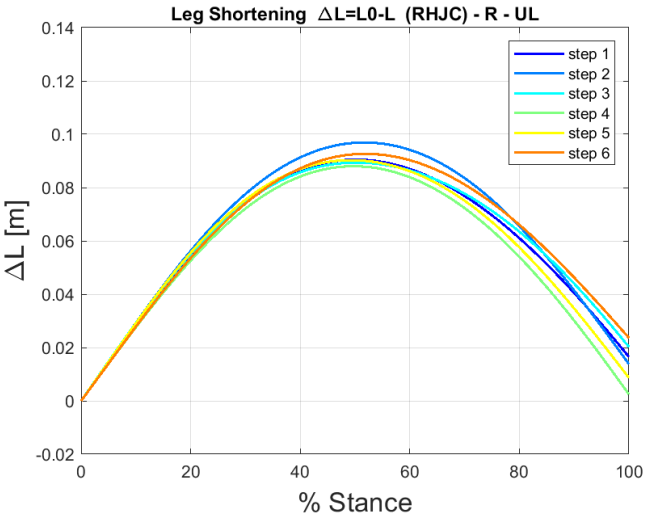
Leg Shortening ΔL=L0-L (RHJC) - R - UL
ΔL [m]
% Stance
step 1
step 2
step 3
step 4
step 5
step 6

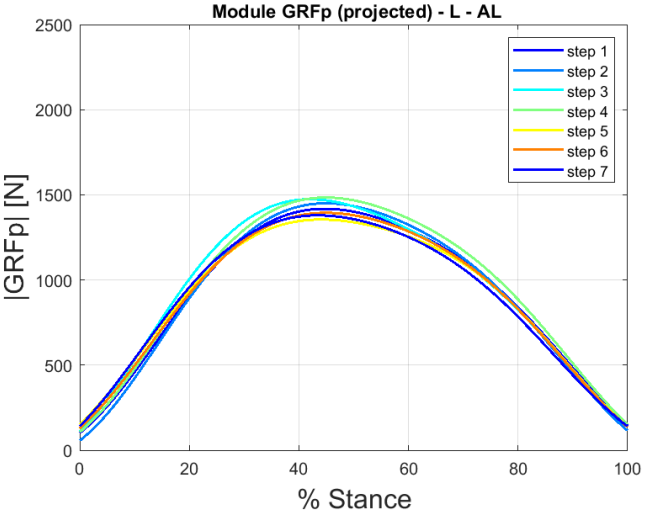
Module GRFp (projected) - L - AL
|GRFp| [N]
% Stance
step 1
step 2
step 3
step 4
step 5
step 6
step 7

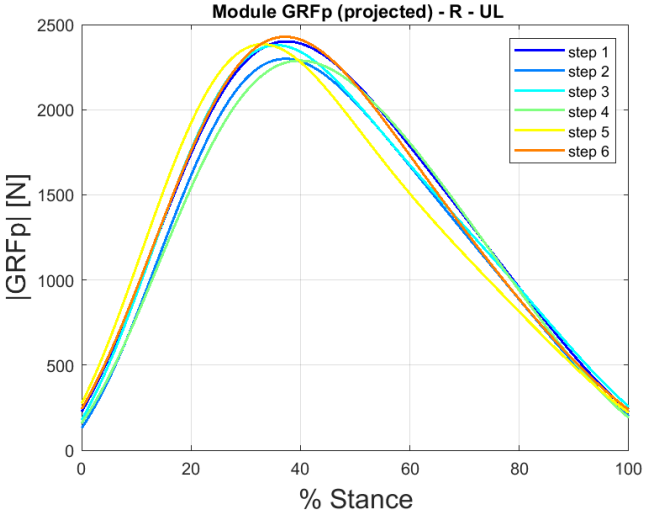
Module GRFp (projected) - R - UL
|GRFp| [N]
% Stance
step 1
step 2
step 3
step 4
step 5
step 6

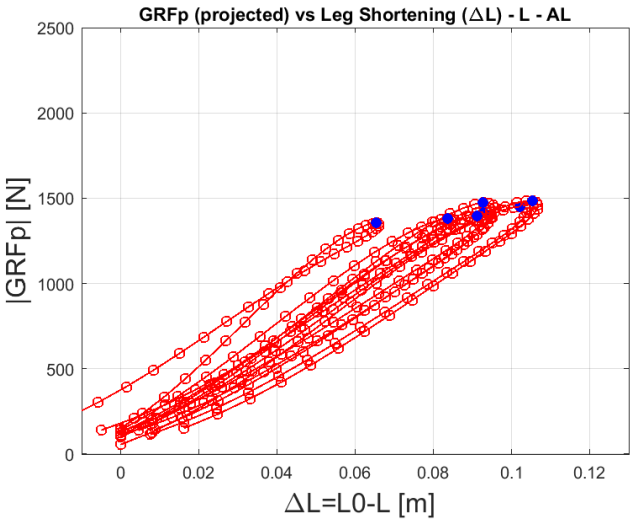
GRFp (projected) vs Leg Shortening (ΔL) - L - AL
|GRFp| [N]
ΔL=L0-L [m]

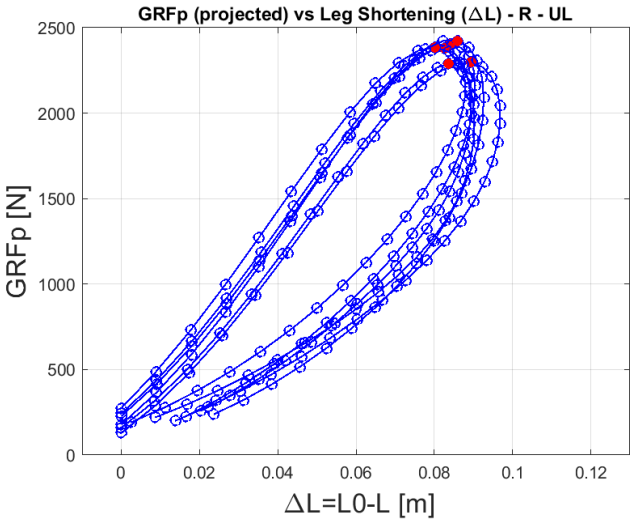
GRFp (projected) vs Leg Shortening (ΔL) - R - UL
GRFp [N]
ΔL=L0-L [m]

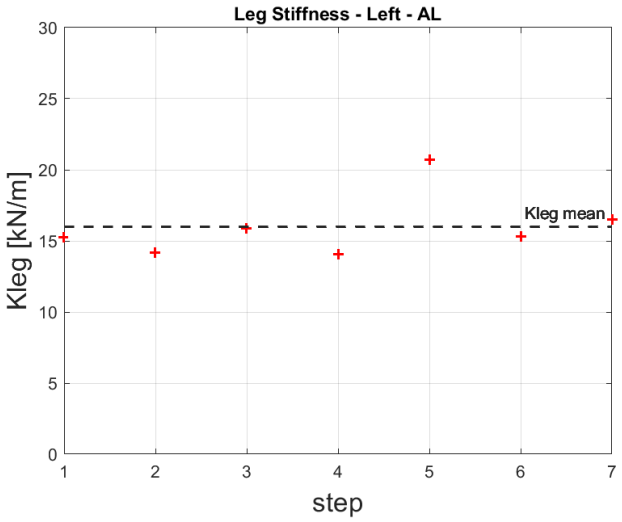

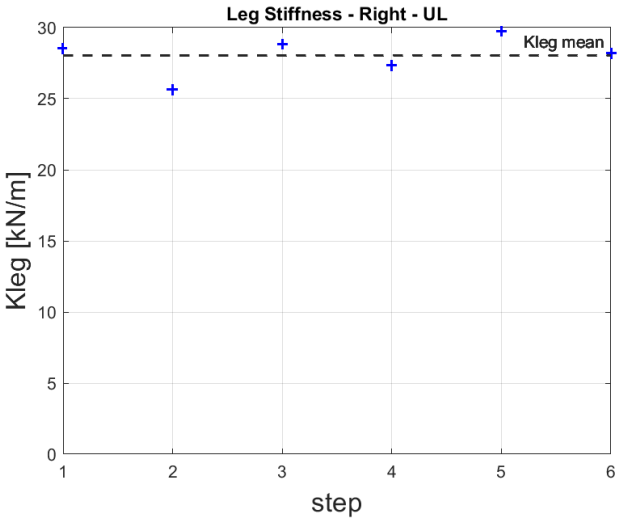

Leg Stiffness Model

Method 2: P=HJC

Alignment: A3

The K_{leg} values for each step, with the mean and standard deviation:

AL- Affected Limb

	Step 1	Step 2	Step 3	Step 4	Step 5	Step 6	Step 7	**Mean**	**std**
K_{leg_AL} [kN/m]	15.3	14.2	15.9	14.1	20.7	15.3	16.5	**16.0**	**2.2**

UL- Unaffected Limb

	Step 1	Step 2	Step 3	Step 4	Step 5	Step 6	**Mean**	**std**
K_{leg_UL} [kN/m]	28.6	25.7	28.8	27.4	29.7	28.2	**28.1**	**1.4**

P=HJC	Test Type	Socket Alignment	Limb
Track	TSSR 04	A3 Track	AL

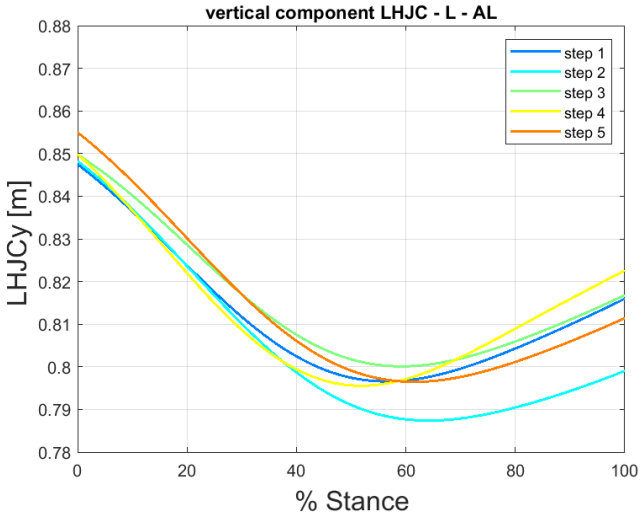

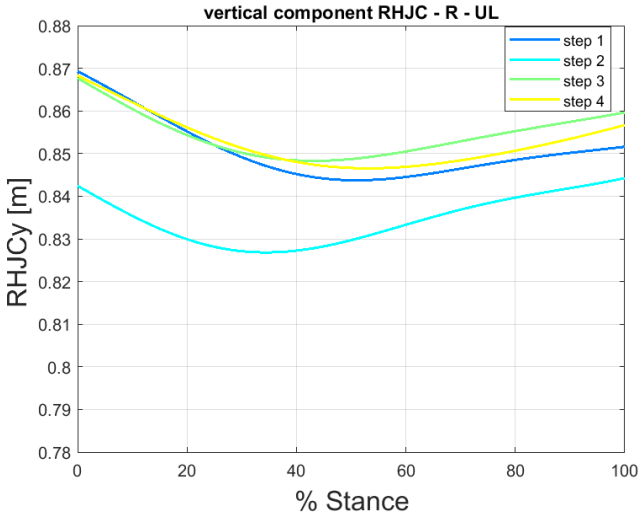

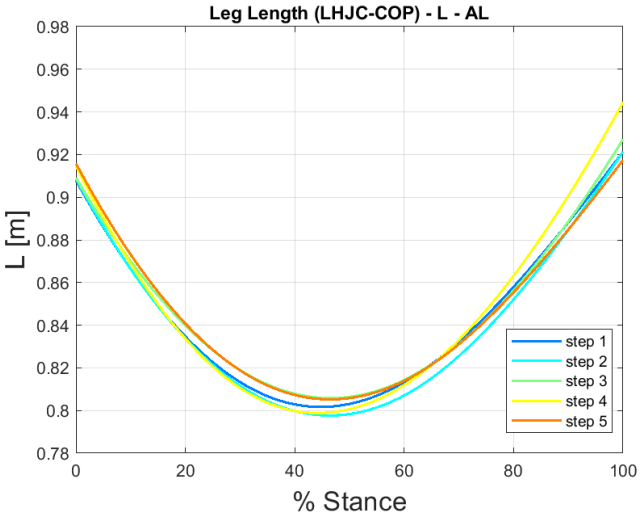

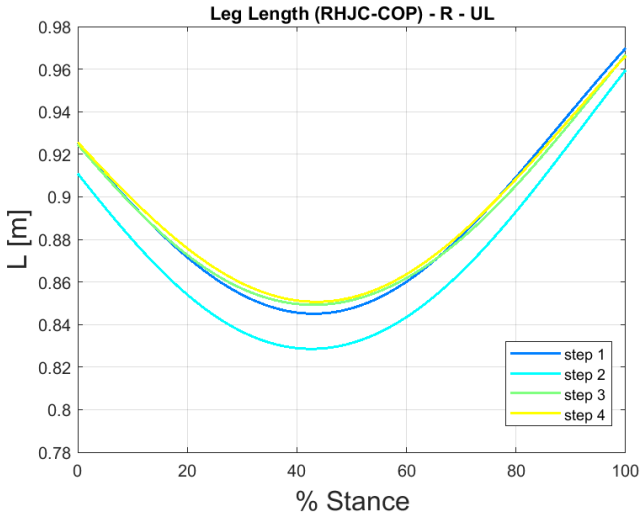

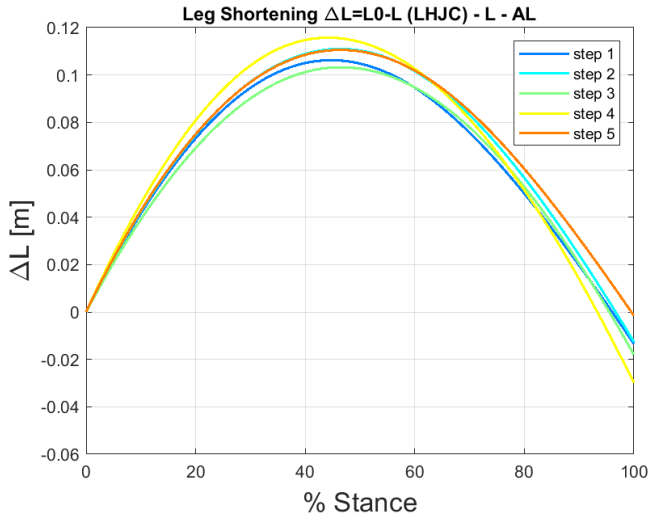

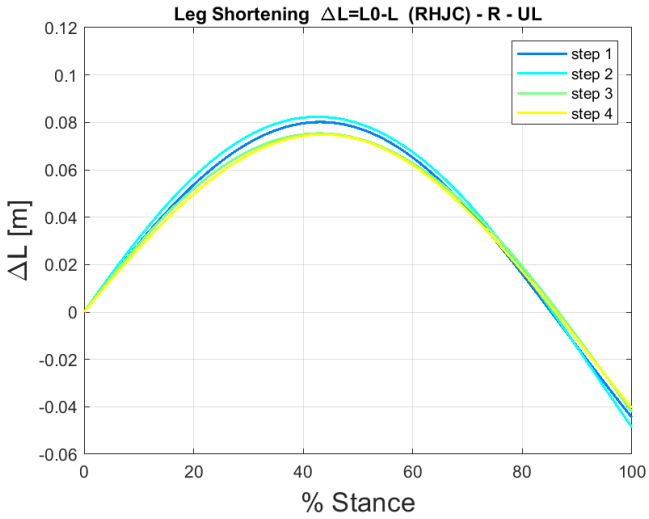

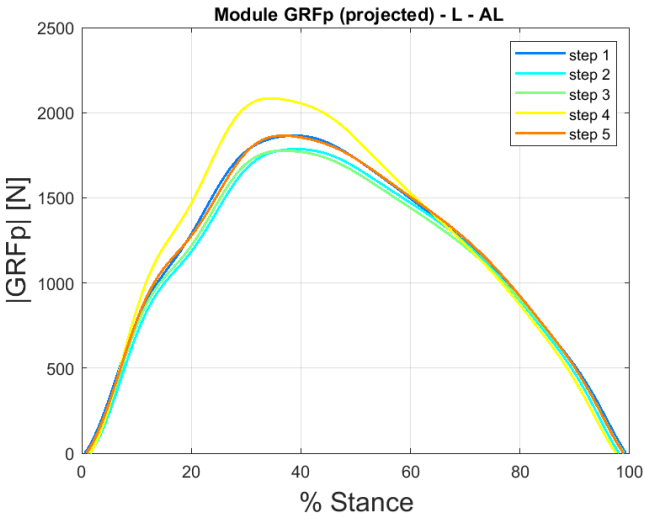

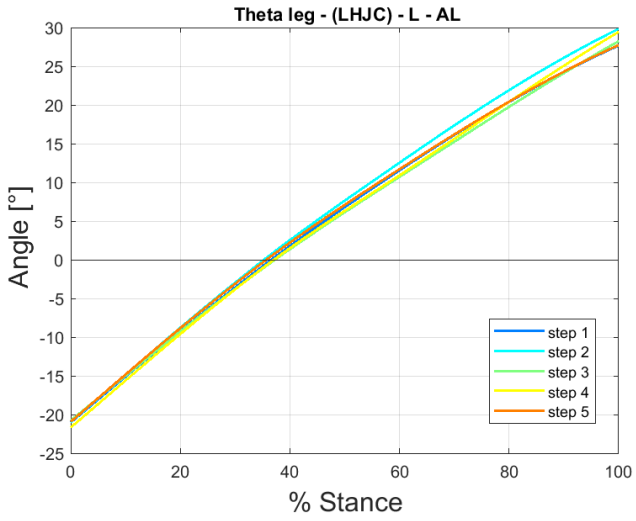

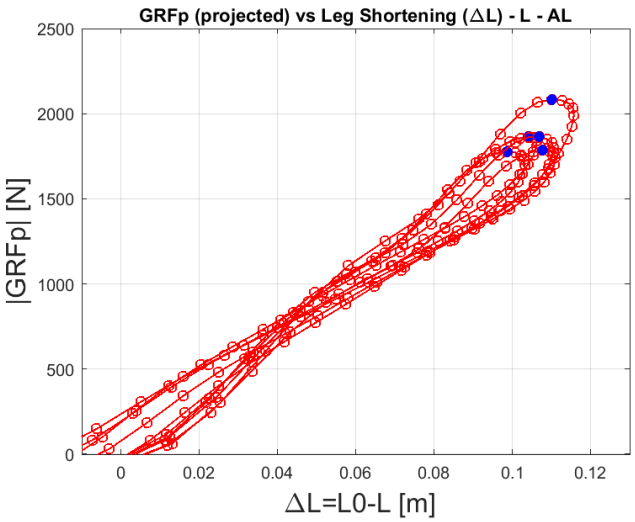

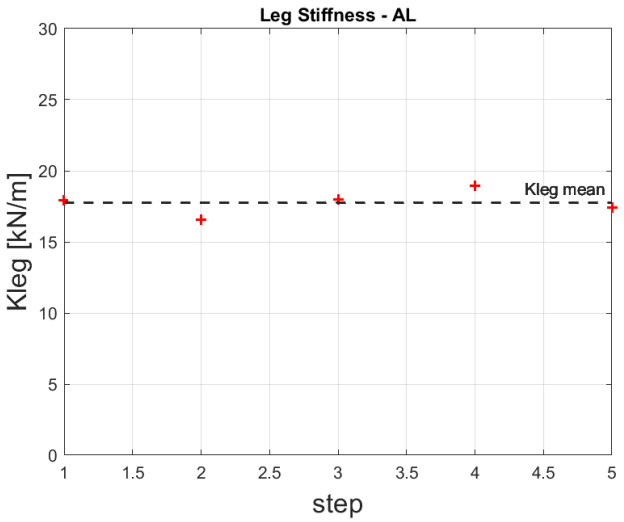

Leg Stiffness Model

Method 2: P=HJC

Alignment: A3 Track (TSSR 04)

The K_{leg} values for each step, with the mean and standard deviation:

AL- Affected Limb

	Step 1	Step 2	Step 3	Step 4	Step 5	Mean	std
K_{leg_AL} [kN/m]	17.9	16.6	18.0	18.9	17.4	17.8	0.9

The following bar plots synthesize the mean values of the Leg Stiffness (K_{leg}) calculated with the Method 2 (P=HJC), for each alignment of treadmill and track test (A3 Track):

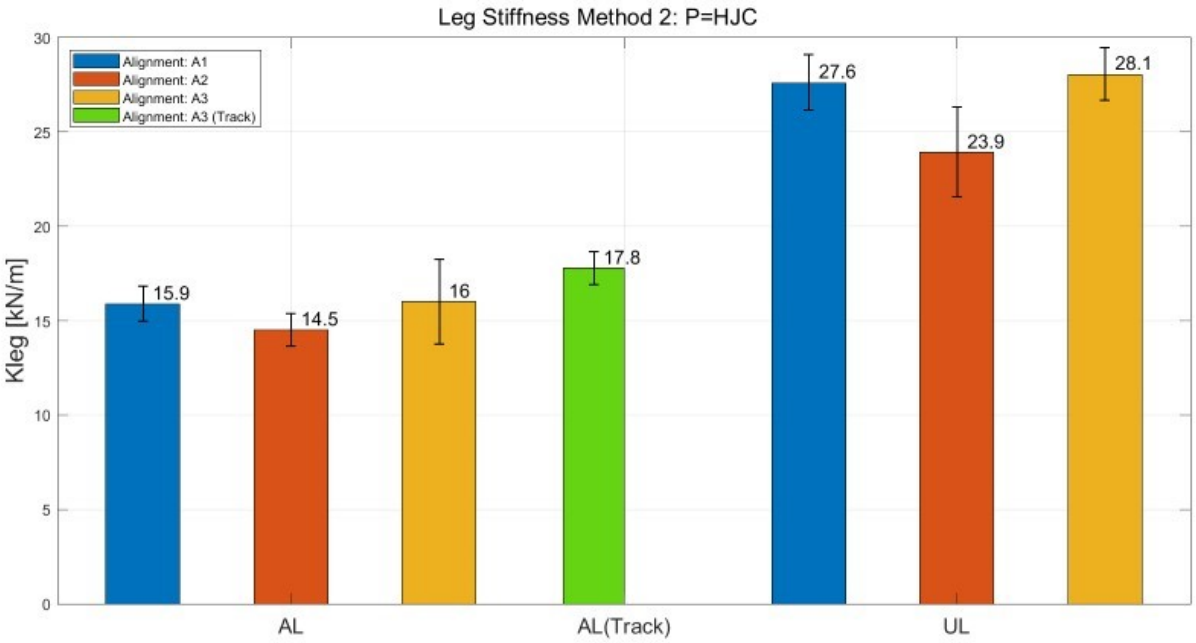

Figure 5.4: Leg Stiffness for the Affected Limb (AL) and Unaffected Limb (UL) for the alignments: A1 in blue, A2 in red and A3 in yellow; A3 (track) in green.

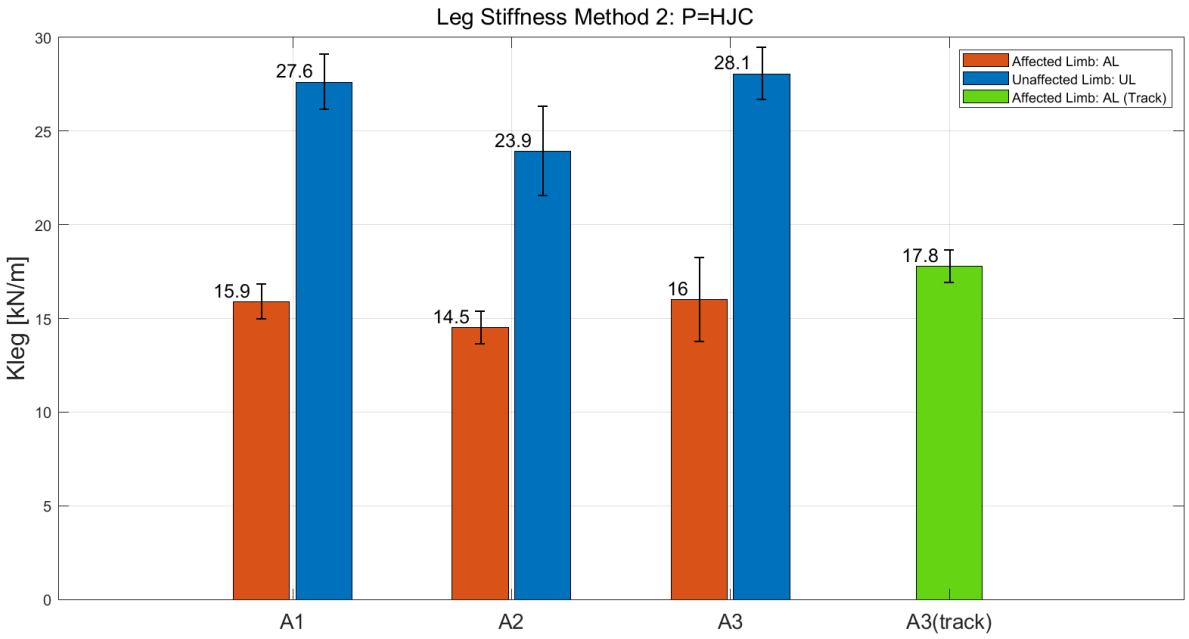

Figure 5.5: Leg Stiffness for all alignments (A1, A2, A3, A3 Track): in red the Affected Limb (AL), in blue the Unaffected Limb (UL) on treadmill. In green the Affected Limb on Track (A3 Track).

L_{HJC} = forward trajectory length of HJC, during stance – 'Contact Length'

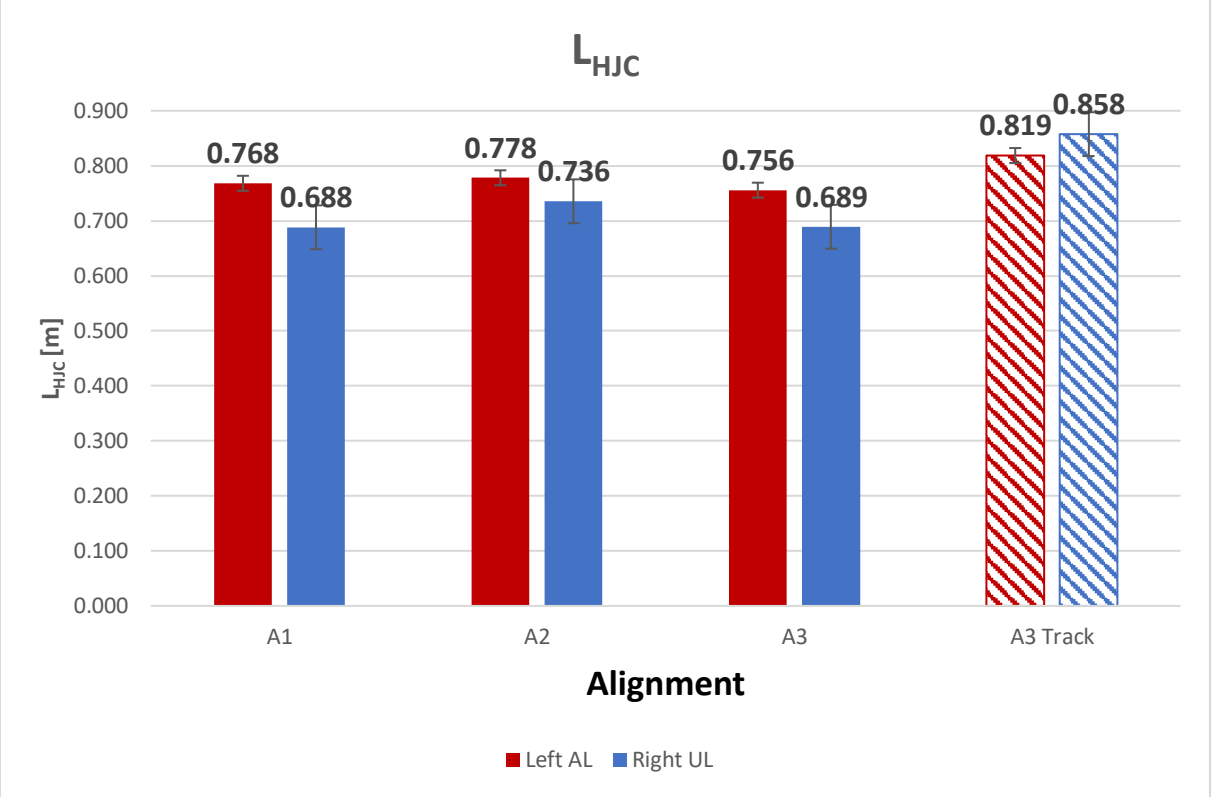

Figure 5.6: L_{HJC} -Contact Length with Method 2 (P=HJC).

2. Foot Stiffness Model

The results from the *Foot Stiffness Model* are also shown, looking at all the different alignments.

For the Affected Limb (left limb for the athlete AS), the meaningful quantities pictured in the analysis are:

- Foot Length (**d**) in % stance.
- Foot Orientation (Theta) in % stance.
- Foot Shortening ($\boldsymbol{\Delta d}$) in % stance.
- Module of the projected GRF ($\left|\overrightarrow{GRF_p}\right|$) in % stance.
- The projected GRF ($\left|\overrightarrow{GRF_p}\right|$) vs Foot Shortening ($\boldsymbol{\Delta d}$)
- The Foot Stiffness for each step of the acquisition.

P=CL	Test Type	Socket Alignment	Limb
Treadmill	SSR	A1	AL

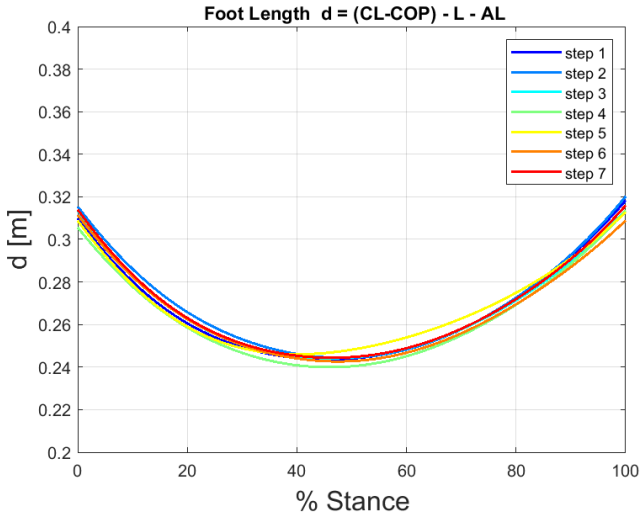

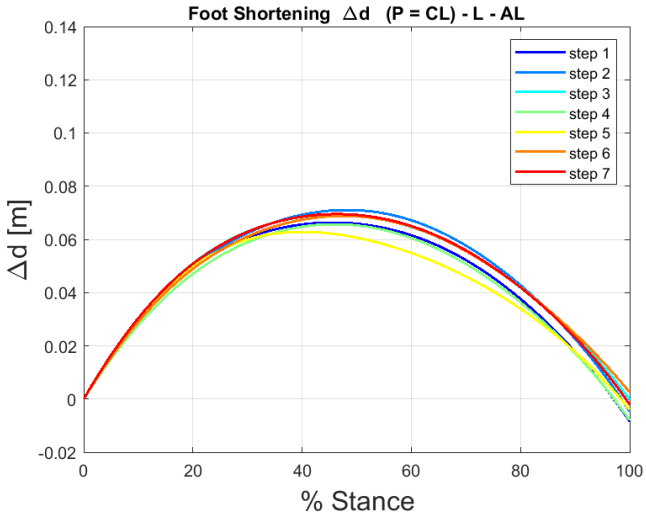

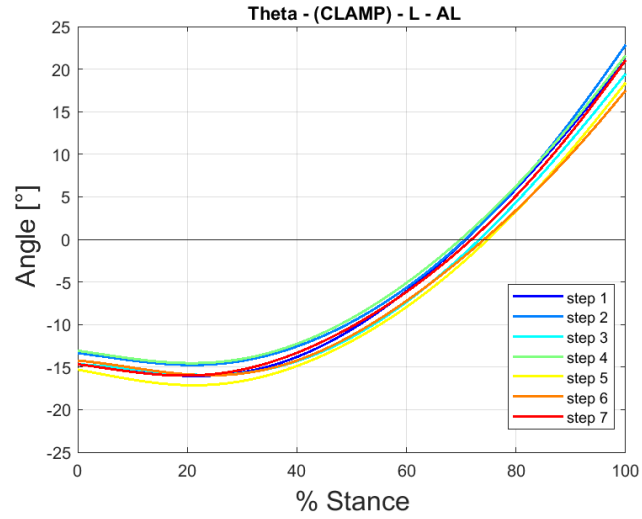

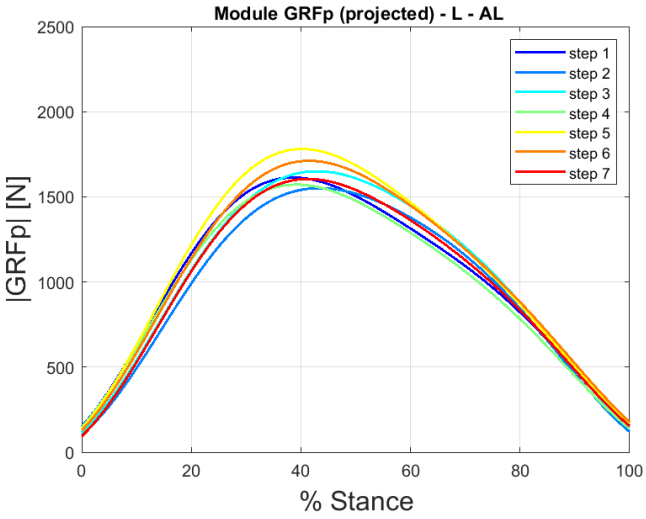

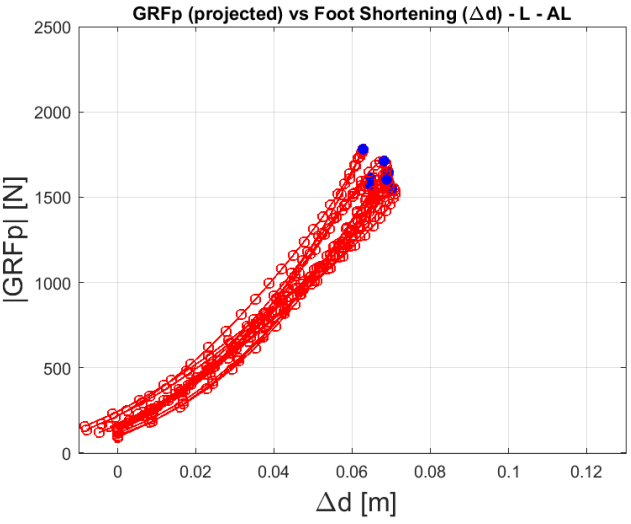

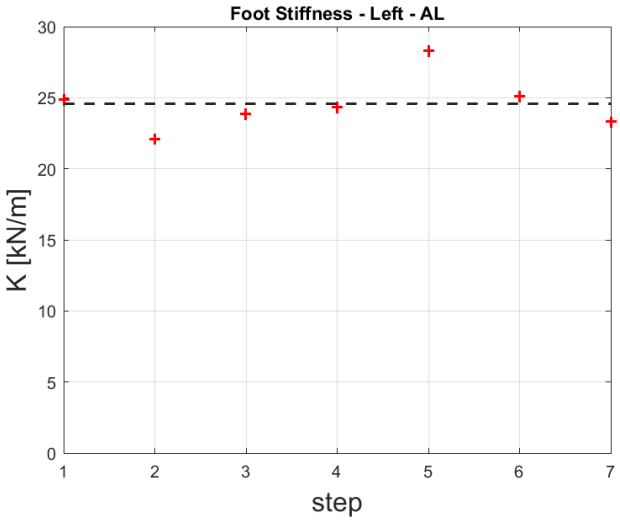

P=CL	Test Type	Socket Alignment	Limb
Treadmill	SSR	A2	AL

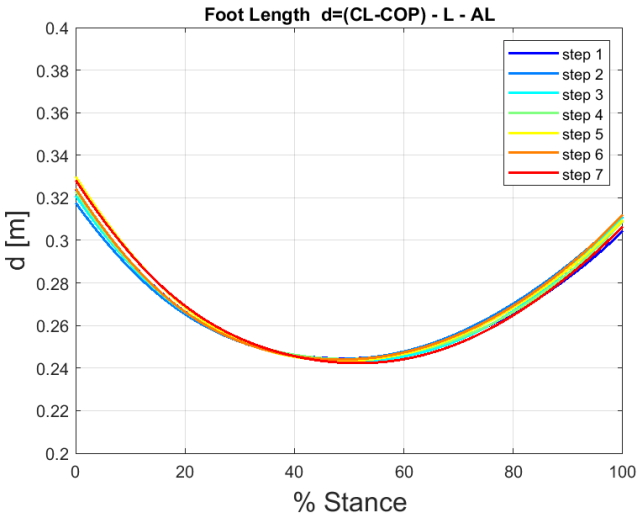

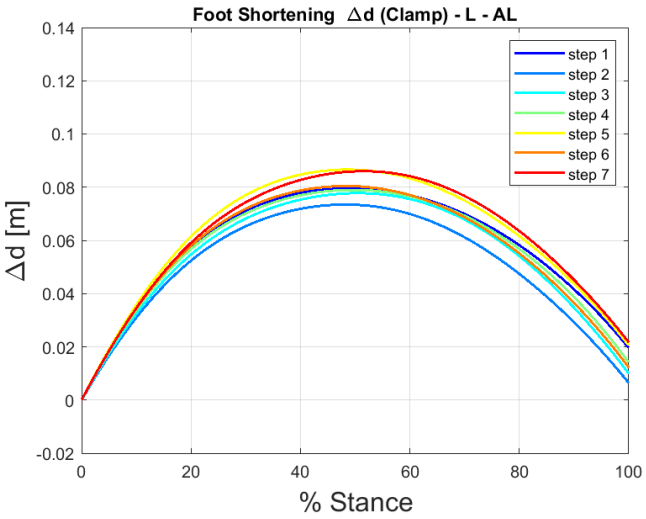

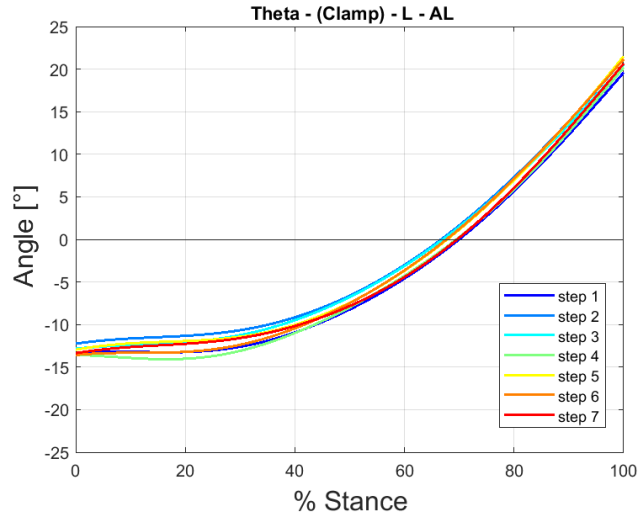

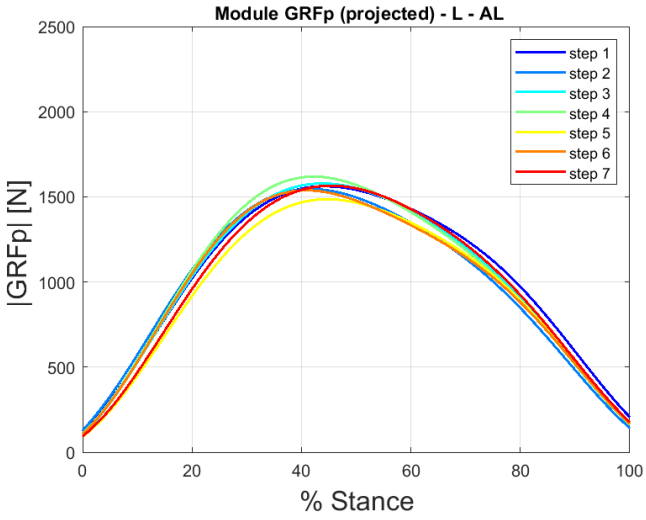

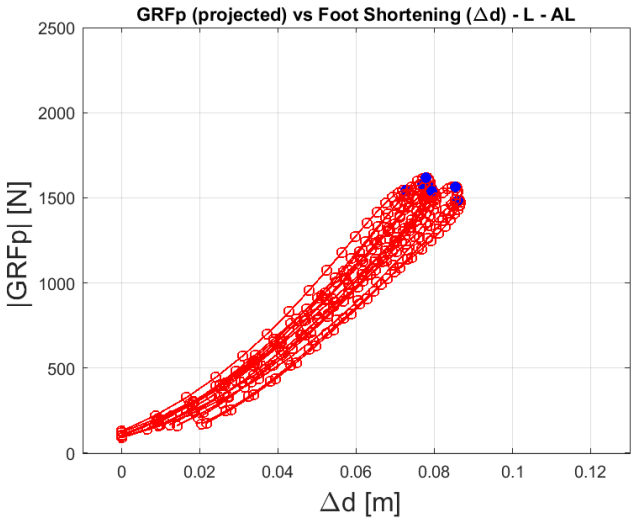

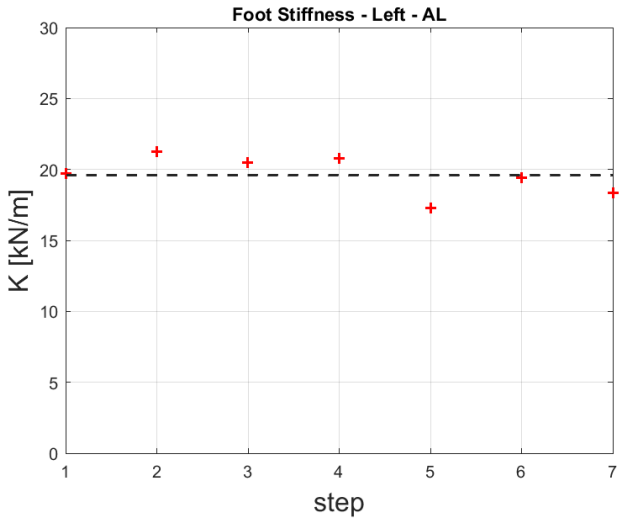

P=CL	Test Type	Socket Alignment	Limb
Treadmill	SSR	A3	AL

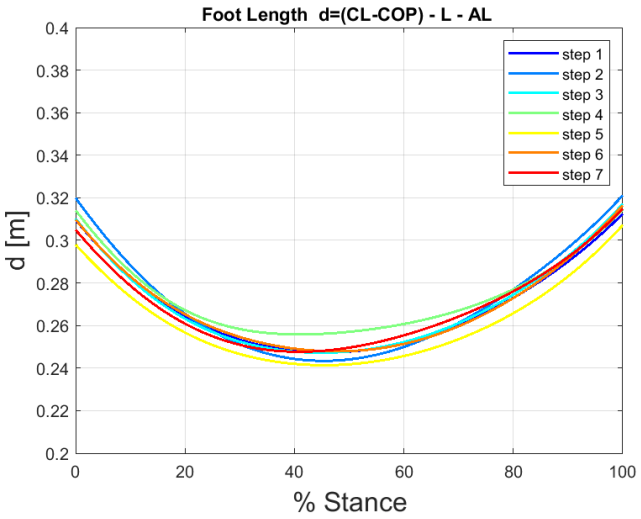

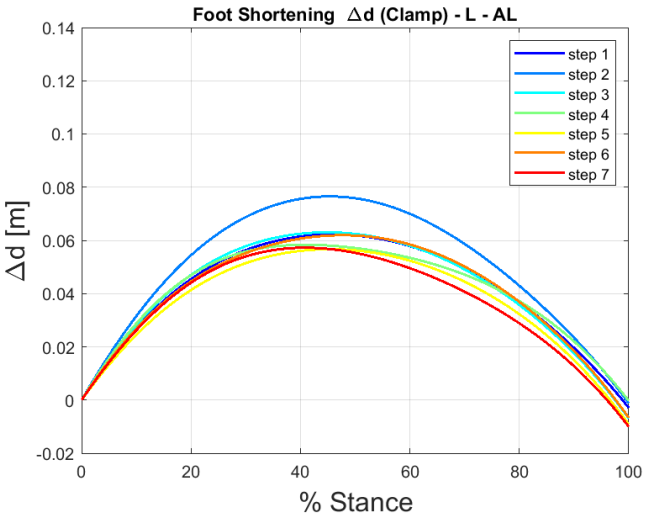

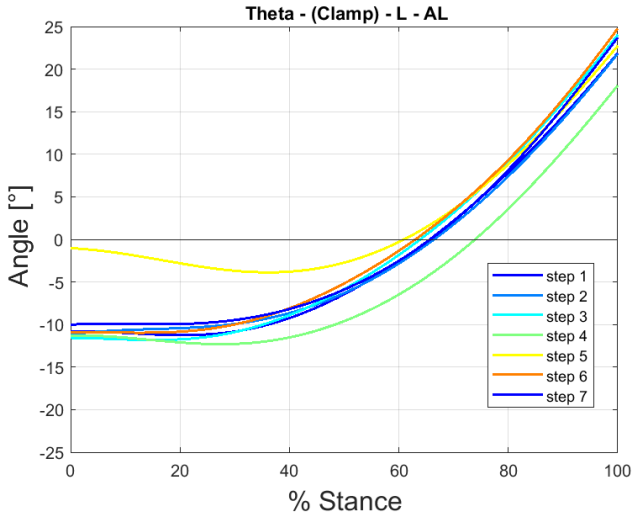

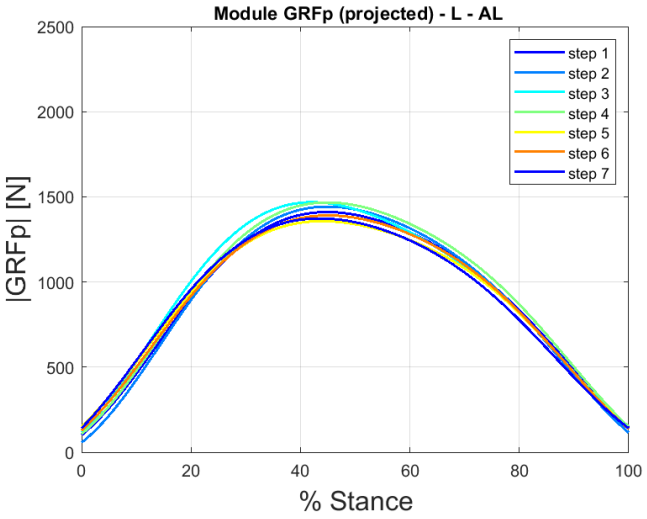

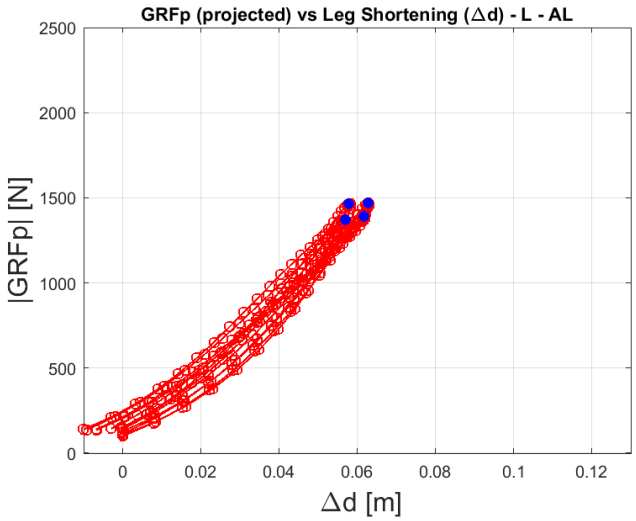

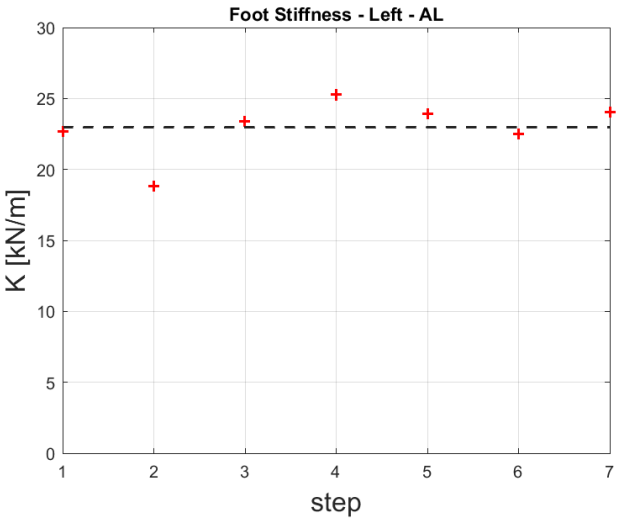

P=CL	Test Type	Socket Alignment	Limb
Treadmill	TSSR 04	A3 Track	AL

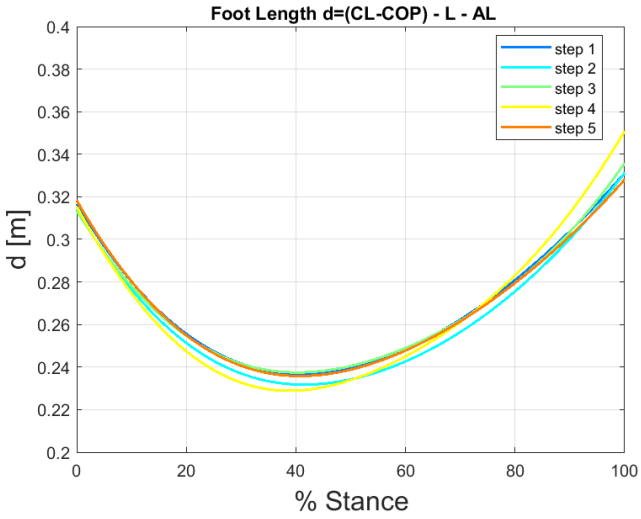

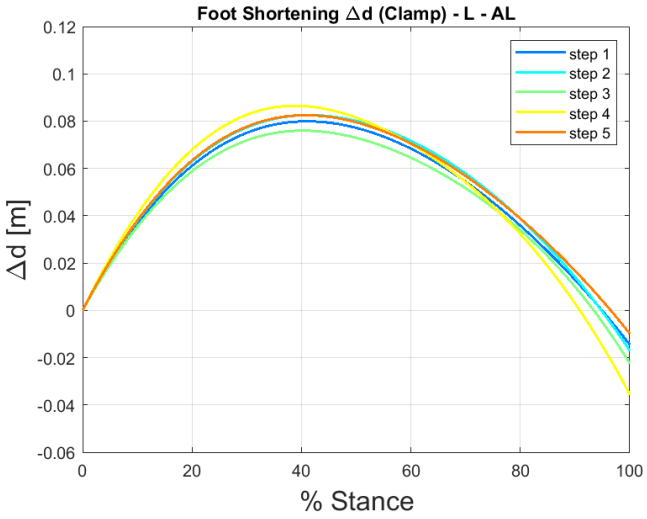

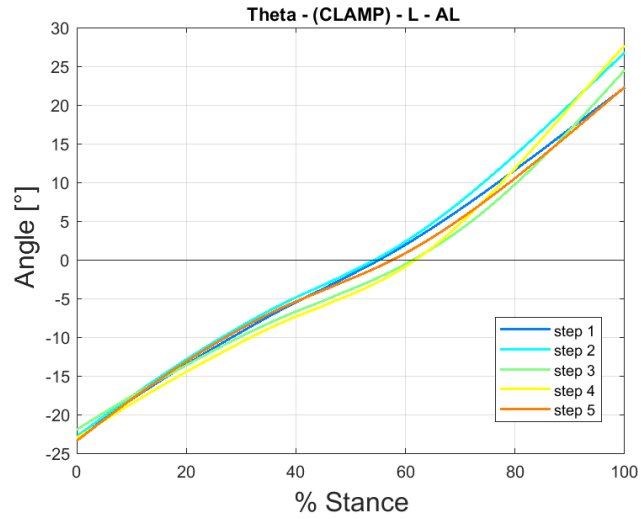

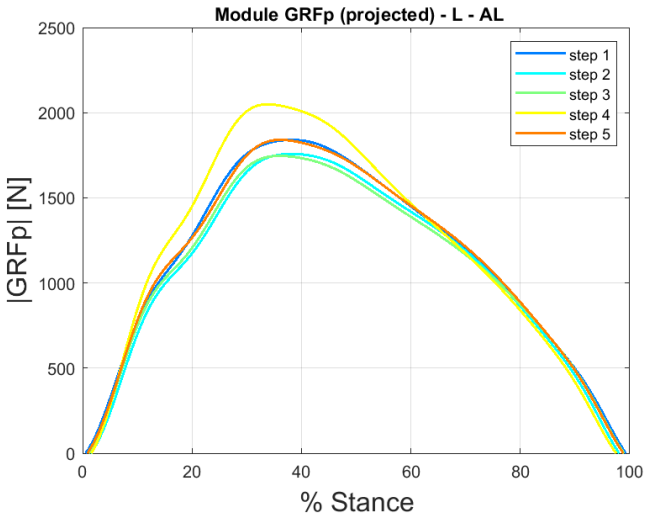

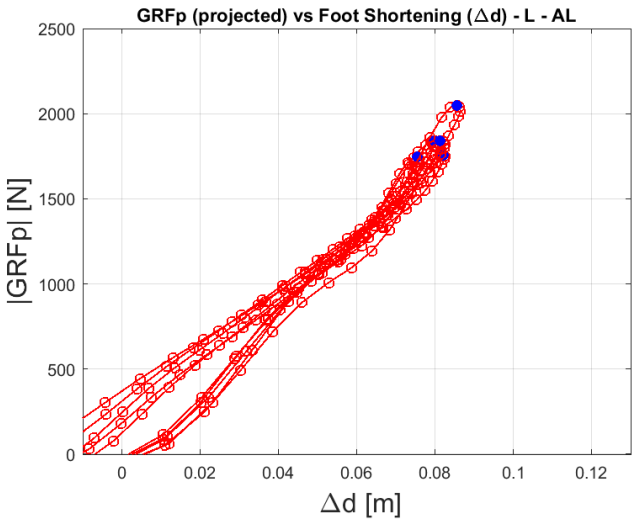

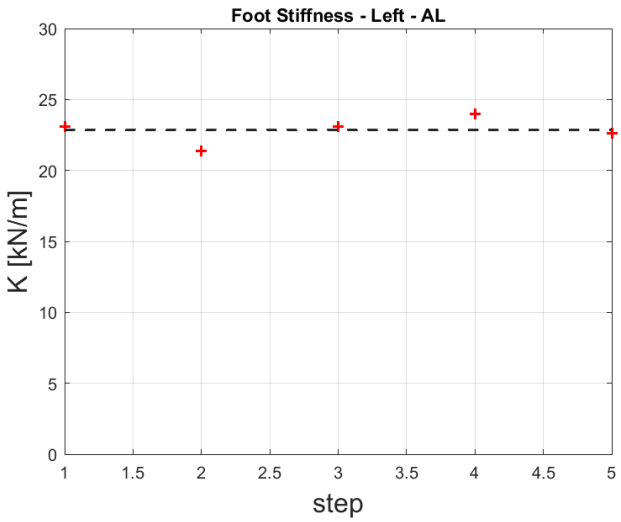

Chapter 6: Discussion and Conclusion

Discussion

The aim of this work was to calculate the *Leg Stiffness* in unilateral amputee elite athletes, during treadmill running and track sprinting. Furthermore, it was possible to investigate the influence of the prosthetic foot, with its foot stiffness, and the residual limb on the overall leg stiffness.

This is a case study, due to the fact that only an athlete has been investigated: the data from the in-vivo experimental test were carried out with the gold medallist sprinter Ambra Sabatini.

A spring-mass model has been implemented, considering different methods of calculation, related to the choice of the proximal point of the model:

- Method 1: P=COM
- Method 2: P=HJC

The results showed in the chapter 5, are summarized in the following tables: for the in-vivo experimental session, either for the treadmill or track tests and all the socket alignments (A1, A2, A3, A3 Track).

Leg Stiffness Model - Method 1: P=COM

Alignment	**A1**	**A2**	**A3**	**A3 Track**
K_{leg_AL} [kN/m]	15.4 ± 1.0	14.2 ± 0.8	15.3 ± 1.8	17.5 ± 1.0
K_{leg_UL} [kN/m]	25.6 ± 1.4	23.2 ± 1.8	26.3 ± 1.5	-

Leg Stiffness Model - Method 2: P=HJC

Alignment	**A1**	**A2**	**A3**	**A3 Track**
K_{leg_AL} [kN/m]	15.9 ± 0.9	14.5 ± 0.9	16.0 ± 2.2	17.8 ± 0.9
K_{leg_UL} [kN/m]	27.6 ± 1.5	23.9 ± 2.4	28.1 ± 1.4	-

Given the model, with its assumptions and simplifications, it was possible to study and quantify additional considerations regarding the leg stiffness:

a) What is the difference on the K_{leg} between AL e UL?
b) What is the difference on the K_{leg} between Treadmill and Track?
c) Are there any changes on the K_{leg} considering different socket alignment? (A1, A2, A3)

a) Differences between AL and UL

Since for test on track no forces have been measured for the unaffected limb, the investigation of the differences between AL and UL is possible only for the treadmill tests.

The *Kleg* estimated is very stable for each step in both limbs. An example of these results is showed below:

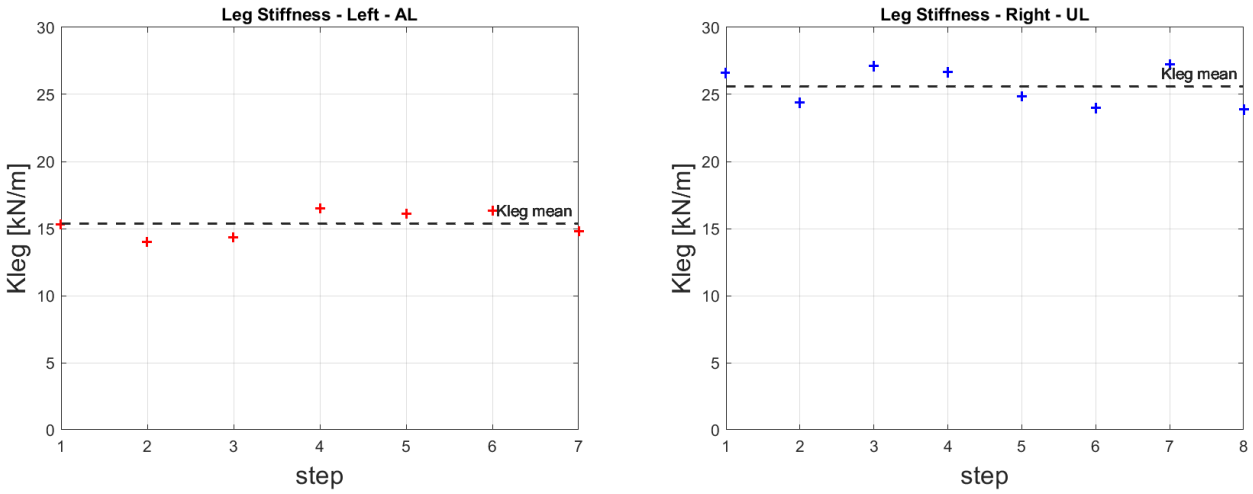

Figure 6.1: Leg Stiffness values for each step with alignment A1 (treadmill) calculated with Method 1 (P=COM).

The mean values of the Leg Stiffness calculated with Method 1 (P=COM) are represented in the bar plots below:

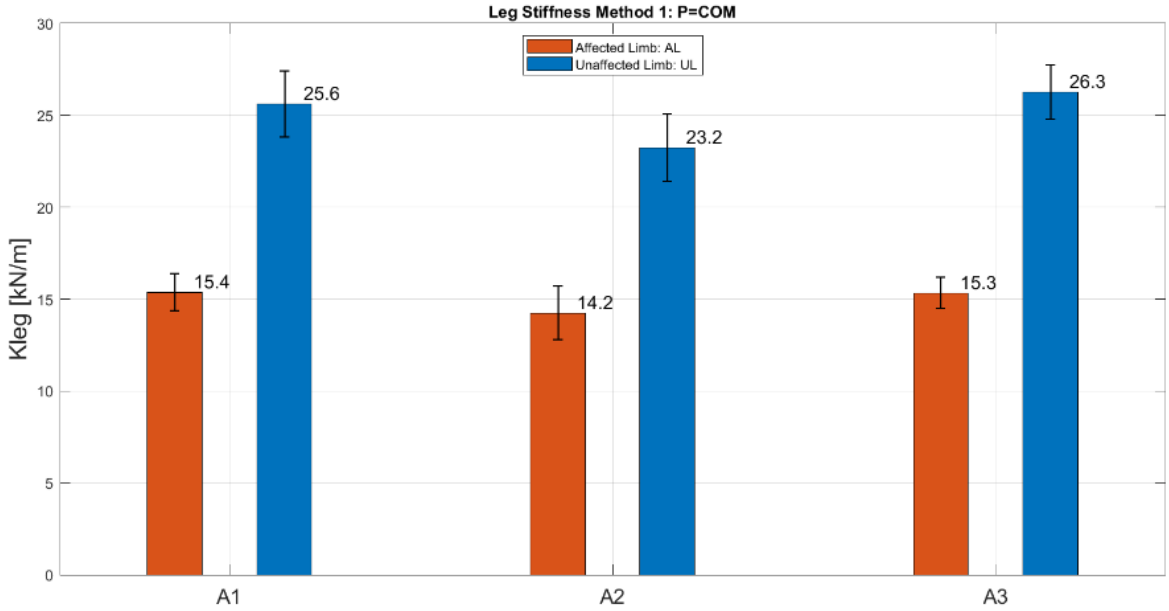

Figure 6.2: Leg Stiffness on treadmill, calculated with Method 1 (P=COM)

With Method 1 (P=COM) the differences in the Leg Stiffness between the Affected Limb (AL) and the Unaffected Limb (UL) are:

- AL 40% lower than UL with alignment A1
- AL 38.7% lower than UL with alignment A2
- AL 41.7% lower than UL with alignment A3

With method 2 (P=HJC) the mean values of the Leg Stiffness calculated represented in the bar plots below:

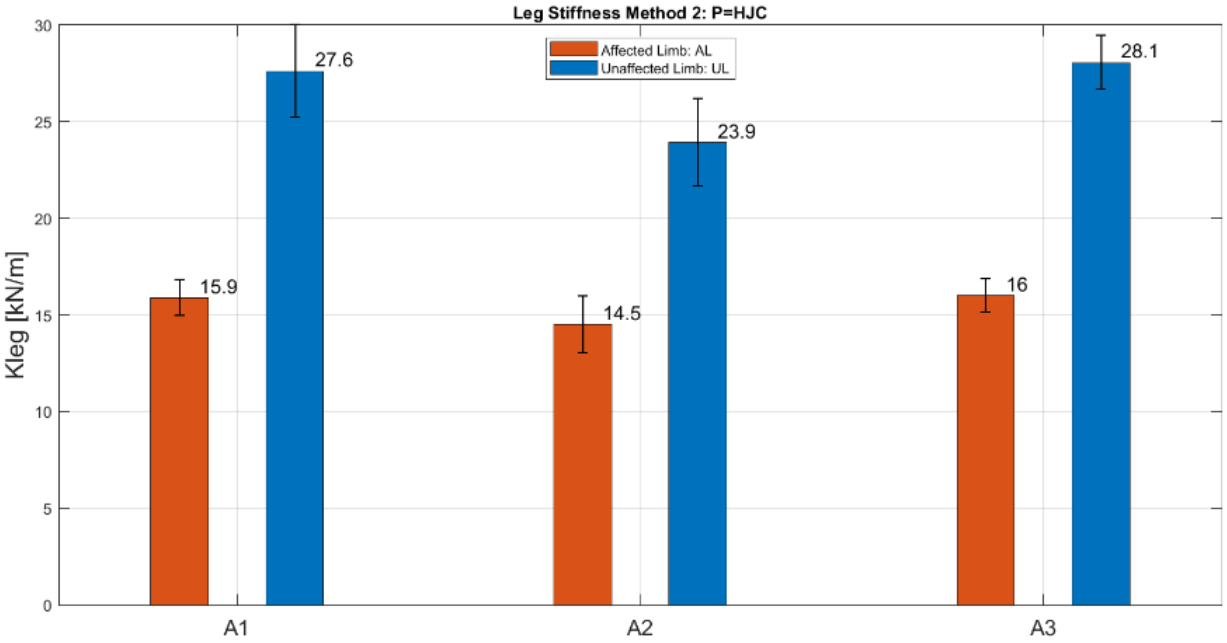

Figure 6.3: Leg Stiffness on treadmill, calculated with Method 2 (P=HJC)

With Method 2 (P=HJC) the differences in the Leg Stiffness between the Affected and the Unaffected Limb are:

- AL 42.5% lower than UL with alignment A1
- AL 39.4% lower than UL with alignment A2
- AL 43% lower than UL with alignment A1

These results, both for the Method 1 (P=COM) and Method 2 (P=HJC), highlight that the K_{leg} was smaller in the affected limb than the unaffected limb. This is in accordance with previous studies demonstrating that K_{leg} during sprinting for the affected limb was lower than for the unaffected limb in unilateral amputees wearing RSPs [26]–[28].

Unilateral amputees wearing RSP therefore present bilateral asymmetry in K_{leg} while running. It is what one might expect, seeing the difference between the projected GRF ($|\overrightarrow{GRFp}|$) in this study.

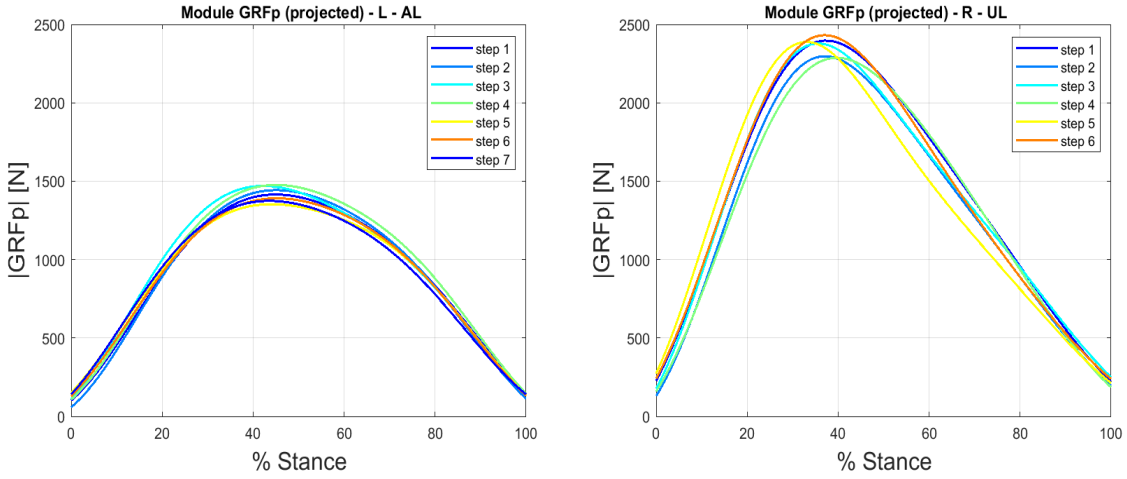

Figure 6.4: Example of $|\overrightarrow{GRF_p}|$ of this study (Method 1(P=COM), alignment A3-Treadmill)

The maximum magnitude of the projected Ground Reaction Force ($\left|\overrightarrow{GRF_p}\right|_{\max}$), which occurs approximately at 40% of the stance, is greater in the Unaffected Limb: the impairment in force generation comes from the fact that people with transtibial and transfemoral amputations are missing part of their foot and ankle musculature, which provides much of the energy used to accelerate the body. RSPs cannot generate new mechanical energy power, but only behave like a spring, which store and release elastic energy [38].

Additionally, asymmetry between limbs in unilateral amputees has been found also in joint kinematics and joint moments [12], [14], [39].

b) Differences between treadmill and track

Stiffness during running tasks has been evaluated during both treadmill and typical over ground sprinting conditions.

On track the athlete run with the socket alignment A3: for this reason, only the alignment A3 on treadmill is considered to make a comparison between values of the Leg Stiffness:

P = COM	**A3**	**A3 Track**
K_{leg_AL} [kN/m]	15.3 ± 1.8	17.5 ± 1.0

- K_{leg} A3 Track 14.3 % greater than K_{leg} A3 (treadmill) with Method 1 (P=COM).

P = HJC	**A3**	**A3 Track**
K_{leg_AL} [kN/m]	16.0 ± 2.2	17.8 ± 0.9

- K_{leg} A3 Track 11.1 % greater than K_{leg} A3 (treadmill) with Method 2 (P=HJC).

Looking at these differences, it should be remembered that the measurements performed on the treadmill give slightly different values of kinematic variables compared to the analysis carried out under field conditions: the parameters measured with a treadmill are comparable but not directly equivalent to those measured for over ground running [37]. Treadmill-based analysis of running mechanics can be generalized to over ground running mechanics, provided the treadmill surface is sufficiently stiff and belt speed is adequately regulated.

Different speeds could affect values of leg stiffness: evidence from literature showed that K_{leg} in transtibial and transfemoral amputee sprinters remained constant or increased with speed in intact limbs, while it remained constant or decreased in limbs using RSPs. In this work, it must be remarked that the treadmill test was performed with a constant speed of 5 m/s while in track the average speed maintained in the central part of the run was 6.7 m/s: looking at the different speed and the results of this study it would appear that they are in contrast with literature. It could be more probable that the difference between Treadmill and Track comes from the different experimental setup and instrumentation, instead of difference in speed. A definitive answer will be reached with the validation of the data acquired through wearable sensors: this could be done once the athlete will run with the same equipment over a farce platform placed on the ground; data from platforms and from load cell should then match.

In addition, the athlete used a different foot sole to ensure better grip while running on the Tartan of the track: this is possibly another effect on this difference.

c) Different socket alignment (A1, A2, A3)

Comparison with the different socket alignments could be done considering treadmill trials, since on track only the A3 was used.

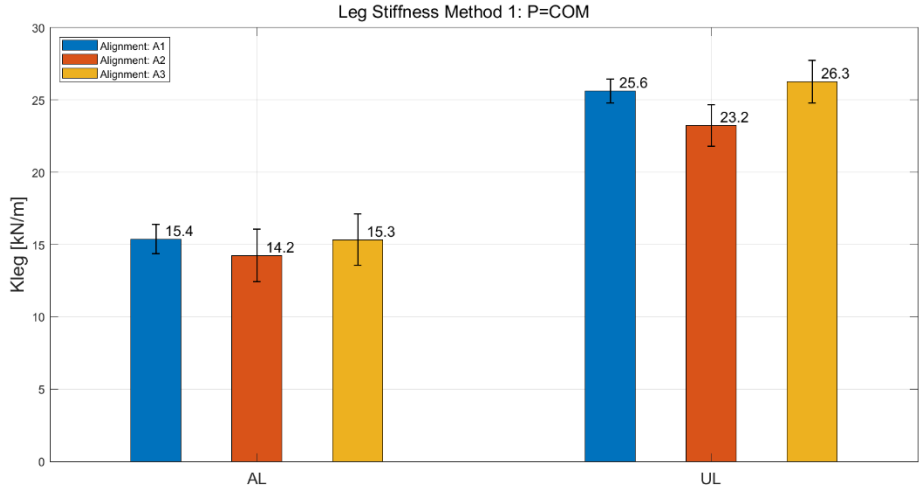

Figure 6.5: Leg Stiffness for AL and UL of treadmill trial, considering the alignment A1(blue), A2 (red), A3 (yellow), calculated with Method 1 (P=COM..

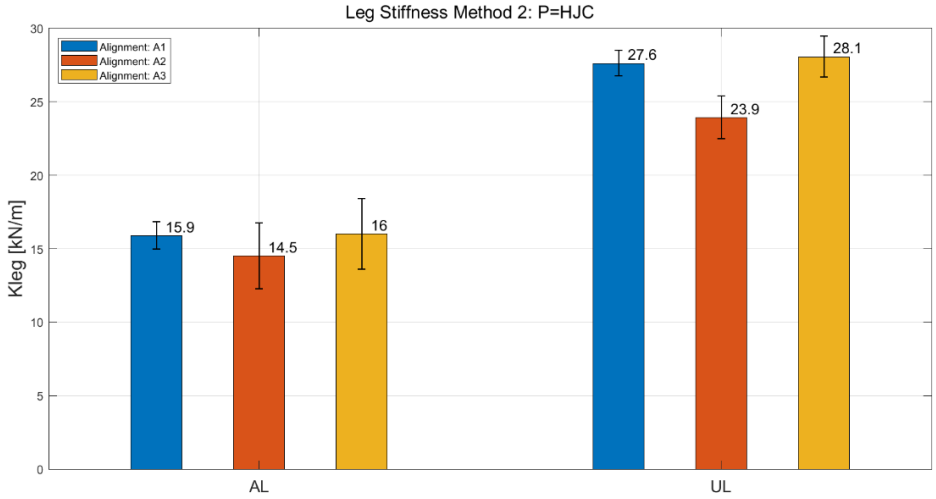

Figure 6.6: Leg Stiffness for AL and UL of treadmill trial, considering the alignment A1(blue), A2 (red), A3 (yellow), calculated with Method 2 (P=HJC).

Among the three alignments (A1, A2, A3), the results from the alignment A2 are not consistent from the others: this is in accordance with the kinematics results, which showed differences as well. The run with the A2 socket alignment was the first trial of the session, and therefore discrepancies in the results could be ascribed to the fact that the athlete was not familiar with the treadmill yet.

Although several studies [40], [41] suggested that RSP stiffness and prosthetic alignment could influence running performance through the regulation of stiffness in lower-extremity amputees, from the data obtained, it is difficult to say whether the different alignment has a significant effect on Leg Stiffness.

Different method of analysis

The Leg Stiffness model has been implemented using as a proximal point the Centre of Mass for the Method 1 and the Hip Joint Centre for the Method 2.

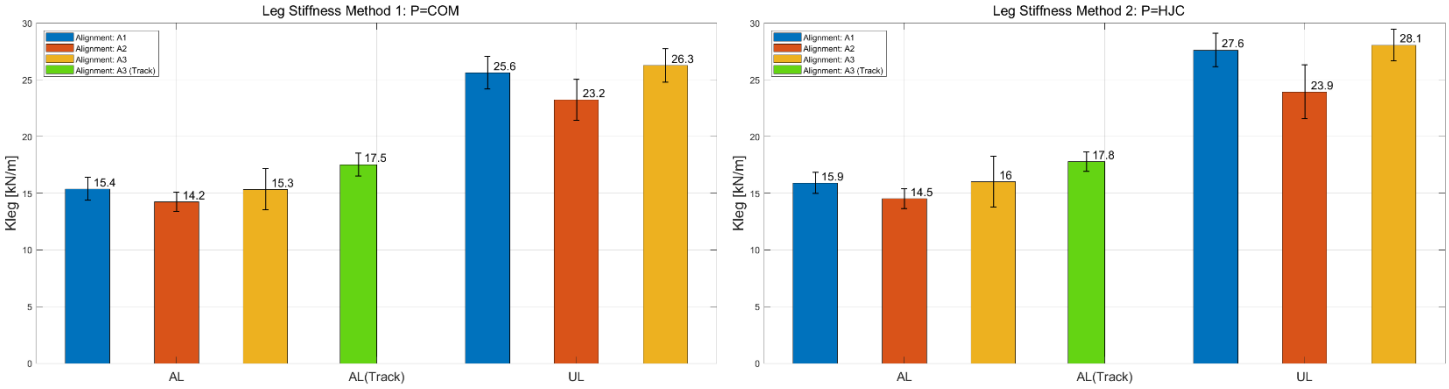

Figure 6.7: Comparison of Leg Stiffness calculated with Method 1 (P=COM) and Method 2 (P=HJC)

Looking at the two different methods of analysis, considering each alignment:

- A1: with method 2 (P=HJC) is 3.5 % higher than with method 1 (P=COM)
- A2: with method 2 (P=HJC) is 1.9 % greater than with method 1 (P=COM)
- A3: with method (P=HJC) is 4.5 % greater than with method 1 (P=COM)
- A3 Track: with method 2 (P=HJC) is 1.5% greater than method 1(P=COM)

Therefore, the leg stiffness calculated by the Method 2 (P=HJC) is slightly higher than that calculated with the method 1 (P=COM).

This small difference could be explained by the fact that in any case HJC and COM are anatomically close, both are calculated with respect to the pelvis. In fact, it is necessary to remember that the Centre Of Mass has been calculated as the centroid of the markers placed on the anterior (RASIS, LASIS) and posterior (RPSIS, LPSIS) iliac spines: perhaps, considering the true COM would lead to larger differences between the two methods.

Anyway, looking at the full body, the COM should be considered, while if looking only at the limb, the HJC should be the choice as proximal point of the model to calculate the leg stiffness.

In this work, the values of the Leg Stiffness calculated with the method 2 (P=HJC) are also used to investigate the effect of the prosthetic foot and the contribution of the residual limb on the overall leg stiffness.

Foot Stiffness

In the prosthetic leg, the stiffness was expected to be highly influenced by the fixed stiffness of the RSP.

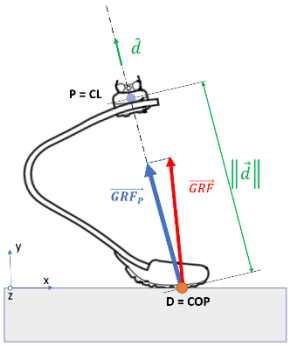

Figure 6.8: Foot Stiffness Model

The analysis with the *Foot Stiffness Model* has given the following values of Foot Stiffness:

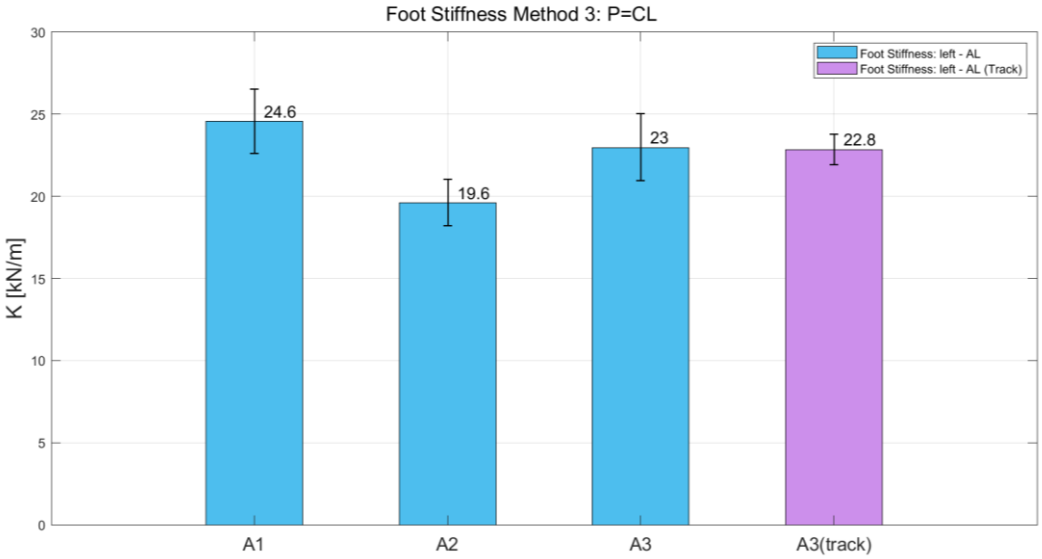

Figure 6.9: Foot Stiffness mean values.

Foot Stiffness Model - P=CL

Alignment	**A1**	**A2**	**A3**	**A3 Track**
K_{foot} [kN/m]	24.6 ± 2.0	19.6 ± 1.4	23.0 ± 2.0	22.8 ± 0.9

Despite the foot used is the same (Ottobock 1E91 standard, category 3.5) for each alignment, the value of foot stiffness for A2 (K_{foot}=19.6 ± 1.4 kN/m) is different from the others: this is in accordance with what it has been seen for the Leg Stiffness.

It is relevant to underline the value of the foot stiffness with the alignment A3 treadmill (K_{foot}=23.0 ± 2.0 kN/m) it is almost the same with the A3 Track (K_{foot}=22.8 ± 0.9 kN/m), even if the Foot Shortening ($\Delta \boldsymbol{d}$) and module of the projected GRF ($\left|\overrightarrow{GRF_p}\right|$) are different: this could be a limit of this model that considers only the peak value of the projected GRF ($\left|\overrightarrow{GRF_p}\right|$) not looking at the evolution of the stiffness during all the stance time.

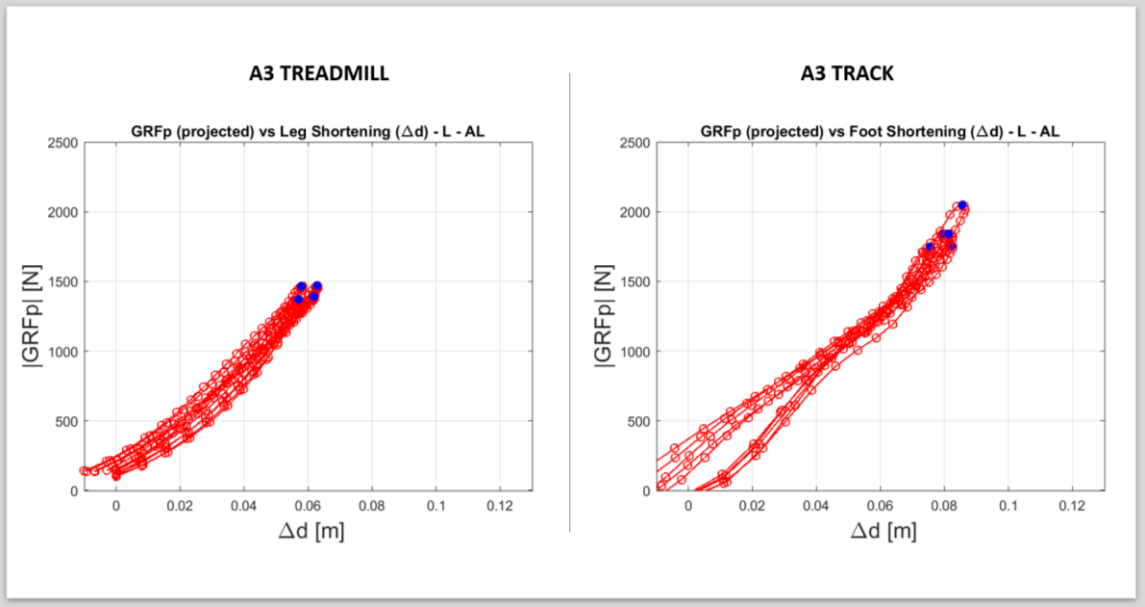

The study of Oudenhoven et al,.[25] confirms that RSP stiffness has a large effect on total leg stiffness and therefore can have an important influence on running performance. Moreover, it suggests also that socket-stump interface could contribute to the K_{leg} regulation during running.

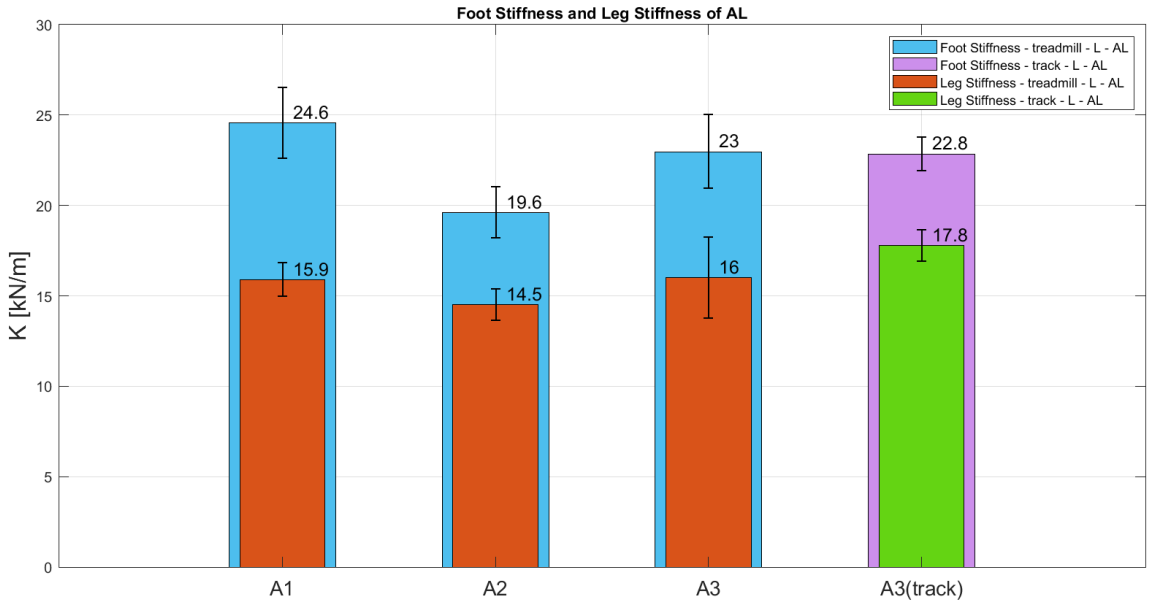

Figure 6.10: Foot Stiffness and Leg Stiffness for each alignment

Nevertheless, since prosthetic leg stiffness is considerably lower than stiffness of the RSP, compliance of the residual limb should not be ignored when selecting RSP stiffness.

A substantial contribution of the residual leg, called K_{stump}, to total leg stiffness is observed:

Figure 6.11: K_{stump} for each alignment (A1, A2, A3, A3 Track)

A difference can be seen between the contribution of the stump between track and treadmill trial: with the alignment A3, the K_{stump} on track is 52% higher than on treadmill.

It seems that athlete using RSP are not capable of regulating the stiffness of the residual leg to adjust the total leg stiffness.

Probably this result is due to the different socket used, even if the alignment is the same (A3).

Figure 6.12: RSP for treadmill (left) and track (right) trials.

In the study of Beck et al. [10], overall leg stiffness of athletes with bilateral amputation are modelled as two in-series springs: the prosthetic stiffness values averaged 22.9 ± 2.3 kN/m and the residual limb stiffness values ranged between 18.7 to 82.8 kN/m.

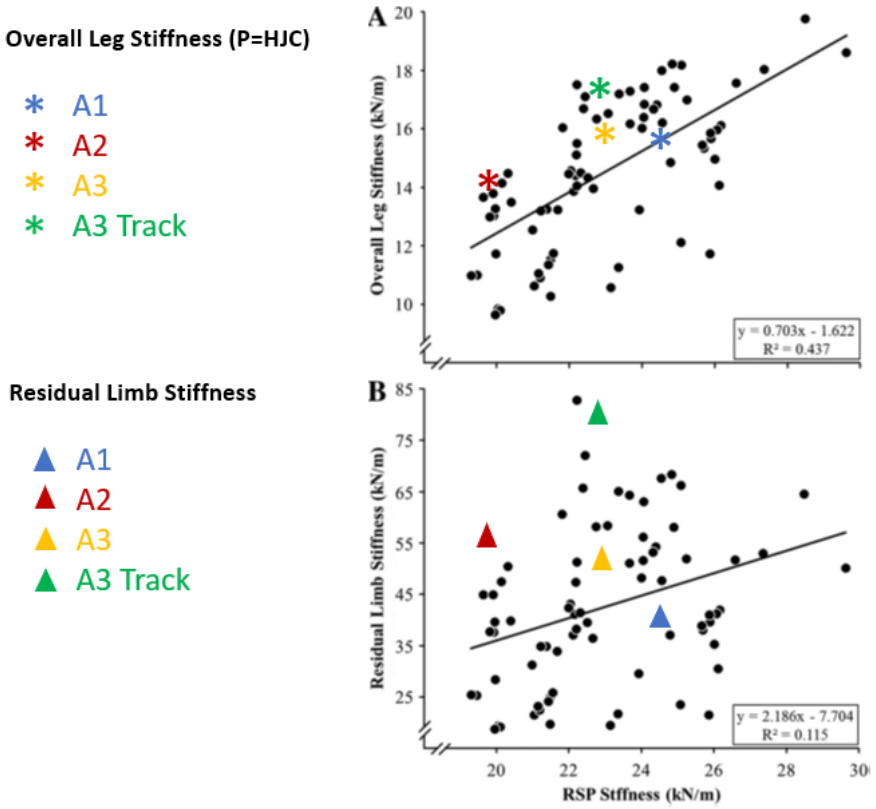

Figure 6.93: Overall leg stiffness compared with running-specific prosthesis (RSP) stiffness (A) and residual limb stiffness compared with prosthetic stiffness (B) [10]*. The quantities calculated in this work are highlighted for the different alignment with different colours (A1 -blue, A2 – red, A3 – yellow, A3 Track-green).*

With these values is not possible to perform a direct comparison due to the different experimental setup and athlete characteristics: anyway, the graph could give us an idea of the order of magnitude for the quantities calculated. The table below show the quantities calculated in this work.

Table 2: Summary of quantities calculated in this work.

		Stiffness [kN/m]	**A1**	**A2**	**A3**	**A3 Track**
Leg	**P = COM**	K_{leg_AL}	15.4 ± 1.0	14.2 ± 0.8	15.3 ± 1.8	17.5 ± 1.0
		K_{leg_UL}	25.6 ± 1.4	23.2 ± 1.8	26.3 ± 1.5	-
	P = HJC	K_{leg_AL}	15.9 ± 0.9	14.5 ± 0.9	16.0 ± 2.2	17.8 ± 0.9
		K_{leg_UL}	27.6 ± 1.5	23.9 ± 2.4	28.1 ± 1.4	-
Foot	**P = CL**	K_{foot} *(RSP)*	24.6 ± 2.0	19.6 ± 1.4	23.0 ± 2.0	22.8 ± 0.9
Stump		K_{stump}	40.5	55.6	52.7	81.1

Contact Length

Leg stiffness can be study not only looking at the influence of runnig speed, but also considering the step frequency.

Able - bodied athletes can adapt leg stiffness to regulate step frequency during running: indeed, increases in step frequency at a given running speed are known to increase the K_{leg} in non – amputees; however, little is known about stiffness regulation in unilateral transfemoral amputee. The affected limb of unilateral transfemoral amputee cannot modulate K_{leg} across a range of step frequency at a given speed and the leg stiffness regulation strategy differs between the affected and unaffected limb [30].

Leg stiffness largely influences the length of ground contact time and hence the step frequency [42], [43]. Moreover, Hobara et al., [44] showed that the contact length of the affected limb is a major biomechanical determinant of the top running speeds in para-athletes with unilateral transfemoral amputation during maximal effort sprinting while running on an instrumented treadmill.

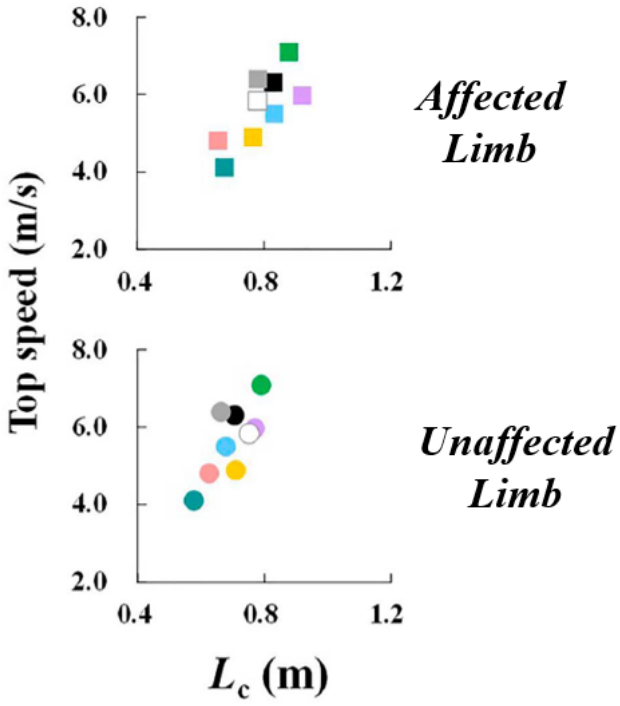

Figure 6.104: Contact Length – Lc (m) - Hobara et al 2022 [44].

'L_c' denotes the contact length (forward distance covered by the COM during the contact period). It is calculated by multiplying the contact time (t_c) with the treadmill belt speed.

Below the values of contact length calculated in this work are showed:

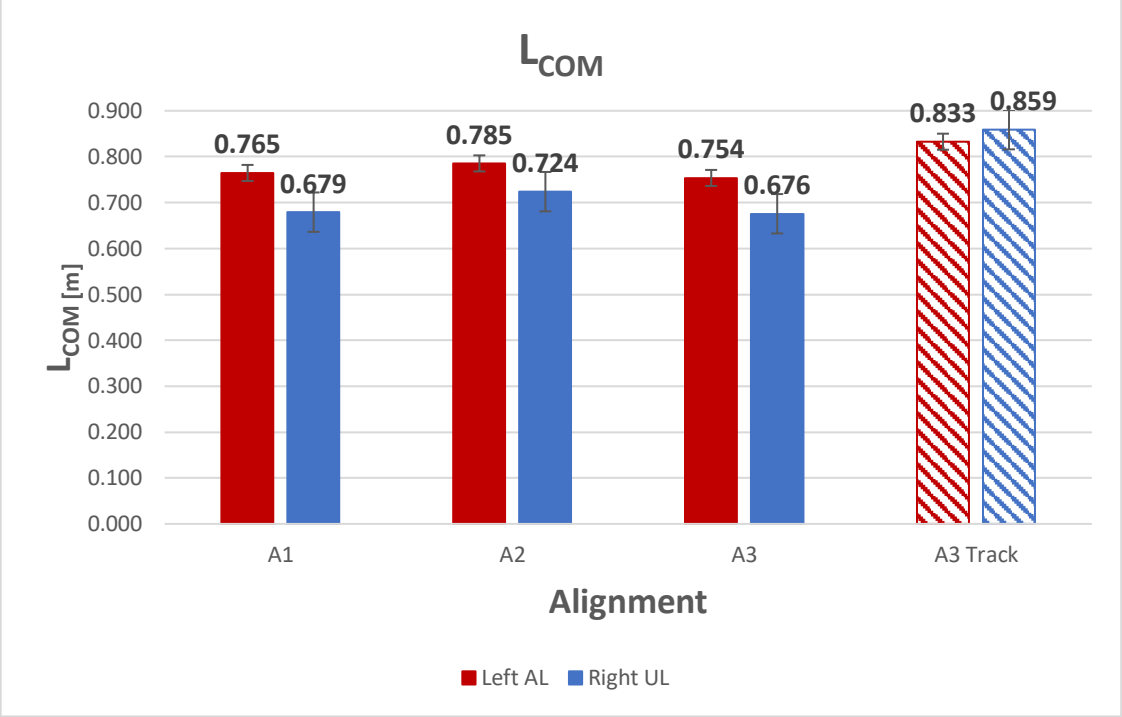

Figure 6.115: Contact Length – L_{COM} - Method 1 (P=COM)

In accordance with previous studies [13], [44] , L_{COM} is longer for the AL compared to UL during treadmill running considering the alignment A1, A2, A3.

However, the results coming from the track test are in contrast: in fact, with A3 Track the L_{COM} for AL is shorter than for UL.

It is possible to think that when running on a treadmill, the increase in step length is limited to the size of the belt: although our treadmill belt was relatively long (1.700 m) compared to maximal observed contact length (0.785 m) this might have affected the step length and influenced the athlete's running technique. Anyway, further investigations are needed to give a proper answer.

Limitations

Several factors and limitations should be considered when interpreting these results.

First, the distal point ‘D’ used in the model implemented, is not the real COP, but a marker on the foot: thus, the oscillations of the centre of pressure in the foot area are neglected.

The proximal point ‘P’ is always reconstructed considering the markers related to the pelvis: in particular is not considered the real COM for the Method 1 of the analysis.

Only one participant has been investigated while running at constant speed: the study has a limited statistical power. Further studies involving more subjects are needed.

Another limitation is related to the instrumentation setup: the athlete AS was not used to run on a treadmill, so the speed was lower than the actual speed during overground sprinting; this is a common problem in many research works, which are based on biomechanics measurements collected in a controlled environment where the conditions are quite different from a real competition.

In the *Simplified Model* implemented, the contribution of the joint’s stiffness was neglected in the unaffected limb. In fact, the ‘leg-spring’ model is dependent also on hip, knee, and ankle kinematics.

In the affected limb the stiffness of the knee was not determined: as demonstrated by previous findings, the stiffness of each prosthetic component should be addressed to determine stiffness regulation during running using RSPs [7], [25], [29].

Future Developments

- Future studies should focus on investigating the effect of greater running speeds and different step frequencies on spring-like behaviour in amputee running, to better compare the results of this model with the studies in literature.
- In this study, the leg/foot stiffness is calculated considering the peak value of the module of the projected GRF ($|\overrightarrow{GRF_p}|$): it could be interesting the estimation of the leg/foot stiffness during all the stance time.
- Study more subjects to reach a statistical relevance for this *Simplified Model*.
- The implementation of new models:
  a. to investigate the Leg Stiffness of the unaffected limb considering all the joint stiffness.

     The *Joint Stiffness* could be calculated with the 'torsional spring model' [3]:

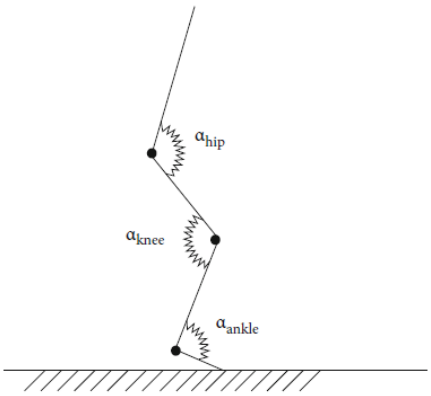

Figure 6.126: Example of torsional spring model used to estimate ankle, knee, and hip joint stiffness during running tasks [3].

The K_{joint} can be calculated as:

$$K_{joint} = \frac{M}{\Delta\alpha}$$

where M denotes the deforming torque and Δα is the angle of deformation [3].

  b. to calculate the leg stiffness for the affected limb, depending on the amputation level of the athlete: TT for transtibial and TF for transfemoral.
  c. to calculate the stiffness considering the multidimensionality of the prosthetic foot: "2-D Stiffness" considering two springs element in the model.
  d. Multiparametric prosthetic model: with the integration of all the geometric parameters of the prosthesis (socket geometry, height…), COM, HJC, stiffnesses, hip moment (M_{hip}) and the contribution of the cam.

Palaindoor Padova

Among the goals of the Olimpia project there is the creation of a sensorised running track to carry out biomechanical analysis to study and improve performances of athletes, with the advantage of using a much more confident environment than a laboratory: the Palaindoor of Padua [45].

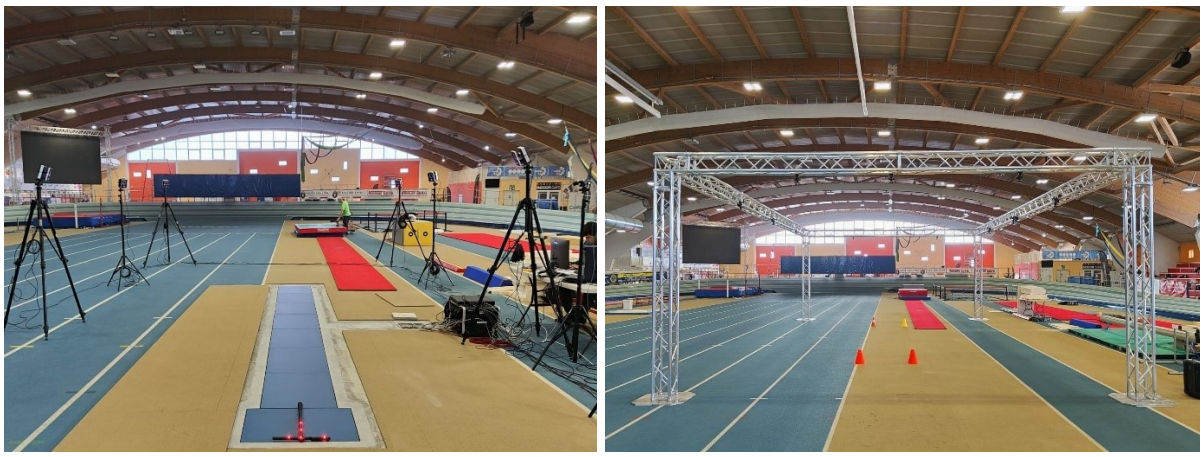

Figure 6.17: New instrumentation at the Palaindoor of Padua: Force platforms (left) and framework (right).

A moving framework (13 x 7 x 3.5 m) has been built to allow the attachment of optoelectronic cameras for motion capture; in addiction, force platforms have been placed on the ground in order to acquire kinematic and kinetic data while the athletes are performing either a sprint or a long jump.

With this instrumentation it will be possible to measure the real Centre Of Pressure and Ground Reaction Forces of the athlete while running: it will be also possible the validation of the method of estimation of the COP using the forces and torque at the load cell.

Further in-vivo experimental sessions will be taken place at the Palaindoor, with the current 'gold standard' instrumentation in term of Motion Capture, to improve kinematics and kinetics analysis and validate new models.

Conclusion

The aim of this study was to analyse the *Leg Stiffness* of the affected limb (AL) and the unaffected limb (UL) of a unilateral elite amputee athlete, during treadmill running and track sprinting.

For this reason, a spring-mass model has been implemented to describe the running action during the stance phase.

The data used for the analysis had been acquired from treadmill and track in-vivo experimental sessions, in which the gold medallist sprinter Ambra Sabatini took part.

The implementation of the '*Simplified Model*', considering all the assumptions and simplifications explained, allows the calculation of the Leg Stiffness that results very stable for each step of running in both limbs.

It has been highlighted that the K_{leg} was smaller in the affected limb than the unaffected limb, both for the Method 1 (P=COM) and Method 2 (P=HJC): unilateral amputees wearing RSP therefore present bilateral asymmetry in K_{leg} while running.

Although several studies suggested that RSP stiffness and prosthetic alignment could influence running performance through the regulation of stiffness in lower-extremity amputees, from the data obtained in this study, it is difficult to say whether the different alignment has a significant effect on Leg Stiffness, because not significantly changes has been observed considering the different socket alignments.

To make a comparison between the values of the *Leg Stiffness* in treadmill and in track only the alignment A3 was considered: the K_{leg} A3 Track was greater than K_{leg} A3 Treadmill. It should be underlined that the parameters measured with a treadmill are comparable but not directly equivalent to those measured for over ground running and it must be remarked that the treadmill test was performed with a constant speed of 5 m/s while in track the average speed maintained in the central part of the run was 6.7 m/s.

It should be noted that different method for calculating the stiffness will likely produce different resuls: the 'Leg Stiffness Model' has been implemented using as a proximal point the Centre of Mass for the Method 1 and the Hip Joint Centre for the Method 2. Looking at the two different methods of analysis implemented the *Leg Stiffness* calculated by the Method 2 (P=HJC) is slightly higher than that calculated with the method 1 (P=COM). Looking at the full

body, the COM should be considered, while if looking at the limb only, the HJC should be chosen as proximal point of the model to perform the analysis.

Furthermore, it was possible to investigate the influence of the prosthetic foot, with its foot stiffness, and the residual limb on the overall leg stiffness.

RSP stiffness has a large effect on total leg stiffness and therefore can have an important influence on running performance. Nevertheless, since prosthetic leg stiffness is considerably lower than stiffness of the RSP, compliance of the residual leg should not be ignored when selecting RSP stiffness; in fact, a substantial contribution of the residual leg, called K_{stump}, to total leg stiffness was observed.

In the end, it is possible to say that the model implemented seems to be a good tool to study the Leg Stiffness, but the outcomes cannot be generalised and caution must be used in the interpretation of these results due to the numerous assumptions and simplifications: further in-vivo experimental sessions will be taken place at the Palaindoor to overcome a good part of the limitations of this study, using the current 'gold standard' instrumentation to improve the quality of the data for the kinematics and kinetics analysis and deepen the investigation of leg and foot stiffness with more detailed models.

Bibliography

[1] 'Inail Centro Protesi'. https://www.inail.it/cs/internet/attivita/prestazioni/centro-protesi-vigorso-di-budrio/ricerca-e-sperimentazione.html (accessed Jul. 01, 2022).

[2] 'Inail.it'. https://www.inail.it/cs/internet/home.html

[3] A. Struzik, K. Karamanidis, A. Lorimer, J. W. L. Keogh, and J. Gajewski, 'Application of Leg, Vertical, and Joint Stiffness in Running Performance: A Literature Overview', *Applied Bionics and Biomechanics*, vol. 2021. Hindawi Limited, 2021. doi: 10.1155/2021/9914278.

[4] G. A. Cavagna, P. Franzetti, N. C. Heglund, and P. Willems, 'The determinants of the step frequency in running, trotting and hopping in man and other vertebrates.', *J Physiol*, vol. 399, no. 1, pp. 81–92, May 1988, doi: 10.1113/jphysiol.1988.sp017069.

[5] T. F. Novacheck, 'The biomechanics of running', 1998.

[6] S. A. Dugan and K. P. Bhat, 'Biomechanics and analysis of running gait', *Physical Medicine and Rehabilitation Clinics of North America*, vol. 16, no. 3. pp. 603–621, Aug. 2005. doi: 10.1016/j.pmr.2005.02.007.

[7] O. N. Beck, P. Taboga, and A. M. Grabowski, 'Characterizing the mechanical properties of running-specific prostheses', *PLoS One*, vol. 11, no. 12, Dec. 2016, doi: 10.1371/journal.pone.0168298.

[8] R. J. Butler, H. P. Crowell, and I. M. C. Davis, 'Lower extremity stiffness: Implications for performance and injury', *Clinical Biomechanics*, vol. 18, no. 6, pp. 511–517, 2003, doi: 10.1016/S0268-0033(03)00071-8.

[9] H. Hobara, 'Running-specific prostheses: The history, mechanics, and controversy', *National Institute of Advanced Industrial Science and Technology (AIST)*, vol. 38, no. 2, pp. 2–3, 2014.

[10] O. N. Beck, P. Taboga, and A. M. Grabowski, 'Reduced prosthetic stiffness lowers the metabolic cost of running for athletes with bilateral transtibial amputations', *J Appl Physiol*, vol. 122, no. 4, pp. 976–984, 2017, doi: 10.1152/japplphysiol.00587.2016.

[11] 'Paralympic.org Classification in Para Athletics'.

[12] F. Hadj-Moussa, C. C. Ngan, and J. Andrysek, 'Biomechanical factors affecting individuals with lower limb amputations running using running-specific prostheses: A

systematic review', *Gait Posture*, vol. 92, no. October 2021, pp. 83–95, 2022, doi: 10.1016/j.gaitpost.2021.10.044.

[13] J. R. Tacca, O. N. Beck, P. Taboga, and A. M. Grabowski, 'Running-specific prosthesis model, stiffness and height affect biomechanics and asymmetry of athletes with unilateral leg amputations across speeds', *R Soc Open Sci*, vol. 9, no. 6, 2022, doi: 10.1098/rsos.211691.

[14] Barbacane S, 'EXPERIMENTAL ANALYSIS OF RUNNING BIOMECHANICS OF ELITE PARALYMPIC AMPUTEE SPRINTERS IN TREADMILL AND TRACK TESTS', Master's Degree Thesis in Bioengineering, University of Padua, Padua, 2022.

[15] G. L. Migliore *et al.*, 'Innovative alignment of sprinting prostheses for persons with transfemoral amputation: Exploratory study on a gold medal Paralympic athlete', *Prosthet Orthot Int*, 2020, doi: 10.1177/0309364620946910.

[16] Migliore G, 'AN INNOVATIVE ALIGNMENT FOR THE SPRINTING PROSTHESIS OF ABOVE-KNEE AMPUTEES: EXPLORATORY STUDY ON A GOLD-MEDAL PARALYMPIC ATHLETE'.

[17] D. R. Coleman, D. Cannavan, S. Horne, and A. J. Blazevich, 'Leg stiffness in human running: Comparison of estimates derived from previously published models to direct kinematic-kinetic measures', *J Biomech*, vol. 45, no. 11, pp. 1987–1991, Jul. 2012, doi: 10.1016/j.jbiomech.2012.05.010.

[18] T. A. Mcmahon and G. C. Cheng, 'THE MECHANICS OF RUNNING: HOW DOES STIFFNESS COUPLE WITH SPEED?'

[19] R. Blickhan, 'THE SPRING-MASS MODEL FOR RUNNING AND HOPPING', 1989.

[20] G. A. Cavagna, P. Franzetti, N. C. Heglund, and P. Willems, 'The determinants of the step frequency in running, trotting and hopping in man and other vertebrates.', *J Physiol*, vol. 399, no. 1, pp. 81–92, May 1988, doi: 10.1113/jphysiol.1988.sp017069.

[21] C. T. Farley and O. Gonzalez, 'LEG STIFFNESS AND STRIDE FREQUENCY IN HUMAN RUNNING', 1996.

[22] D. J. Stefanyshyn and B. M. Nigg, 'Dynamic Angular Stiffness of the Ankle Joint During Running and Sprinting', 1998.

[23] A. Groothuis and H. Houdijk, ‘The Effect of Prosthetic Alignment on Prosthetic and Total Leg Stiffness While Running With Simulated Running-Specific Prostheses’, *Front Sports Act Living*, vol. 1, Aug. 2019, doi: 10.3389/fspor.2019.00016.

[24] L. Nolan, ‘Carbon fibre prostheses and running in amputees: A review’, *Foot and Ankle Surgery*, vol. 14, no. 3. pp. 125–129, 2008. doi: 10.1016/j.fas.2008.05.007.

[25] L. M. Oudenhoven, J. M. Boes, L. Hak, G. S. Faber, and H. Houdijk, ‘Regulation of step frequency in transtibial amputee endurance athletes using a running-specific prosthesis’, *J Biomech*, vol. 51, pp. 42–48, Jan. 2017, doi: 10.1016/j.jbiomech.2016.11.058.

[26] H. Hobara *et al.*, ‘Amputee locomotion: Spring-like leg behavior and stiffness regulation using running-specific prostheses’, *J Biomech*, vol. 46, no. 14, pp. 2483–2489, Sep. 2013, doi: 10.1016/j.jbiomech.2013.07.009.

[27] C. P. McGowan, A. M. Grabowski, W. J. McDermott, H. M. Herr, and R. Kram, ‘Leg stiffness of sprinters using running-specific prostheses’, *J R Soc Interface*, vol. 9, no. 73, pp. 1975–1982, Aug. 2012, doi: 10.1098/rsif.2011.0877.

[28] Y. Sano *et al.*, ‘Leg stiffness during sprinting in transfemoral amputees with running-specific prosthesis’, *Gait Posture*, vol. 56, pp. 65–67, Jul. 2017, doi: 10.1016/j.gaitpost.2017.04.038.

[29] H. Hobara, H. Sakata, S. Hashizume, and Y. Kobayashi, ‘Leg stiffness in unilateral transfemoral amputees across a range of running speeds’, *J Biomech*, vol. 84, pp. 67–72, Feb. 2019, doi: 10.1016/j.jbiomech.2018.12.014.

[30] H. Hobara, H. Sakata, Y. Namiki, G. Hisano, S. Hashizume, and F. Usui, ‘Effect of step frequency on leg stiffness during running in unilateral transfemoral amputees’, *Sci Rep*, vol. 10, no. 1, Dec. 2020, doi: 10.1038/s41598-020-62964-2.

[31] F. Gondoni, ‘Valutazione comparativa dei modelli per la stima di vertical e leg stiffness durante la corsa’, *Master Thesis in Biomedical Engineering, Politecnico di Milano*, 2020.

[32] Y. Blum, S. W. Lipfert, and A. Seyfarth, ‘Effective leg stiffness in running’, *J Biomech*, vol. 42, no. 14, pp. 2400–2405, Oct. 2009, doi: 10.1016/j.jbiomech.2009.06.040.

[33] B. X. W. Liew, S. Morris, A. Masters, and K. Netto, ‘A comparison and update of direct kinematic-kinetic models of leg stiffness in human running’, *J Biomech*, vol. 64, pp. 253–257, Nov. 2017, doi: 10.1016/j.jbiomech.2017.09.028.

[34] S. Breban, F. Bettella, R. Di Marco, G. Migliore, A. G. Cutti, and N. Petrone, ‘GRF ANALYSIS OF TWO ELITE PARALYMPIC SPRINTERS IN STEADY AND RESISTED ACCELERATED TREADMILL RUNNING’, in *40th International Society of Biomechanics in Sports Conference, Liverpool, UK: July 19-23*, 2022. [Online]. Available: https://commons.nmu.edu/isbs/vol40/iss1/22

[35] N. Petrone *et al.*, ‘Development of instrumented running prosthetic feet for the collection of track loads on elite athletes’, *Sensors (Switzerland)*, vol. 20, no. 20, pp. 1–18, Oct. 2020, doi: 10.3390/s20205758.

[36] G. Wu and P. R. Cavanagh, ‘ISB recommendations for standardization in the reporting of kinematic data’, *J Biomech*, vol. 28, no. 10, pp. 1257–1261, Oct. 1995, doi: 10.1016/0021-9290(95)00017-C.

[37] A. L. Bell, D. R. Pedersen, and R. A. Brand, ‘A comparison of the accuracy of several hip center location prediction methods’, *J Biomech*, vol. 23, no. 6, pp. 617–621, 1990, doi: 10.1016/0021-9290(90)90054-7.

[38] A. M. Grabowski, C. P. McGowan, W. J. McDermott, M. T. Beale, R. Kram, and H. M. Herr, ‘Running-specific prostheses limit ground-force during sprinting’, *Biol Lett*, vol. 6, no. 2, pp. 201–204, Apr. 2010, doi: 10.1098/rsbl.2009.0729.

[39] B. Baum, ‘Running after lower extremity amputation with daily-use and running-specific prostheses: A review of biomechanics outcomes’, vol. 23, pp. 121–130, Feb. 2020.

[40] Y. NISHIKAWA and H. HOBARA, ‘Mechanical stiffness of running-specific prostheses in consideration of clamped position’, *Mechanical Engineering Letters*, vol. 4, no. 0, pp. 17-00452-17–00452, 2018, doi: 10.1299/mel.17-00452.

[41] O. N. Beck, P. Taboga, and A. M. Grabowski, ‘How do prosthetic stiffness, height and running speed affect the biomechanics of athletes with bilateral transtibial amputations?’, *J R Soc Interface*, vol. 14, no. 131, Jun. 2017, doi: 10.1098/rsif.2017.0230.

[42] J. B. Morin, P. Samozino, K. Zameziati, and A. Belli, ‘Effects of altered stride frequency and contact time on leg-spring behavior in human running’, *J Biomech*, vol. 40, no. 15, pp. 3341–3348, 2007, doi: 10.1016/j.jbiomech.2007.05.001.

[43] M. Brughelli and J. Cronin, ‘Influence of Running Velocity on Vertical, Leg and Joint Stiffness Modelling and Recommendations for Future Research’, 2008.

[44] H. Hobara *et al.*, ‘Biomechanical determinants of top running speeds in para-athletes with unilateral transfemoral amputation’, 2022, doi: 10.1097/PXR.0000000000000175.

[45] P. Mistretta, M. Scapinello, S. Breban, A. G. Cutti, and N. Petrone, ‘Instrumentation of sprint and long jump tracks of an indoor athletics field to study athletes’ performances’, in *ISEA 2022 – The Engineering of Sport 14, Purdue University, 6-10 June 2022*, 2022.